Fall 12-20-2013

4D evolution of fluvial system and channel-fill architecture of the Cretaceous Blackhawk Formation, Wasatch Plateau, Utah: An integrated fluvial rock record analysis

Hiranya Sahoo
University of New Orleans, hsahoo@uno.edu

4D evolution of fluvial system and channel-fill architecture of the Cretaceous Blackhawk Formation, Wasatch Plateau, Utah: An integrated fluvial rock record analysis

A Dissertation

Submitted to the Graduate Faculty of the
University of New Orleans
in partial fulfillment of the
requirements for the degree of

Doctor of Philosophy
in
Engineering and Applied Science
Earth and Environmental Sciences

by

Hiranya Sahoo

M.Sc. Utkal University, 2003
M.Tech. IIT Bombay, 2006

December, 2013

Acknowledgements

I am extremely indebted to the University of New Orleans for all I have gained throughout these years. Excellent people, vibrant departmental activities, and thriving environment for research have made my stay at UNO utmost enjoyable and memorable. All these years of PhD study at UNO have been of immense personal and professional enrichment. I am thankful to all of those who have rendered their time and efforts towards my progress during this period.

First and foremost, I feel a great privilege to have had Prof. Royhan Gani as my advisor during all these years. His intellectual direction introduced me into the fascinating outcrop exposures of the Western Interior Seaway that eventually became the natural laboratory of my PhD research. This research would not have been possible without his persistent support and faith in me. I admire his outstanding mentorship, incredible guidance, and utmost motivation that I have received during all these years. These have greatly helped in enhancing my professional and personal standing.

My sincere gratitude goes to the other members of my PhD committee for their guidance throughout my research, and timely help to keep me aligned to the plan. I am thankful to Prof. Mark Kulp for his insightful feedbacks that have brought refinements to the sedimentologic-stratigraphic analysis of this research. My thanks goes to Prof. Ioannis Georgiou for providing me new ideas and avenues for complimentary research of ancient vs. modern vs. modeling domain. I thank Prof. Bhaskar Kura for always bringing the interdisciplinary aspects for broader research relevance. I am grateful to Prof. Nahid Gani for her perspectives that have

led to augment the dimensionality of my research. Her research guidance has been of great help in bringing novelty to my outcrop investigation approach in terms of application of cutting-edge photorealistic technology.

I sincerely thank Prof. Gary Hampson of Imperial College London, UK for his stimulating interactions and inputs during the course of collaborative work with him. His feedbacks have greatly augmented the quality and content of my research focuses. Similarly, thanks goes to the group of Prof. John Howell at the University of Bergen, Norway for the collaborative contribution towards LiDAR-integrated outcrop research.

This research has been greatly benefited from financial support by petroleum industry and professional organizations. Corporate support from Chevron and ExxonMobil is sincerely appreciated. Several student grants and fellowships from AAPG, GCSSEPM, IAS, and University of New Orleans have significantly supported towards the completion of this PhD research.

I acknowledge Shell Oil Company for providing me an opportunity to learn real industry practice through its summer internship program. I sincerely thank Dr. Daniel Minisini and Dr. Steven Bergman for their excellent guidance and mentorship during that period. Additionally, I would like to thank Dr. Calum Macaulay, Dr. Mark Barton and other members of the clastic group therein for fruitful interactions and inputs. This internship experience has been an immense professional enrichment for me.

During these years, my stay in the StrataMax Lab at UNO has been extremely pleasurable as I have enjoyed my share with fellow group members. Mr. Andrew Ranson has been of great help during the times of field documentation. Mr. Corey Hinyup has provided

field-support during the final stage of this research. Wonderful friendship and help from Mr. Prabhat Neupane is greatly appreciated.

I am grateful to the department of Earth and Environmental Sciences at UNO for providing me an excellent ambience and fascinating people. My sincere thanks goes to each faculty member, Ms. Linda Miller, Mr. Al Falster, and others for the much help and support I have received during the course of my study.

Above all, my deepest gratitude goes to my family for all I have achieved so far. Unequivocal love and support from my parents, brother and sister have always motivated me to move on in my life. I am extremely grateful to my maternal uncles and aunts for their invaluable contribution to both my personal and professional life. In particular, I owe my professional accomplishments profoundly to the high moral support and guidance of my elder maternal uncle who has always been there for my education and development since my early school days. My deepest love and gratitude goes to my wife Suchismita for her overwhelming support and encouragement during this PhD study. She has been a pillar of strength to me.

Hiranya Sahoo

University of New Orleans

December, 2013

Table of Contents

List of Figures

List of Tables

Abstract

Using an integrated dataset comprising outcrop, core, GPR and LiDAR data, this study targets a high-quality outcrop "window" of the upper Cretaceous Blackhawk Formation in the eastern Wasatch Plateau in central Utah, spanning a fairly large spatial (~30 km^2 area comprising eight contiguous, and vertical cliff faces) and temporal (~4 my) range. This research provides field-validation and -calibration of a wider range of fluvial heterogeneity: 1) large-scale heterogeneity (10's of m vertically and 100's of m laterally), 2) intermediate-scale heterogeneity (1's of m vertically and 10's of m laterally), and 3) small-scale heterogeneity (10's of cm vertically and 1's of m laterally). These sandbody- to facies-scale heterogeneities generate potential for stratigraphic compartmentalization for analogous fluvial reservoirs and prospects. Moreover, these results specifically constitute an outcrop analog to the producing tight-gas fluvial reservoirs of the adjacent hydrocarbon-prolific Uinta and Piceance Basins of Utah and Colorado, including the giant Jonah Field of Wyoming.

3D virtual outcrop model generated from LiDAR-integration has helped in avulsion-scale (~1's-10's kyr) to basin-fill scale (~100's kyr-1's myr) fluvial sandbody organization analysis down to channel-storey level. This high-resolution analysis has brought several intriguing insights. single-storey sandbodies are preferentially attendant to clustering organization, whereas multi-lateral sandbodies (i.e. channel-belt) show compensational-prone behavior. Sandbody organization is broadly compensational for the lower Blackhawk Formation, where the floodplain facies diversity is the highest. In contrast, floodplain diversity decreases

stratigraphically upward such that the upper Blackhawk Formation shows the least heterogeneous floodplain with clustering-prone sandbody organization. In the quest of differentiating autogenic from allogenic signal in dynamic systems where their interplay is complexly intertwined, this study presents two incised-valley examples, where resultant fluvial organization has been interpreted, contrary to conventional wisdom, to be preferentially modulated by a dominant controlling mechanism of autogenic forcing. In filling these incised valley deposits, each of which is up to ~15-20 m thick, the dominating behavior of substrate coal compaction as an autogenic mechanism supplanted allogenic forcing (i.e. sea-level fluctuation).

Keywords: Cretaceous Blackhawk Formation, Utah, stratigraphic compartmentalization, fluvial heterogeneity, compensational vs. clustered stacking, floodplain diversity, autogenic vs. allogenic forcing.

Chapter 1

Introduction

1.1 Motivation

In the realm of rock record investigation, fluvial depositional elements are among the most prominent stratigraphic entities that have persistently generated enormous intellectual interest and, in turn, been extensively studied (e.g. Miall, 2006). Voluminous works on them by both the academic community and petroleum industry provide a context to their importance towards economic and societal progress. Fluvial sandbodies overwhelmingly serve as avenues for subsurface hydrocarbon reservoirs as well as aquifer development. Given this emphasis, a good understanding of geometry and internal architecture of fluvial depositional elements is crucial to fully exploit their potential not only as hydrocarbon reservoirs but also as aquifers (e.g. Rygel and Gibling, 2006). Additionally, latest review and experimental studies in fluvial dynamics have brought some compelling observations on controlling mechanisms (autogenic vs. allogenic forcings) of fluvial organization and its stratigraphic manifestation at spatio-temporal scales (e.g. Muto et al., 2007; Paola et al. 2009; Hajek et al., 2010; Blum et al., 2013). Improved evaluation of these latest findings on fluvial dynamics requires robust outcrop dataset with appropriate geological merits.

Given the constraints of conventional subsurface dataset (e.g. seismic, well-log, core etc.), outcrop characterization is increasingly being pursued towards better fluvial reservoir analysis as well as delineating characteristics of fluvial elements (e.g. Willis 1997, 1998; Reynolds, 1999; Bryant et al., 2000; Willis and White, 2000; Barnaby and Ward, 2007; Hofmann et al., 2011). Modern fluvial analogs render insufficient to illustrate startigraphic manifestation of fluvial elements at spatio-temporal scales. This study pursues an intensive outcrop characterization of Cretaceous fluvial deposits in Cottonwood Creek of the Wasatch Plateau of central Utah. Selection of this fieldsite is extremely advantageous for two reasons. Firstly, the study area is a part of the broader Western Interior Seaway of Utah and Colorado that has served as a natural laboratory for development and refinement of significant stratigraphic concepts due to its clean, sparsely-vegetated, and world-class exposures (e.g. Pattison, 1995; Van Wagoner, 1995; Howell and Flint, 2003; Hampson and Howell, 2005). Secondly, this area is adjacent to the hydrocarbon-prolific Uinta and Piceance Basins of Utah and Colorado. Hence, sedimentologic and stratigraphic information gained from this fieldsite can be integrated towards improved upstream practices of producing reservoirs of those two basins (e.g. Nehring, 2008; Mackel and Thomasson, 2008).

1.2 Research questions

Analysis on characters of producing hydrocarbon reservoirs in the Uinta and Piceance Basins as well as scientific realization from some recent studies in fluvial discipline bring some key concerns: 1) fluvial reservoirs in these two basins are characterized by a wide range of

subsurface complexities that are posing huge exploration and production challenges therein, and 2) there is a need for improved fluvial rock record analysis to test evolving knowledge of fluvial sandbody organization in space and time. This research attempts to address these concerns as specified below.

1. Producing fluvial reservoirs of the adjacent Uinta and Piceance Basins of Utah and Colorado are highly compartmentalized. How to analogously illustrate those range of compartmentalization from adjacent outcrop characterization?
2. In fluvial rock record studies, sandbody organization analysis has been done at the channel-belt scale. What could be the organization below this scale? Does any coupling relationship exist between sandbody organization and floodplain diversity?
3. How to differentiate autogenic from allogenic signals in fluvial records where these two signals are interwoven?

1.3 Approach

For the completion of this doctoral research, extensive fieldwork was carried out that have resulted in detailed documentation of outcrop data. A GPR (Ground Penetration Radar) with 250 MHz frequency has been utilized to document the internal variability of sandbodies. Cutting-edge photorealistic technology using LiDAR (Light Detection and Ranging) has been incorporated to analyze the preserved three dimensionality of fluvial depositional elements. Low-airborne LiDAR data (~20 cm resolution) were acquired and processed to generate 3D virtual outcrop model for fluvial organization analysis. Additionally, one nearby long core (EM-

137C) has been analyzed in detail to provide additional control on sandbody correlation and process sedimentology. This study has been immensely benefited from financial supports from Chevron, and several student grants and fellowships from ExxonMobil, AAPG (American Association of Petroleum Geologists), GCSSEPM (Gulf Coast Society for Sedimentary Geology), IAS (International Association of Sedimentologists), and University of New Orleans (Geology and Geophysics research fund, and graduate enhancement research grant). During the course of this research, collaborative works with Imperial College London and University of Bergen (Norway) have augmented both dimensionality and clarity of several research focuses. Individual research focus has been comprehended as three separate chapters of this dissertation that constitute three standalone manuscripts.

Chapter two provides field-validation and -calibration of the entire range of fluvial heterogeneity captured on a single outcrop dataset. Analysis demonstrates that large-scale heterogeneity (10's m vertically and 100's m laterally) is associated with channelized fluvial sandbodies encased within coastal-plain fines. Intermediate-scale heterogeneity (1's m vertically and 10's m laterally) is related to the type and distribution of architectural elements like bar-accretion and crevasse splays units within individual sandbodies. Small-scale heterogeneity (10's cm vertically and 1's m laterally) is attributed to lateral and vertical facies variations within individual architectural elements. These fluvial heterogeneities illustrating sandbody continuity and connectivity, net-to-gross variation, and architectural element and facies distributions generate potential for stratigraphic compartmentalization at field-scale for analogous fluvial reservoirs and prospects, especially for low net-to-gross system. These results, as an outcrop analog, provide particular insight for improved upstream practice of

producing tight-gas reservoirs of the Uinta and Piceance Basins of Utah and Colorado. Moreover, study results bear a matching correlation to the reservoir characteristics of the giant, gas-producing Jonah field of Wyoming.

Third chapter brings to the attention that far robust sedimentologic and stratigraphic results can be achieved by integrating emerging technology to conventional outcrop investigation. Utilizing photorealistic technology like the LiDAR, this study has successfully extracted three dimensionality of fluvial sandbodies encased within pervasive coastal-plain fines using a 3D virtual outcrop model. Upon paleoflow correction, nearly-perfect and fully-preserved sandbodies have been populated to analyze fluvial organization at architecture- (e.g. avulsion cycle ~1's-10's kyr) to basin-scale (~100's kyr-1's myr). Compared to published works that have focused fluvial sandbody organization at channel-belt scale, this LiDAR-integrated characterization has been able to pursue fluvial sandbody organization down to individual channel-storey level. Analysis on sandbody organization (clustered vs. compensationally-stacked) has been done at three stratigraphic levels of the Blackhawk Formation (lower, middle, and upper). Relationship of these end-member organization types to attendant channel-storey types (single vs. multi-storey) has been established for the first time in literature. Additionally, study has provided insights on plausible links between type of sandbody organization (clustered or compensationally-stacked) and associated floodplain diversity.

The analysis in fourth chapter brings a significant new perspective to fluvial paradigm. In the light of recent knowledge that fluvial autogenic dynamics has equivalent potential in operating over similar temporal range as well as sculpting identical fluvial sandbody organization that are traditionally inferred as modulating mechanism of allogenic forcings, the

latest review on paleovalley fluvial architecture (i.e. Blum et al., 2013) urges to find ways in differentiating autogenic from allogenic signals in preserved fluvial organization. However, it renders a huge challenge to de-convolve autogenic from allogenic signals in a dynamic system like paleovalley where these two signals can easily be intertwined complexly. Using two interpreted incised valley fill deposits, this study brings a finding of differentiating autogenic controls by carefully illustrating resultant trends of fluvial organization in relation to substrate coal thickness. Instead of allogenic control, dominant autogenic behavior shows a supplanting mechanism in guiding paleovalley sandbody organization.

Chapter 2

Facies- to sandbody-scale heterogeneity in a tight-gas fluvial reservoir analog: Blackhawk Formation, Wasatch Plateau, Utah, USA

Abstract

Using photomosaics, measured sections, and ground-penetrating radar data, this study characterizes facies- to sandbody-scale heterogeneity in the fluvial and coastal-plain deposits of the Blackhawk Formation of the Wasatch Plateau, Utah, USA, as an outcrop analog for tight-gas reservoirs of the adjacent Uinta and Piceance Basins. Analysis on eight contiguous, and vertical cliff-faces comprising both depositional-dip- and -strike-oriented segments provides field-validation and calibration of entire range of fluvial heterogeneity, where: 1) large-scale heterogeneity (10's of m vertically and 100's of m laterally) is associated with stacking of channelized fluvial sandbodies encased within coastal-plain fines, 2) intermediate-scale heterogeneity (1's of m vertically and 10's of m laterally) is related to type and distribution of architectural elements like bar-accretion and crevasse-splay units within individual sandbodies, and 3) small-scale heterogeneity (10's of cm vertically and 1's of m laterally) is attributed to lateral and vertical facies variations within individual architectural elements.

Individual sandbodies are medium-grained, 1-17 m thick, 29-724 m wide, and they constitute single-storey to multi-storey lateral (i.e. channel-belt) to channel-belt complexes.

Along each lateral-accretion bed within a sandbody, updip fine-grained sandstones become distinctly coarser-grained and amalgamated downdip. A crevasse-delta deposit (c. 7 m thick) shows down-clinoform facies change from proximal, rippled sandstones to distal, silty mudstones over a length of ~ 50 m. At a ~ 100 m pseudowell spacing, > 50% channelized sandbodies and > 90% crevasse-splay sandbodies show very limited well intersection (one or two at most). Studied dataset analogously constrain subsurface characteristics of the giant, tight-gas producing Jonah field.

2.1 Introduction

Tight-gas sandstone reservoirs form a key component of U.S. unconventional gas production with an enormous projected potential (Smith et al., 2010). Growing energy consumption and a persistent drive for secure and environmentally-clean energy have emphasized the importance of tight-gas resources, particularly in the Rocky Mountain region (Nehring, 2008). However, many tight-gas plays and reservoirs are associated with significant appraisal and extraction challenges, including low net-to-gross ratios, anomalous petrophysical behavior, and pronounced production variability, that restrict commercial production to “sweet spot” areas (Surdam, 1997). Addressing these challenges requires improved geologic understanding to calibrate, validate, and evaluate heterogeneities and uncertainties in tight-gas reservoirs (e.g., Cumella et al., 2008).

Significant work has been carried out on fluvial tight-gas reservoir evaluation and performance in order to document their facies characteristics (e.g., Shanley, 2004),

petrophysical properties (e.g., Shanley et al., 2004), and fracture distributions and diagenetic overprints (e.g., Laubach and Gale, 2006; Higgs et al., 2007; Olson et al., 2009; Tobin et al., 2010) from cores, cuttings, well logs, and seismic data. However, these subsurface analyses are insufficient for an understanding of reservoir sandbody geometry, connectivity, and stacking patterns that is integrated with detailed documentation of their internal heterogeneities. For example, core and well-log data capture the vertical dimension of depositional elements, but do not constrain their lateral extent. Also, well-log data cannot extract bed-scale sedimentary structures (i.e., dune-stratification, ripple-lamination, parallel-lamination etc.). Likewise, lithologic contrasts between sandstones and mudstones may not generate sufficiently strong impedance contrasts at conventional seismic tuning and resolution to be imaged (e.g., House and Shemeta, 2008). Even high-quality 3D seismic data cannot resolve lithological variations within sandbodies (Shanley, 2004). Therefore, these descriptions fall short of fully delineating the degree of heterogeneity development at inter-well scale. In contrast, such heterogeneities can be constrained in outcrop analogs that allow sandbodies and mudstones, which respectively form flow conduits and baffles or barriers, to be characterized in the context of their stratigraphic architecture, geometry, and net-to-gross variation at a range of scales. In fact, outcrop studies can furnish significant inputs to reservoir connectivity analysis that usually relies on core, well log, seismic, and conceptual modeling data (Larue and Hovadik, 2006).

Published outcrop studies on analogous tight-gas sandstone reservoirs have compiled dimensional data for fluvial sandbodies (e.g., Cole and Cumella 2005; Pranter et al., 2009) and focused on heterogeneity at the scale of architectural elements within such sandbodies (e.g., Pranter et al., 2007). However, heterogeneity in fluvial reservoirs is complex, and ranges in size

from small-scale (10's of cm vertically and 1's of m laterally; e.g., facies transitions and cross-stratification style) to intermediate-scale (1's of m vertically and 10's of m laterally; e.g., stacking of architectural elements) to large-scale (10's of m vertically and 100's of m laterally; e.g., spatial distribution of channelized sandbodies encased within floodplain mudstones) (Miall, 1988; Jones et al., 1987; Larue and Hovadik, 2006). Heterogeneity at each of these scales can potentially give rise to stratigraphic reservoir compartmentalization that is defined by segregation of flow units with distinctly different porosity and permeability properties. Aimed towards an intensive analysis of this entire range of fluvial heterogeneity and its constraining effect on subsurface tight gas reservoir complexity, this study focuses on three objectives: (1) detailed characterization of a single outcrop dataset, comprising a series of contiguous cliff faces oriented in both depositional-dip and –strike directions, that illustrates facies distributions, stratigraphic architecture, and fluvial heterogeneity across a range of scales in the lower Blackhawk Formation, Wasatch Plateau; (2) assessment of how these heterogeneities influence potential stratigraphic compartmentalization and development of "sweet spots" at field scale; and (3) analysis of the controls on amalgamation of channelized sandbodies, which significantly increases the localized net-to-gross ratio.

The studied succession contains numerous coal seams, and thus, is an analog for direct-type unconventional gas systems that are characterized by a gas-prone source rock and short migration distances (Law, 2002; Law and Spencer, 2004), such as part of the Mesaverde Total Petroleum System of Johnson and Roberts (2003). The Wasatch Plateau study area in east-central Utah flanks the southwestern part of the Uinta Basin (Figure 2.1B), and serves as a direct analog for fluvial tight-gas reservoirs in the western, subsurface part of the Wasatch

Plateau (an immature tight-gas basin *sensu* Meckel and Thomasson, 2008) and, more importantly, to the adjacent Uinta and Piceance Basins of Utah and Colorado (Figure 2.1B), a key area of current tight-gas production with significant remaining potential (Nehring, 2008).

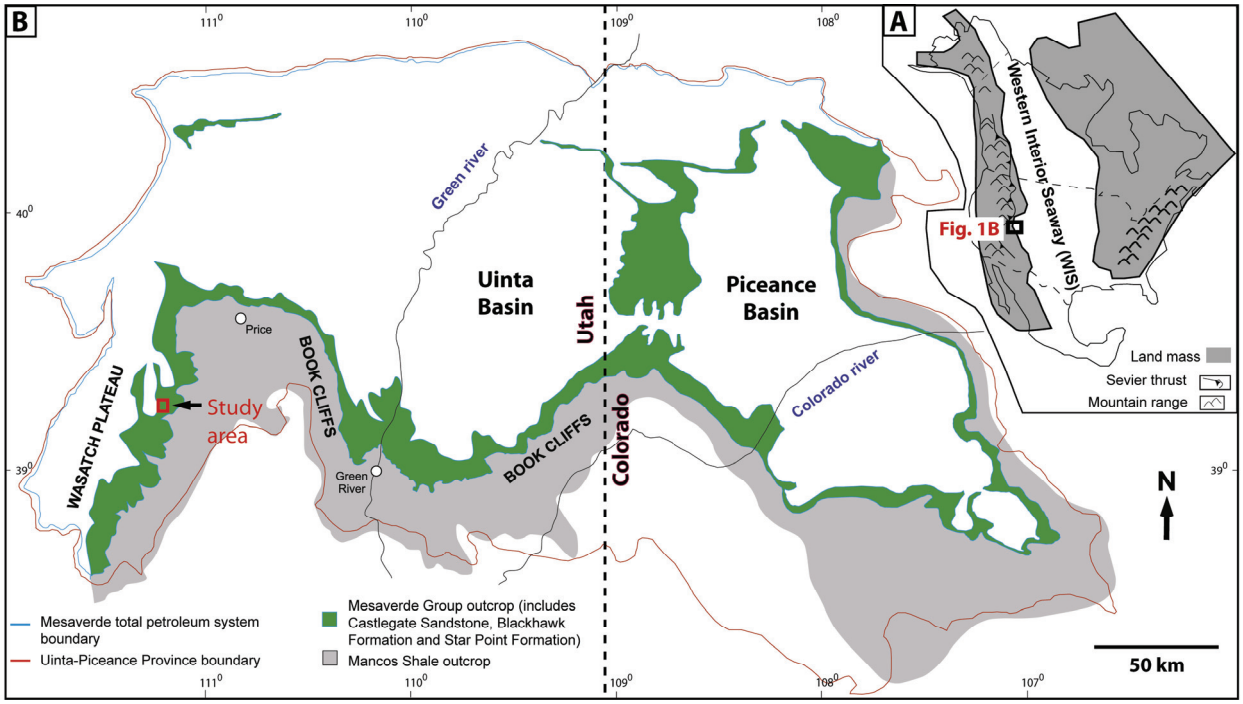

Figure 2.1. A) Late Cretaceous paleogeography of the study area (after Gani and Bhattacharya, 2007). B) Location of the study area in the Wasatch Plateau, central Utah. The Upper Cretaceous Blackhawk Formation, Mesaverde Group, crops out in the study area (modified from Johnson and Roberts, 2003; Hampson, 2010). The study area is adjacent to the Uinta-Piceance province in Utah and Colorado that constitutes one of the key areas of current US tight-gas production (Nehring, 2008).

2.2 Geologic Setting

The studied outcrop section is from Cottonwood Creek in the Wasatch Plateau, central Utah (Figure 2.1). The Wasatch Plateau is contiguous with, and crops out approximately perpendicular to the extensively studied Book Cliffs of Utah and Colorado, which have served as the natural outcrop laboratory underpinning sequence stratigraphic concepts in shallow- and marginal-marine settings (e.g., Van Wagoner, 1995; Howell and Flint, 2003). These strata were deposited in the Cretaceous Western Interior Seaway that formed in response to higher sea-level during greenhouse late Cretaceous as a vast epicontinental sea stretching from Alaska to northern Mexico. The Seaway occupied the retro-arc foreland basin formed by subduction-related kinematics of the Farallon Plate (e.g., Liu et al., 2011), and was bordered by the tectonically active highlands of the Sevier orogenic belt in the west and by stable, cratonic lowlands in the east (Kauffman and Caldwell, 1993; DeCelles and Coogan, 2006). The coeval Columbian-Sevier orogeny uplifted areas west of the seaway, and rivers sourced from these highland fold-and-thrust zones dispersed sediments eastward to the Seaway over a source-to-sink distance of over 100 km. This sediment flux resulted in the development of prograding siliciclastic wedges of coastal-plain and shallow-marine deposits that transition eastward into offshore mudstones (e.g., Young, 1955; Hampson, 2010). The combined effect of subduction tectonics, eustasy, and varying sediment supply from the Sevier fold-and-thrust zone principally controlled relative sea-level fluctuations in the Seaway, as reflected in the stratal stacking pattern of shallow-marine sandstones and their intertonguing relationships with offshore shales (Houston et al., 2000; Miall and Arush, 2001; Hampson, 2010).

In comparison to strata exposed in the Book Cliffs, the contemporaneous strata of the Wasatch Plateau are markedly less well documented. The study provides a detailed outcrop characterization of the Cretaceous Blackhawk Formation, Mesaverde Group (Figure 2.2) from part of the outcrop belt exposed in cliff faces in the eastern Wasatch Plateau, which forms a continuous 100-km long escarpment oriented roughly parallel to regional depositional strike. Here, the Blackhawk Formation is mudstone- and coal-prone (proportion of sandstone is c. 10-30% over the outcrop belt; Hampson et al., 2012), and consists of marginal-marine, coastal-plain deposits in its lower part that transition to continental, alluvial-plain deposits in its upper part (e.g., Flores et al., 1984; Dubiel et al., 2000; Adams and Bhattacharya, 2005; Hampson et al., 2012). The studied section belongs to the lower Blackhawk Formation and comprises channelized sandbodies, coastal-plain mudstones, and numerous coal seams.

The Blackhawk Formation extends into subsurface of the Uinta Basin (Figure 2.1) where it has attained burial maturity (Nuccio and Roberts, 2003), and hosts tight-gas reservoirs of the Mesaverde Play System (Johnson and Roberts, 2003). The play comprises discontinuous, low net-to-gross sandstones as reservoir rock and coal as source rock in a coastal-plain depositional setting. The coal quality, sandbody thickness and distribution patterns, and depositional characteristics of the Blackhawk Formation in the study area are similar to those of producing tight-gas reservoirs in the Mesaverde Group in the Piceance Basin, Colorado (Yurewicz et al., 2008). Therefore, the Blackhawk Formation in the study area provides a reservoir analog to tight-gas plays in these two basins.

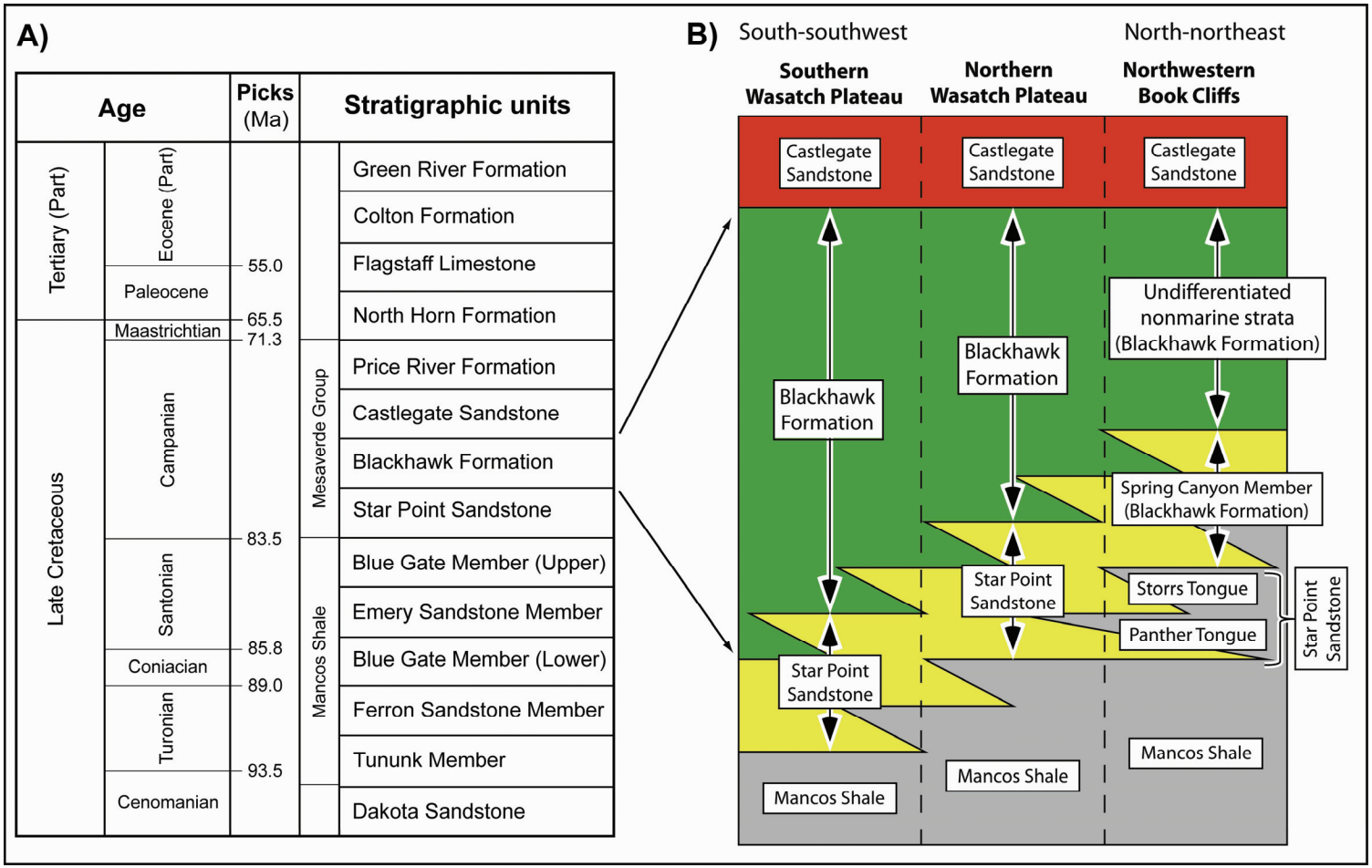

Figure 2.2. A) Stratigraphic succession of the Cretaceous and Tertiary sedimentary rocks in the Wasatch Plateau (modified from Henry and Finn, 2003). B) Lithostratigraphic summary chart of the Blackhawk Formation and surrounding strata in the Wasatch Plateau and northwestern Book Cliffs (from Hampson et al., 2011). The study area lies in the northern Wasatch Plateau (central column). The Blackhawk Formation comprises coastal-plain to alluvial-plain deposits in the study area. Similar deposits form tight-gas reservoirs in the Mesaverde Group in the Uinta-Piceance province (Figure 2.1).

2.3 Dataset and Methodology

Using photomosaics, measured sections, and ground-penetrating radar (GPR) data, a detailed sedimentological investigation was conducted on a single, encompassing outcrop dataset comprising eight contiguous, and vertical cliff faces in Cottonwood Creek, eastern Wasatch Plateau, Utah (Figure 2.3). In combination, these cliff faces crop out a series of depositional-dip and -strike oriented segments with high quality and scales (Figure 2.3). Depositional dip vs. strike orientations were interpreted from paleocurrent analysis (Figure 2.3C). The investigated section belongs to the lower Blackhawk Formation, and is ~100 m thick, ~ 4 km in depositional-dip extent, and ~6 km in depositional-strike extent.

To record the location of collected data, a global positioning system (GPS) of sub-meter accuracy has been used. Sedimentological descriptions, tape measurements, lithological logs, and digital photographs have been used for detailed facies and architectural element analysis. Serial photos covering cliff faces were collected. All photos in each cliff-face were taken serially at the same distance from the cliff face, to ensure scale preservation, and with ~ 30% overlap with adjacent photos, to maintain the continuity of sedimentologic elements during generation of photomosaics. Photomosaics have been constructed by stitching together individual photos in commercially available software ensuring that the correct geometry of sedimentologic elements is maintained with minimal parallax error. Bedding diagrams have been constructed from the photomosaics, documenting the preserved geometry of channelized sandbodies (e.g., apparent thickness and width, truncation relationships) and stratigraphic architecture (e.g., sandbody abundance, horizontal and vertical facies distributions, net-to-gross ratio). Using a high-resolution binocular in the field, all macro- to micro-scale sedimentological structures

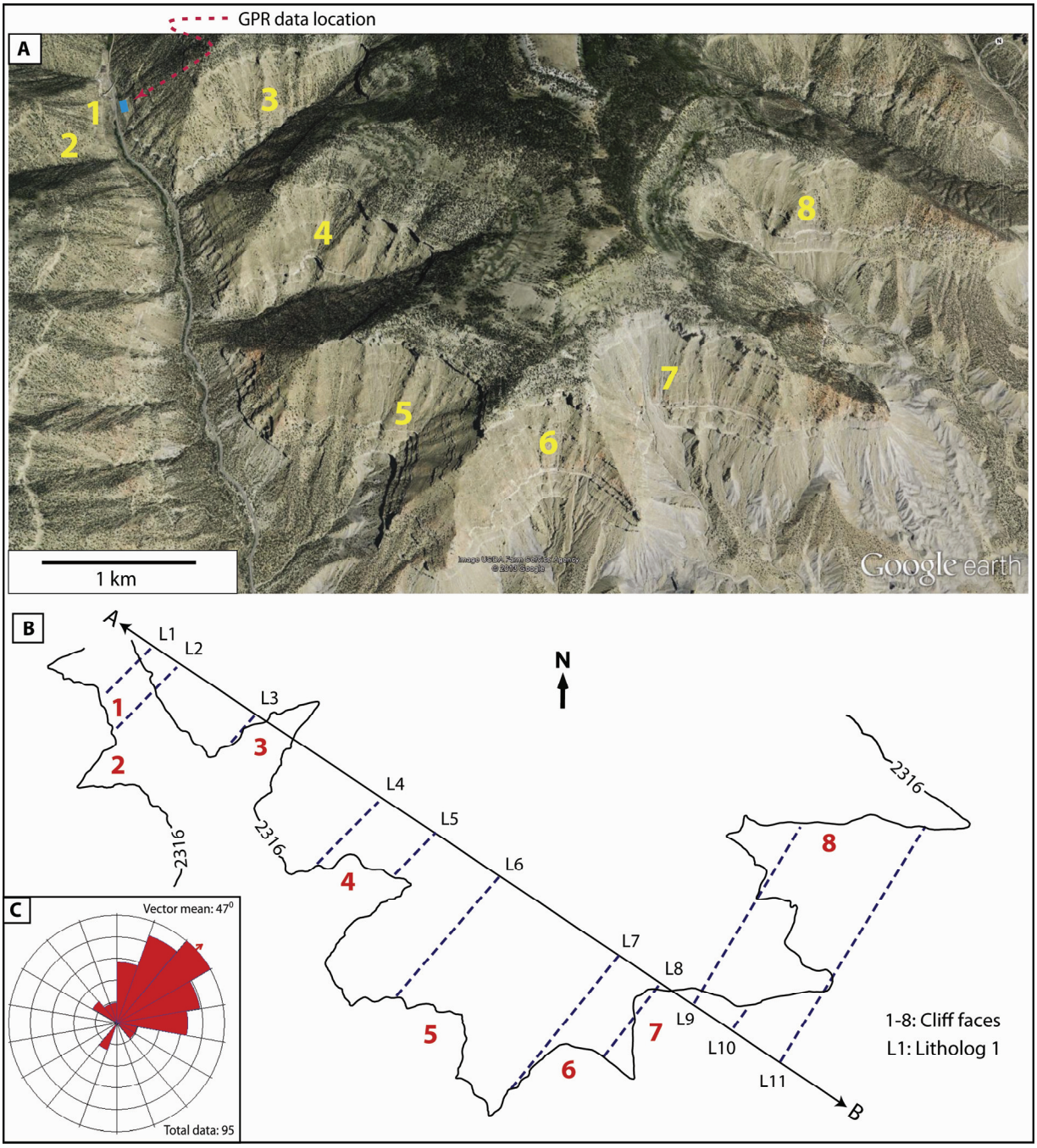

Figure 2.3. A) Studied outcrop dataset comprising eight contiguous, and vertical cliff faces (1-8) (from Google Earth). B) Map view of cliff faces (2316 m contour line is shown for reference). Lithologs (1-11) have been constructed for vertical description of the studied Blackhawk Formation. The line AB has been used as a projection plane for all these lithologs for along-strike correlation used in Figure 2.14. C) Paleocurrent rose diagram for dune and ripple cross-strata of the studied outcrop dataset showing an overall northeast paleoflow direction.

(e.g., barform, dunes, ripples, mud clasts, etc.) have been meticulously populated on their near-accurate spatial position on the bedding-diagram panels. Measured sections (i.e. lithological or lithologs) were generated to document vertical facies distributions, and to calibrate the bedding diagrams (Figure 2.3). Notably, as our dataset adequately comprise a series of both dip- and strike-oriented exposures, for more appropriate lateral dimensional estimates of channel sandbodies and other architectural elements, we have targeted only strike-oriented rather than dip-oriented segments. Hence, we have purposefully avoided lateral dimensional statistics of dip-oriented segments that could have brought spurious quantification inconsistent to paleoflow-constrained estimates. Paleocurrent data have been synthesized in rose diagrams to analyze the overall paleoflow directions.

A GPR survey was conducted on an accessible, relatively flat, and sparsely-vegetated top surface of a channelized sandbody (Figure 2.3) in a rectangular grid pattern (~25 m length; ~10 m width) to record data along both depositional-strike and depositional-dip orientations. For this data acquisition, a shielded 250 MHz antennae mounted on a road cart was pulled by hand on the near-clean, flat exposed surface to minimize artifacts and noise. Topographic data (X, Y, and Z) for the radar profiles were synchronously collected by attaching a GPS of sub-meter accuracy to the survey tool. GPR data were processed to enhance the signal and correct for surface topography, prior to interpretation. Thickness variations of each coal seam (of Axel Anderson coal zone; Sanchez and Brown, 1986, Hampson et al., 2012) were documented at accessible outcrop locations. In addition, subsurface coal thickness data of mining areas behind studied cliff faces have been utilized for channel sandbody vs. coal thickness correlation. For net-to-gross estimation, pseudowells were positioned spanning the entire dataset at ~ 100 m

well spacing. Quantified datasets of channel sandbodies and other architectural elements along with collected GPS readings have been utilized in ArcGIS software to generate geo-referenced, spatial distribution maps.

2.4 Results

Six depositional facies (Table 2.1; Figure 2.4) and five architectural elements (Table 2.2; Figure 2.5) have been recognized in the studied succession (Figure 2.3).

2.4.1 Facies Analysis

Six facies have been recognized in this study (Table 2.1): (1) trough cross-stratified sandstones, (2) parallel-laminated sandstones, (3) thinly interbedded mudstones, siltstones and rippled sandstones, (4) mudstones and siltstones, (5) carbonaceous mudstones, and (6) coal. These facies are characterized and differentiated mainly on the basis of grain size, lithology, and sedimentary structures. Measured sections (e.g., lithologs 1 to 11 in Figure 2.3) provide vertical description of these facies.

Trough cross-stratified sandstones (facies 1) are mostly medium-grained, and contain predominantly (>90%) trough cross-beds resulting from the migration of dune-scale bedforms with minor (<10%) current-ripple cross-lamination (Figures 2.4A, B). Mostly, ripple cross-laminations occur towards the upper part of this facies. Cross-stratification sets range from 10 to 50 cm in thickness and are commonly stacked vertically into cosets. The facies is characterized by erosional bases, which exhibit curved, concave-upward geometries at some

Table 2.1 Facies recognized in the lower Blackhawk Formation in the Cottonwood Creek outcrops.

Facies	Lithofacies description	Figure	Depositional Process
Facies 1: trough cross-stratified sandstones	Medium-grained; trough cross-stratification with 10-50 cm set thickness; subordinate ripple cross-lamination towards top part when grain size grades to fine to very fine; erosional bases with rip-up clasts; scattered mud-clasts throughout; soft-sediment deformation (i.e. convolued bedding up to ~ 2m) with outsized clasts (up to ~ 10 cm) at some locations.	2.4A & 2.4B	Migration of sandy dunes and ripples in response to unidirectional flow.
Facies 2: parallel-laminated sandstones	Parallel-laminated, fine-grained sandstones; bed thickness of 0.1-1 m; commonly intercalated within mudstones and siltstones (facies 4).	2.4C	Deposition under upper-plane bed conditions during high-stage flooding events in nearby channels.
Facies 3: thinly interbedded mudstones, siltstones and rippled sandstones	Interbedded mudstones, siltstones and very fine- to fine-grained, rippled sandstones; subordinate parallel lamination in sandstones.	2.4D	Episodic fluctuations in flow velocity and sand supply.
Facies 4: mudstones and siltstones	Mudstones to sandy siltstones; dirty-white to light-gray color; massive to fissile.	2.4E	Suspension settling in floodplains during waning flooding stage.
Facies 5: carbonaceous mudstones	Organic-rich mudstones with leaf impressions and plant debris; root-penetrated (root height up to ~ 20 cm) at some locations; intertonguing with coal (facies 6).	2.4E	Vegetated muddy environment; high organic content indicates poorly oxygenated environment; root-penetration indicates plant colonization on floodplain.
Facies 6: coal	Coal seams (~1-2 m thick, traceable for ~ 0.5 km laterally), intertonguing with carbonaceous mudstones (facies 5); *Teredolites* burrows at some locations.	2.4F	Peat preservation in coastal-plain environments; episodic marine influence.

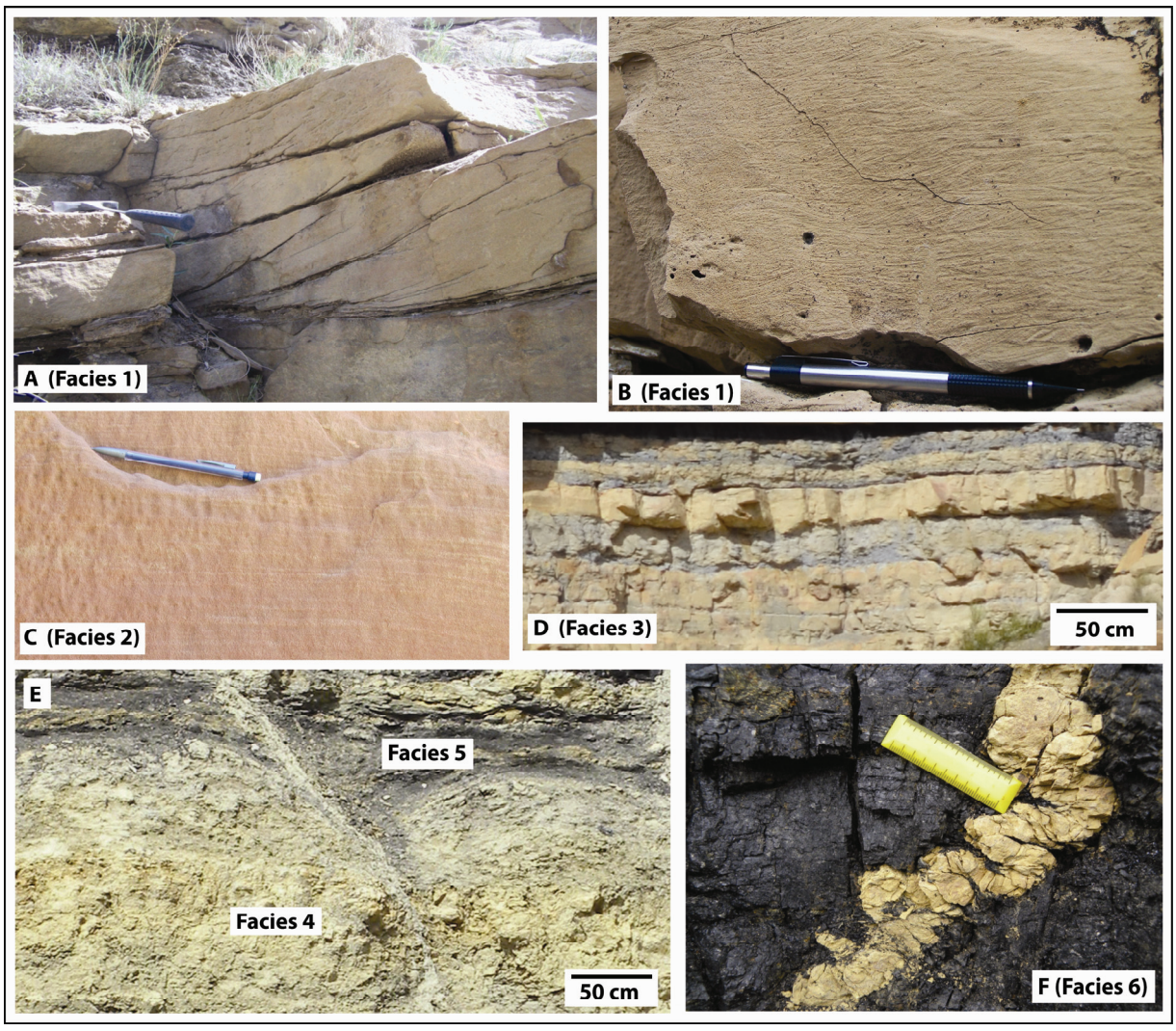

Figure 2.4. Representative photos of facies in the lower Blackhawk Formation at Cottonwood Creek (Table 2.1). A, B) Facies 1: trough cross-stratified sandstones (A) with subordinate current-ripple cross-lamination (B). C) Facies 2: parallel-laminated sandstone. D) Facies 3: heterolithic deposit comprising thinly interbedded mudstones, siltstones and rippled sandstones. E) Facies 4 (mudstones and siltstones) and facies 5 (carbonaceous mudstones). F) Facies 6: Coal seam showing highly compacted and ptygmatically folded burrow. Scale bar is 5 cm long. A high compaction factor (at least 10) was calculated for coal-precursor peat by restoring the burrow to its original shape, which was assumed to be gently sinusoidal.

locations, and a progressively fining-upward grain-size trend. A few numbers of sole marks have been found at the erosional bases. Rip-up mudclasts are common and scattered throughout sandbodies, but unusually large clasts (up to ~ 10 cm in diameter) occur locally within convoluted patches. Dune and ripple data shows unimodal paleocurrent distribution (Figure 2.3C). The cross-stratified sandstones are interpreted to be deposited by migration of dunes and ripple bedforms in response to unidirectional currents. The facies shows a good correspondence between grain-size and bedform types. For example, dune-scale cross-strata are present in medium-grained sandstones whereas ripple-scale cross-laminations occupy fine-grained sandstones usually towards the top of a sandbody. Cross-stratification arrangement from set to coset indicates superposition of migrating dunes. Localized presence of large clasts with convolution indicates deposition due to soft-sediment deformation likely related to liquefaction process (e.g., Owen, 1986). In combination, trough cross-stratified sandstones are predominant facies in the studied sections (e.g., Figures 2.6-2.8).

Parallel-laminated, fine-grained sandstones (facies 2) are encased within mudstones (facies 4) (Figure 2.4C). This facies (facies 2) forms thin (~ 0.1-1 m thick), but laterally persistent sheets that occur at the margins of channelized bodies of trough cross-stratified sandstone (facies 1). Mud rip-up clasts are rarely present. Parallel-lamination within the sheet bodies is attributed to deposition under upper-plane bed conditions during high-stage flooding events in nearby channels. They form only a small proportion on outcrop panels (Figures 2.6, 2.7), but more distinct proportion on Figure 2.8.

Thinly interbedded mudstones, siltstones, and rippled sandstones (facies 3) represent a heterolithic deposition wherein bed-scale thickness variation is distinct laterally. Rippled-

sandstones are sheet-type and fine-grained. Intercalated mudstones and siltstones are generally structureless to crudely planar-bedded (Figure 2.4D). This facies grades laterally into mudstones (facies 4) in floodplain area. The thinly interbedded mudstones, siltstones, and rippled sandstones record floodplain deposition in response to episodic fluctuations in flow velocity and sand supply during flooding events.

Mudstones and siltstones (facies 4) are massive and show nodular to fissile weathering features. Rootings and pedogenesis were observed locally. This facies records suspension fall-out deposition of unconfined flows in floodplain area during waning stage of flooding events adjacent to main channels. The facies is pervasive in outcrop panels (Figures 2.6-2.8).

Carbonaceous mudstones (facies 5) are gray to light black in color, and marked by abundant plant material and leaf impressions (Figure 2.4E). Localized root penetration (up to ~ 20 cm) is visible in places, indicating plant colonization. Hence, this facies was likely developed in a partly subaerial, highly vegetated floodplain environment. Carbonaceous mudstones appear adjacent to and interbedded with coal (facies 6) on outcrop panels that implies its deposition in swampy conditions similar to those for coals.

Coal (facies 6) is distinct, easily recognized (Figure 2.4F) and appears as numerous individual seams (~ 1-2 m thick) showing as much lateral-continuity (up to ~ 500 m) on outcrop panels (Figures 2.6, 2.7). In places, coal beds have been moderately bioturbated (BI = ~ 2), showing *Teredolites* burrows at the base of coal seams. The accumulation of coal, notably in the lower Blackhawk Formation, has been attributed to favorable peat preservation in a swampy environment during periods of clastic sediment starvation (Flores et al., 1984). Although coal constitutes a small proportion of the outcrop data (Figure 2.3), its presence is significant for

stratigraphic correlation and stratal subdivision of the Blackhawk Formation in the Wasatch Plateau (e.g., Flores et al., 1984; Dubiel et al., 2000; Hampson et al., 2012).

2.4.2 Architectural Element Analysis

Hierarchy of architectural units is represented by bounding-surface relationships which range in spatial scale from ripple-scale cross-stratification sets (1^{st} order), dune-scale cross-stratification sets (2^{nd} order), bar-accretion increment (3^{rd} order), individual bar macroform (4^{th} order), channel storey (5^{th} order), channel belt (6^{th} order), to channel-belt complex (7^{th} order) (e.g., Miall, 1988). We illustrate this hierarchical arrangement through detailed documentation of bounding surfaces and architectural elements on cliff-face photomosaics (Figures 2.6-2.8). We also evaluate external and internal geometry, and dimensions and facies composition of architectural elements. Five architectural elements have been recognized on the outcrop panels (Table 2.2): (A) channel, (B) bar-accretion macroform, (C) overbank fines, (D) crevasse delta, and (E) overbank and crevasse splays.

A: Channel (Figure 2.5A)

Channel-fill sandbodies are typically 1-17 m thick, medium-grained, and white to light-brown colored. They comprise facies 1 (Table 2.1, Figure 2.5A), and are commonly found laterally adjacent to coeval bar deposits (architectural element B) and overbank fines

Table 2.2. Architectural elements of the lower Blackhawk Formation in the Cottonwood Creek outcrops.

Architectural elements	Description	Figure	Facies assemblage
A: Channel	Lens or sheet geometry; concave-up, erosional basal surface with rip-up clasts indicating thalweg scouring and filling; fining-upward succession with gradational top; dominated by trough cross-stratification with ~ 10-50 cm set thickness with minor ripple-scale cross-lamination; localized, scattered mud-clasts throughout channel bodies.	2.5A	Facies 1
B: Bar-accretion macroform	Wedge or sheet geometry; distinct development of lateral accretion surfaces dipping ~ 6-11˚, mostly oblique or nearly perpendicular to mean paleocurrent direction; dominated by dune-scale cross-stratification with minor ripple-scale cross-lamination; incremental and persistent bar growth on inner bank of sinuous channel produced laterally extensive sandstone sheet.	2.5B	Facies 1
C: Overbank fines	Thin to thick blanket geometry; fine-grained deposition on floodplain during flooding events and commonly intercalated with thin sandstone beds (architectural element E); contains carbonaceous shale and coal at specific horizons where peat was accumulated and preserved.	2.5A	Facies 3-6
D: Crevasse delta	Heterolithic coarsening-upward unit (~7 m thick, ~50 m wide) developed as delta lobe due to progradation of successive crevasse splays on to floodplain during high energy flooding events; individual beds form clinoforms (dip <10˚) in which grain size decreases with increasing distance from channel.	2.5C	Facies 2-3
E: Overbank and Crevasse splays	Isolated, thin (0.1-1 m thick), ribbon to sheet (10s-100s m lateral extent), nearly horizontal sandstone beds or thicker (0.7-3.9 m), lenticular (2-65 m) sandstone beds deposited on floodplain during high-stage flow events; commonly interbedded with overbank fines (architectural element C).	2.5D	Facies 2-3

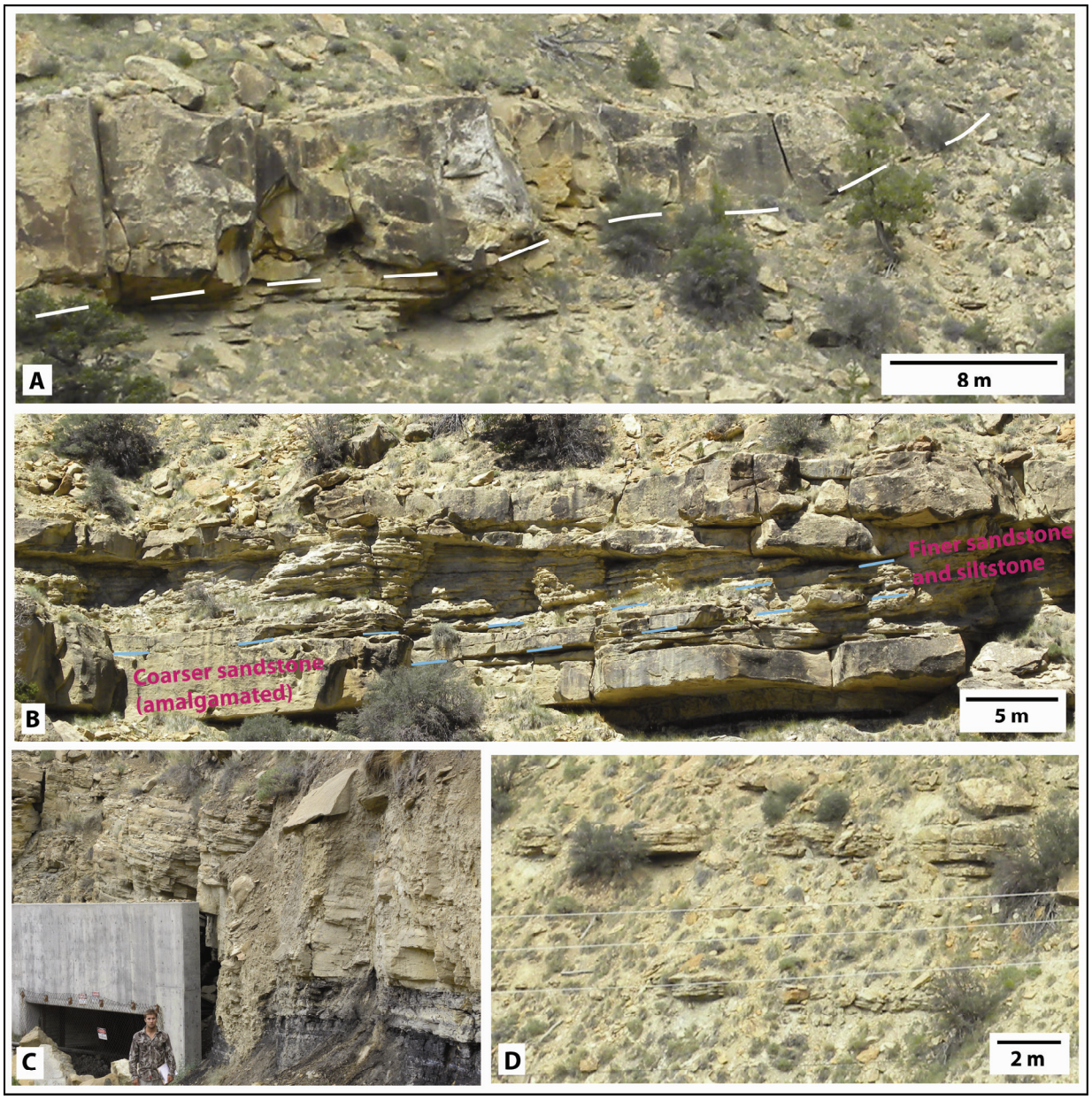

Figure 2.5. Representative photos of architectural elements in the lower Blackhawk Formation at Cottonwood Creek (Table 2.2). A) Channel element (architectural element A) encased within overbank fines, and overbank and crevasse splays (architectural elements C and E, respectively). B) Bar-accretion macroform (architectural element B) with distinct development of inclined lateral accretion-strata, which shows individual beds are amalgamated and coarser-grained downdip that gradually transitions updip to finer sandstones and siltsones. This is a product of helical turn of the paleochannel flow at the meander loop. C) Crevasse delta (architectural element D) developed as prograding clinoformal package (dipping to the right) underlain and overlain by overbank fines (architectural element C). D) Overbank and crevasse splays (architectural element E) developed as package of stacked, thin, parallel-laminated sandstone beds encased in overbank fines (architectural element C).

(architectural element C). Sedimentary structures include dune-scale trough cross-stratification with set thickness ranging from 10 cm to 50 cm, and subordinate ripple cross-lamination that principally occurs towards channel-fill tops and defines a fining-upward trend. Channel bases are commonly concave-upward erosional surfaces lined by discontinuous lags of mud rip-up clasts. Mud clasts are also scattered throughout channel-fill sandbodies.

Channel elements represent the fills of formative rivers. The medium-sand grain size and predominance of dune-scale cross-stratification indicates that the paleochannels had a modest stream competency. To estimate water depths of paleorivers from dune cross-set thickness data, methods of Bridge and Tye (2000), Leclair and Bridge (2001), and Bhattacharya and Tye (2004) have been pursued. From the compiled dune cross-set thickness data (ranges from 10 to 50 cm), mean cross-set thickness (s_m) and standard deviation (s_{sd}) were calculated. When s_m/s_{sd} is ~ 0.88, average dune height h_m was estimated using equation (Bridge and Tye 2000; Bridge 2003):

$$h_m = 5.3\,\beta + 0.001\beta^2 \quad (\text{where } \beta \approx s_m/1.8)$$

As the flow-depth scales to 6-10 times of average dune height (Allen 1984; Bridge and Tye 2000; Leclair and Bridge, 2001; Li et al., 2010), the water depths of paleorivers were estimated as ~ 2-15 m which provides a good correspondence to measured thickness (1-17 m) of channel sandbodies on outcrop data (e.g., Figures 2.6-2.8). The overall paleoflow direction recorded by dune-scale cross-bedding, ripple-scale cross-lamination, bar-accretion bedding, and sole marks

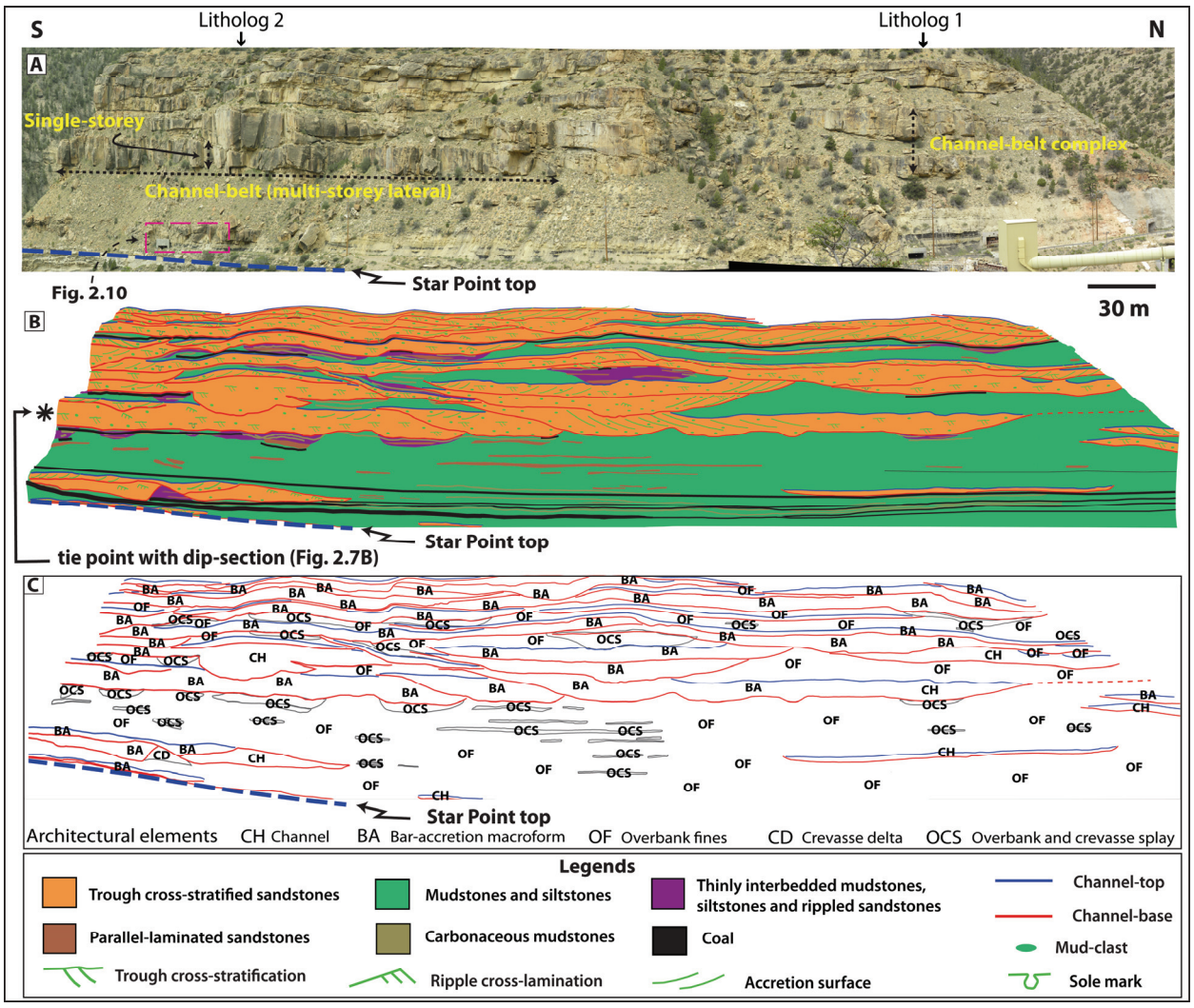

Figure 2.6. A) Photomosaic of cliff face 1 (Figure 2.3), which is oriented along depositional-strike (i.e. perpendicular to paleoflow). B, C) Line drawings of interpreted facies distributions (B) and architectural elements (C) of this photomosaic that demonstrates decreases in net-to-gross ratio and channel-sandbody amalgamation from left (south) to right (north). Marked measured sections (Lithologs 1 and 2) provide vertical facies descriptions for the contrasting sandbody stacking patterns in two locations along the cliff face. A coal seam near the base of the panel thins from left (1.8 m) to right (1 m).

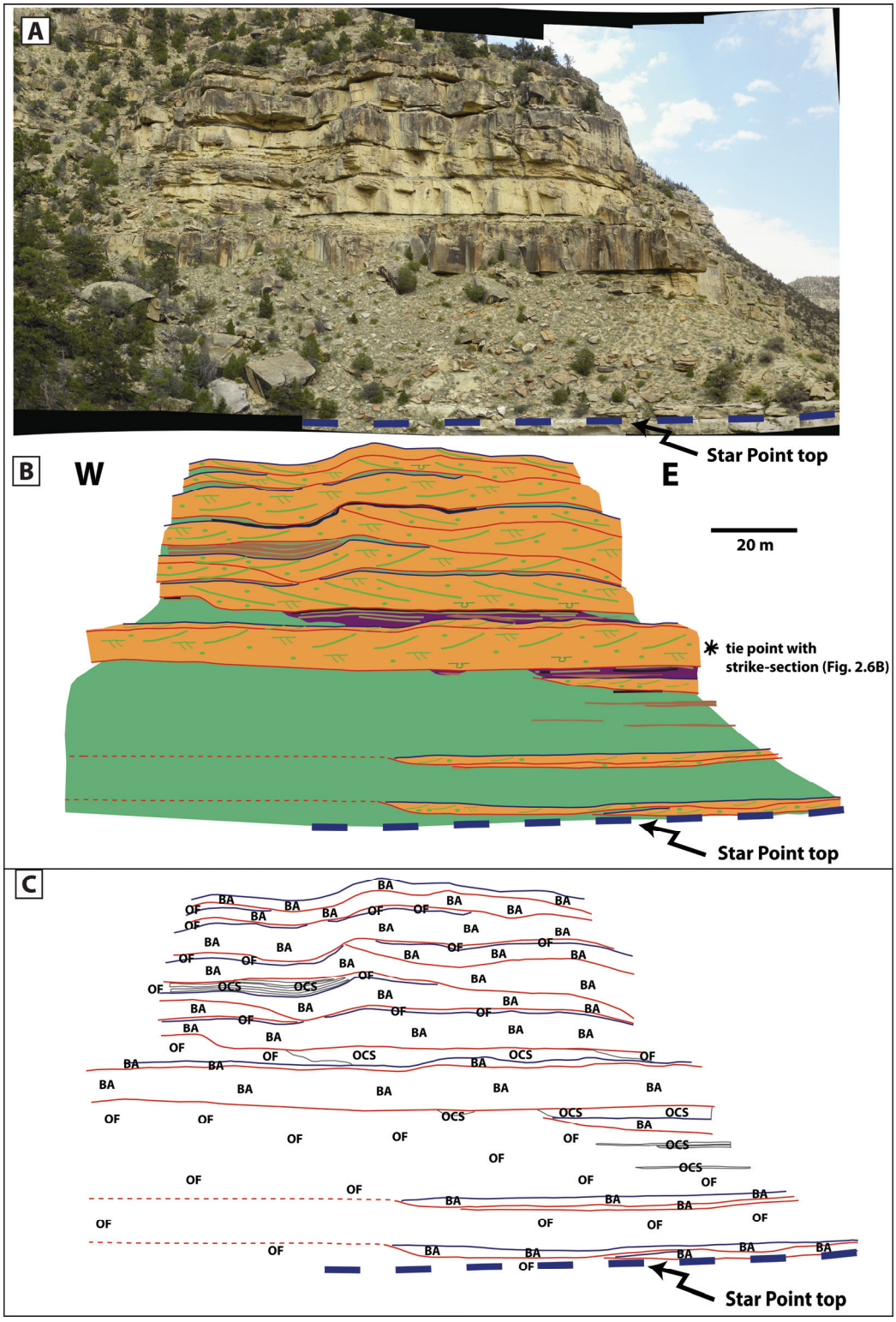

Figure 2.7. A) Photomosaic of cliff face 2 (Figure 2.3), which is oriented along depositional-dip (i.e parallel to paleoflow). B, C) Line drawings of interpreted facies distributions (B) and architectural elements of this photomosaic (C). Note increase in channel-sandbody amalgamation towards the right (east), at the junction with strike-oriented panel (Figure 2.6). For legend, see Figure 2.6.

was towards northeast (Figure 2.3C), which broadly matches to documented regional paleoflow trend of the area (e.g., Kamola and Van Wagoner, 1995; Hampson et al., 2012).

B: Bar-accretion macroform (Figure 2.5B)

Bar deposits comprising accretion units are distinctly developed and abundant on outcrop panels (e.g., Figures 2.6-2.8). Locally, they pass laterally to adjacent, coeval channel-fill sandbodies or overbank fines (architectural elements A and C, respectively). Individual bar-accretion elements range in thickness from 2 m to 15 m, but appear as laterally continuous, sheet sandbodies on the outcrop panels (e.g., Figures 2.6-2.8), as a result of continuous accretion increments. Internally these elements comprise facies 1 (Table 2.1, Figure 2.4A-B), and show predominantly trough cross-stratification with subordinate ripple cross-lamination. Their basal surfaces are erosional (Figures 2.6-2.9), whereas their top surfaces are relatively gradational. Accretion surfaces dip gently (6-11˚, calculated from both outcrop and GPR data; Figures 2.6-2.9) in directions mostly oblique or nearly perpendicular to mean paleocurrent flow.

Upward-fining, bar-accretion macroform elements are formed by deposition on the inner bend of sinuous channel reaches (Allen 1963, 1970). Dip directions of accretion beds that are nearly perpendicular to mean paleoflow direction indicates a greater lateral than downstream component of accretion development. Their abundance in the study area attributes to sinuous, and possibly meandering (sinuosity >1.5), nature of individual channels that developed point-

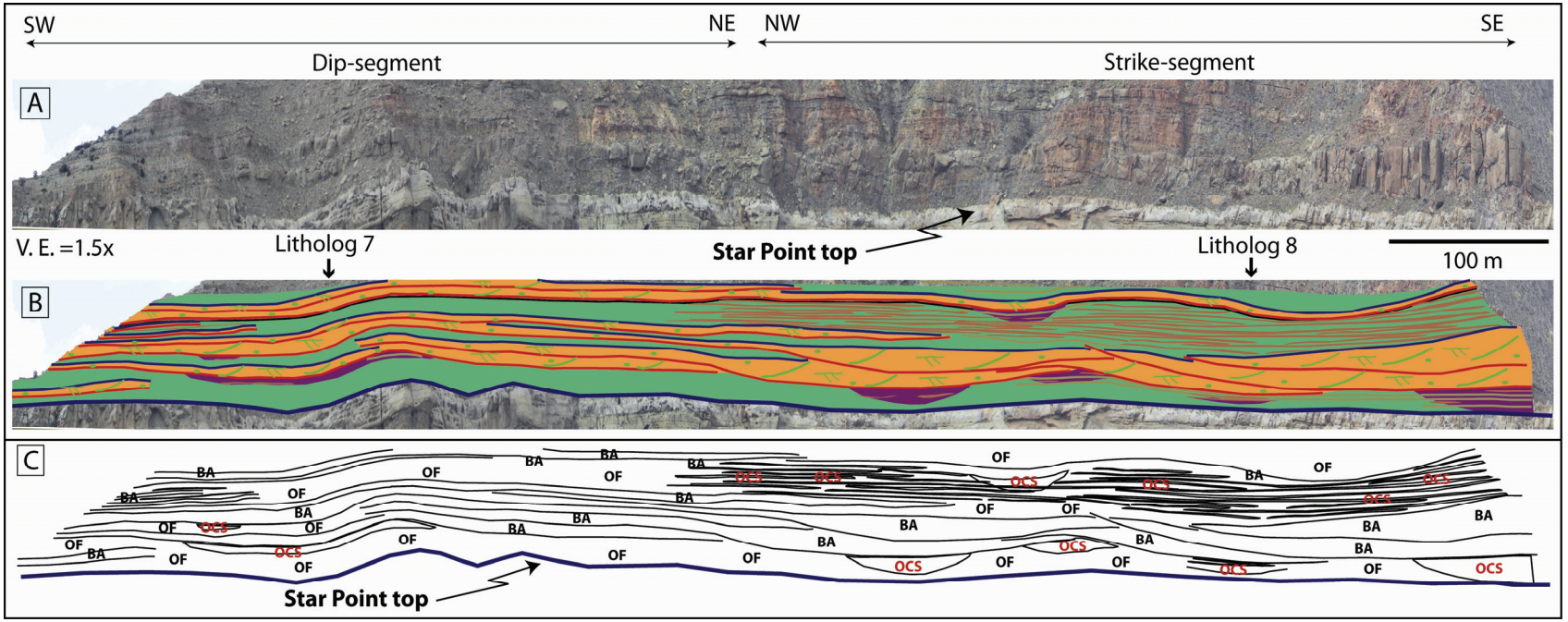

Figure 2.8. A) Photomosaic of cliff face 6 (Figure 2.3), which comprises both depositional-dip- and –strike-oriented segments. B, C) Line drawings of interpreted facies distributions (B) and architectural elements of this photomosaic (C). For legend, see Figure 2.6.

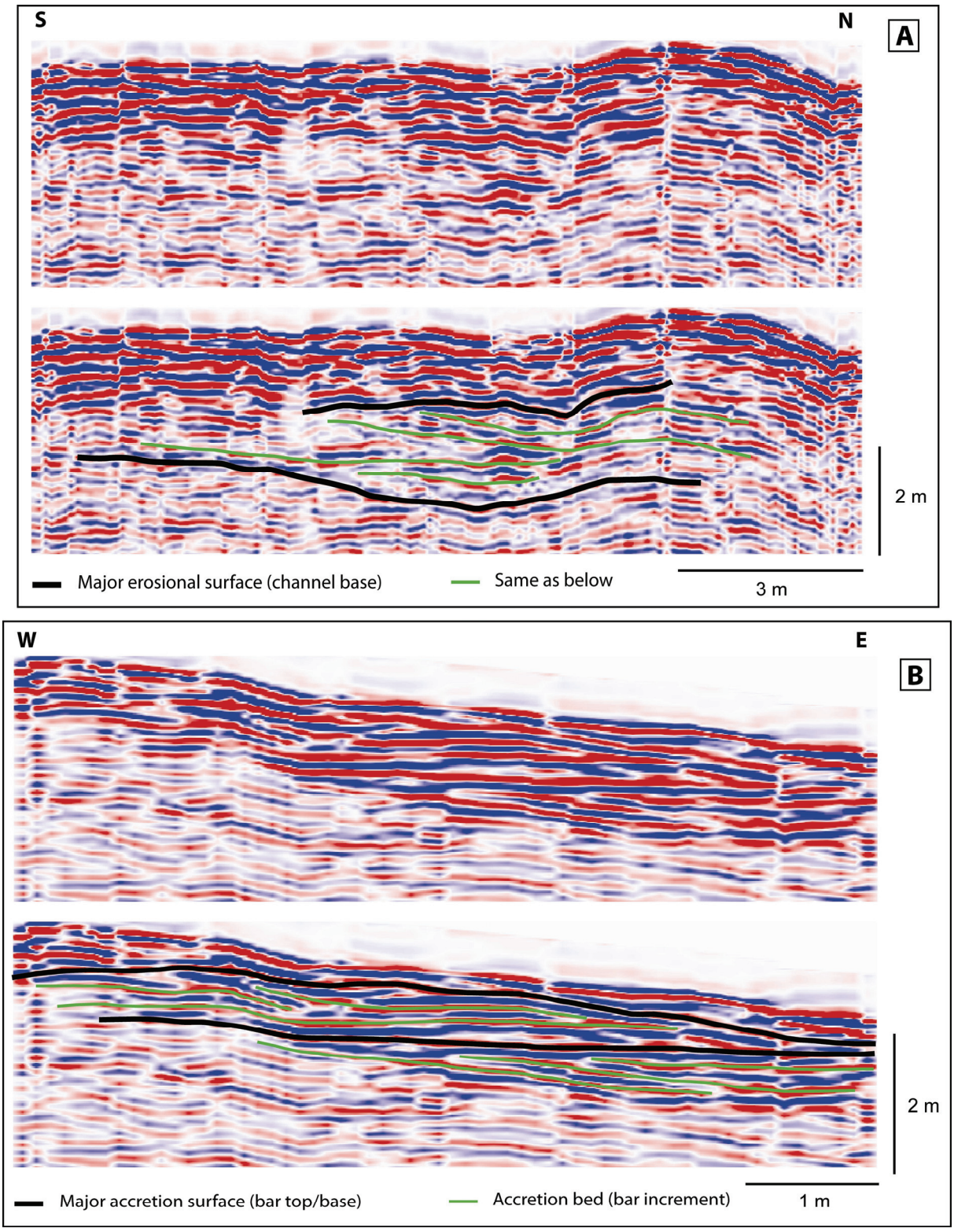

Figure 2.9. Representative GPR sections (250 MHz frequency) revealing the geometry of bar-accretion macroforms (architectural element B) within a stratigraphically-equivalent channelized-sandbody across cliff face 1 (Figure 2.3A). A) Un-interpreted (upper) and interpreted (lower) GPR section showing

erosional channelized-sandbody base and onlapping bar deposits in depositional-strike orientation. B) Un-interpreted (upper) and interpreted (lower) GPR section showing lateral accretion surfaces within bar-accretion macroforms (architectural element B) in the same channelized-sandbody in depositional-dip orientation.

bar deposits on their inner banks. To estimate the sinuosity of paleorivers, we have used the method of Schumm (1972):

$$P = 3.5 * (W / D)^{-0.27}$$

Where P = sinuosity, W = bankfull channel width, D = bankfull channel depth

Using this relationship, moderate-to-high sinuosity values (~ 1.5-1.7) have been estimated for the paleorivers.

C: Overbank fines (Figure 2.5A)

Overbank fines comprise mostly mudstones and siltstones (facies 4; Table 2.1, Figure 2.4E), carbonaceous mudstones (facies 5; Table 2.1, Figure 2.4E) and coal (facies 6; Table 2.1, Figure 2.4F). Mudstones are pervasive, and carbonaceous mudstones and coals occur at distinct stratigraphic levels. Overbank fines were probably deposited on the floodplain during the waning stage of flooding events or during channel avulsion (e.g., Smith et al., 1989). The occurrence of laterally continuous coal seams of moderate thickness (~ 1-2 m) suggests favorable conditions for accumulation and preservation of peat, as a result of a high water table and clastic sediment starvation (Bohacs and Suter, 1997). Overbank fines element occurred as laterally continuous thick to thin sheet-type deposits as well as patchy, discontinuous deposits as it was eroded away laterally by channel and bar elements.

D: Crevasse delta (Figure 2.5C)

A coarsening-upward, lenticular, and heterolithic unit (c. 7 m thick, ~ 50 m wide), containing distinct clinoformal beds (<10˚ dip), shows a lateral facies change from proximal, ripple-laminated sandstones to distal, silty mudstones (Figure 2.10). Sandstones in the package are fine-grained, parallel-laminated, and contain abundant plant debris (facies 2; Table 2.1, Figure 2.4C). Individual sandstone beds intertongue with siltstones, mudstones and carbonaceous mudstones (facies 3; Table 2.1, Figure 2.4D). The package is overlain by channel-fill and bar-accretion elements (architectural elements A and B, respectively) (Figure 2.10).

The heterolithic, convex-upward, and coarsening-upward unit is interpreted as crevasse delta deposit that developed on the floodplain due to rapid deceleration in flow velocity through a breached levee and on to the floodplain, where flow was poorly confined and dissipated as a jet (Allen, 1965; Kraus, 1987). The stacking of multiple clinoformal sandstone beds into a clinoform set demonstrates delta buildup via repeated, episodic flow events that are separated by waning-flow mudstones. The proximal delta, being adjacent to the source channel, shows high energy deposition and thus coarser grain size (Litholog 1 of Figure 2.10), whereas the distal delta is finer grained and contains more mud content and plant debris, consistent with deposition further from the channel (Litholog 3 of Figure 2.10). The measured thickness (c. 7 m) and width (~ 50 m) of this architectural element refers only to its minimum preserved dimensions, as the element has been eroded by an overlying channelized sandbody (Figure 2.10).

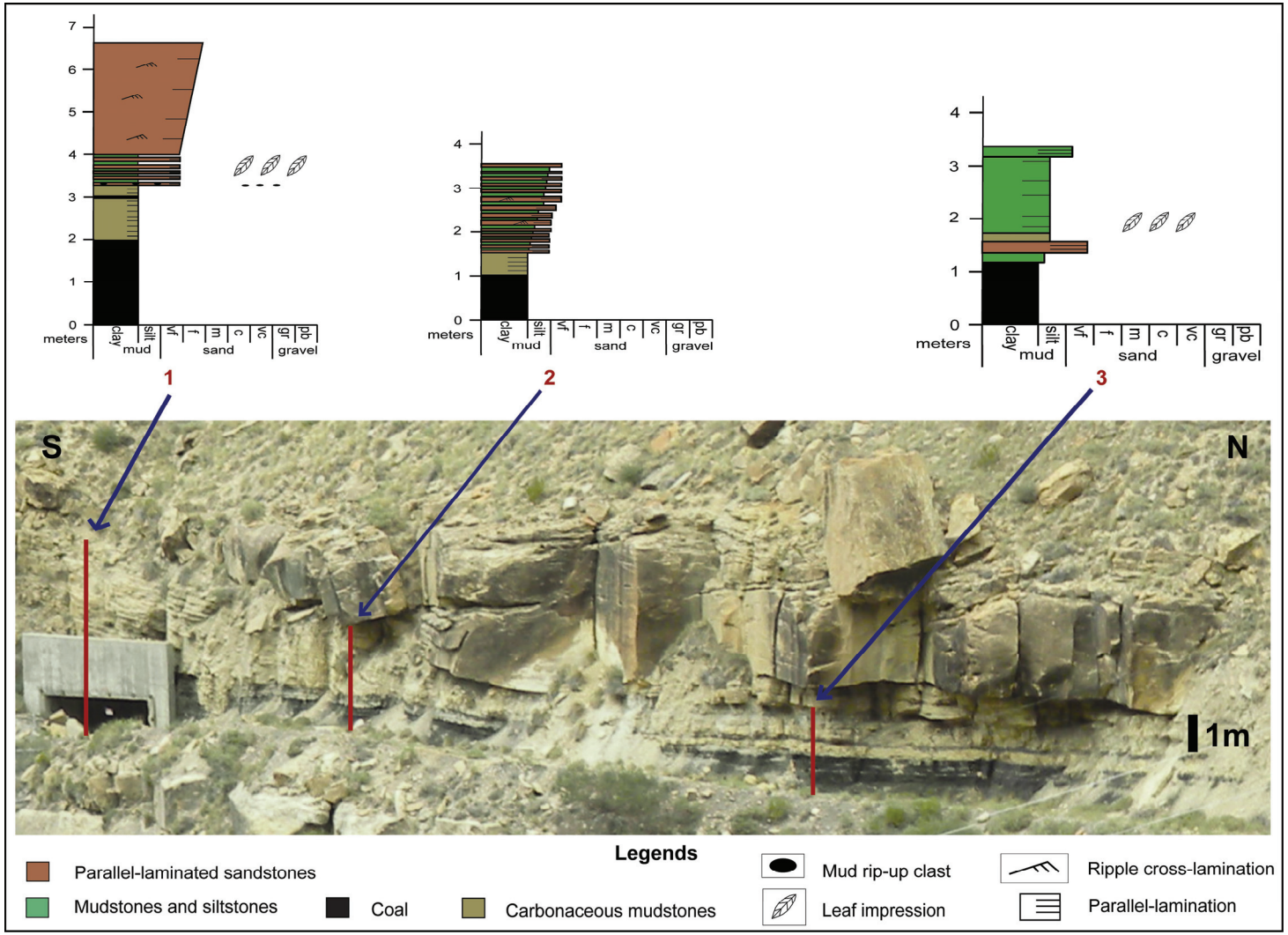

Figure 2.10. Photo of crevasse delta (architectural element D) containing distinct clinoforms, erosionally truncated by an overlying channelized sandbody. The delta is represented by a heterolithic, coarsening-upward succession in measured sections 1 and 2 that laterally transitions to overbank fines (architectural element C) in measured section 3. The photo is located in Figure 2.6A.

E: Overbank and crevasse splays (Figure 2.5D)

This architectural element is composed of both overbank and crevasse splays deposits. Overbank splays occur as thin (0.1-1 m), isolated sandbodies that extend laterally over tens to hundreds of meters. Overbank splay sandstone beds have ribbon and sheet geometries, and comprise parallel-laminated, nearly horizontal-bedded, fine-grained sandstones and siltstones (Facies 2; Table 2.1, Figure 2.4C) that lack basal erosional relief. The overbank splay sandstone beds are gradational with overbank fines (architectural element C).

In contrast, crevasse splay deposits, comprised of both parallel-laminated sandstones (Facies 2; Table 2.1), and thinly interbedded mudstones, siltstones and rippled sandstones (Facies 3; Table 2.1), show a lenticular cross-sectional geometry, notably in strike-oriented sections (e.g., Figures 2.6, 2.8), and characteristic lateral and vertical grain-size trends. They comprise fine-grained sandstones proximal to the source channel that gradually pass distally into siltstones and mudstones. Individual bed commonly forms a fining upward trend, but successive beds stacked vertically, usually form coarsening-upward successions with erosional basal surfaces in proximal locations that become gradational at more distal locations. These coarsening-upward packages have thicknesses of ~0.7-9.5 m and lateral extents of ~2-131 m (Figure 2.11). They lack the clinoforms that characterize crevasse delta (architectural element D; Figure 2.10).

The thin, sheet-sandstone beds interpreted as overbank splay deposits were formed when sediment-laden floodwaters from main river channel spilled into the adjoining floodplain during high-stage flooding events, without breaching the channel levee. The ribbon to sheet geometry of these beds, with their high aspect ratios (i.e. width/thickness) is suggestive of relatively low-

energy sand influx to the floodplain, consistent with the interpretation of overbank splays. In contrast, when excess discharge during flooding events breached the channel levee, crevasse splay deposits characterized by proximal scour, high-energy flow, and tapering lens and wedge geometries accumulated on the floodplain. The absence of clinoformal geometries within crevasse splay successions suggests a lack of repeated clastic influx via the same route to topographically low basins on the floodplain, which implies that crevasse splay networks were isolated and short-lived.

2.4.3 Lithologic Heterogeneity

A significant challenge in characterization and modeling of fluvial reservoirs is presented by the various scales of heterogeneity that exist between and within fluvial depositional elements (Jackson, 1977; Miall, 1988; Willis, 1989; Sharp et al., 2003). These heterogeneities constrain the distribution of, and contrasts between lithologic and petrophysical properties in inter-well volumes, and hence, their evaluation is critical to channelized reservoir connectivity and producibility (Richardson et al., 1978; Lasseter et al., 1986; Tyler and Finley, 1991; Hartkamp-Bakker and Donselaar, 1993; Larue and Hovadik, 2006; Pranter and Sommer, 2011). Below we assess the length scales and organization of heterogeneity in the studied outcrop analog.

Large-scale heterogeneity (10's of m vertically, 100's of m laterally)

Large-scale heterogeneity pertains to the spatial distribution of channelized fluvial sandbodies encased within fine-grained coastal-plain deposits. For representative field-validation, we

target cliff faces 1, 2, and 6 (Figures 2.3, 2.6-2.8) where these channelized sandbodies (thickness range: 1-17 m, and width range: 29-724 m; Figure 2.11B) exhibit internal organizations that define: 1) single-storey channel bodies, 2) channel-belts, and 3) channel-belt complexes (Figures 2.6-2.8). A single lateral-accretion bar macroform (architectural element B) combined with a laterally adjacent channel-fill deposit (architectural element A) constitutes a single-storey channel body (~ 1-11 m thick and ~ 50-300 m wide; Figures 2.6, 2.7) (sensu, Friend et al., 1979). Discrete bar-macroform deposits that are laterally stacked together at the same stratigraphic level comprise a channel-belt (~ 15 m thick and ~ 230 m wide; Figures 2.6, 2.7), which typically appears as a laterally-amalgamated sandstone sheet in the outcrop panels (Figures 2.6-2.8). Each channel-belt is produced by lateral swing and sweep of an individual channel (Pettijohn et al., 1972). Vertical superposition of channel-belts results in the development of channel-belt complexes (~ 25 m thick and ~ 270 m wide; Figures 1.6, 1.7). Channel-belts and channel-belt complexes are composite sandbodies formed by lateral and vertical amalgamation, respectively, and are thus associated with the development of relatively thick, well-connected sandstones. They represent the dominant portion of sandbodies on outcrop panels (Figures 2.6-2.8), although their proportions and connectedness vary laterally and vertically. Local vertical amalgamation of individual sandbodies is associated with an increase in the net sandstone thickness (e.g., in the southeastern part of cliff faces 1 and 2, towards the left side of Figure 2.6 and the right side of Figure 2.7), whereas lateral

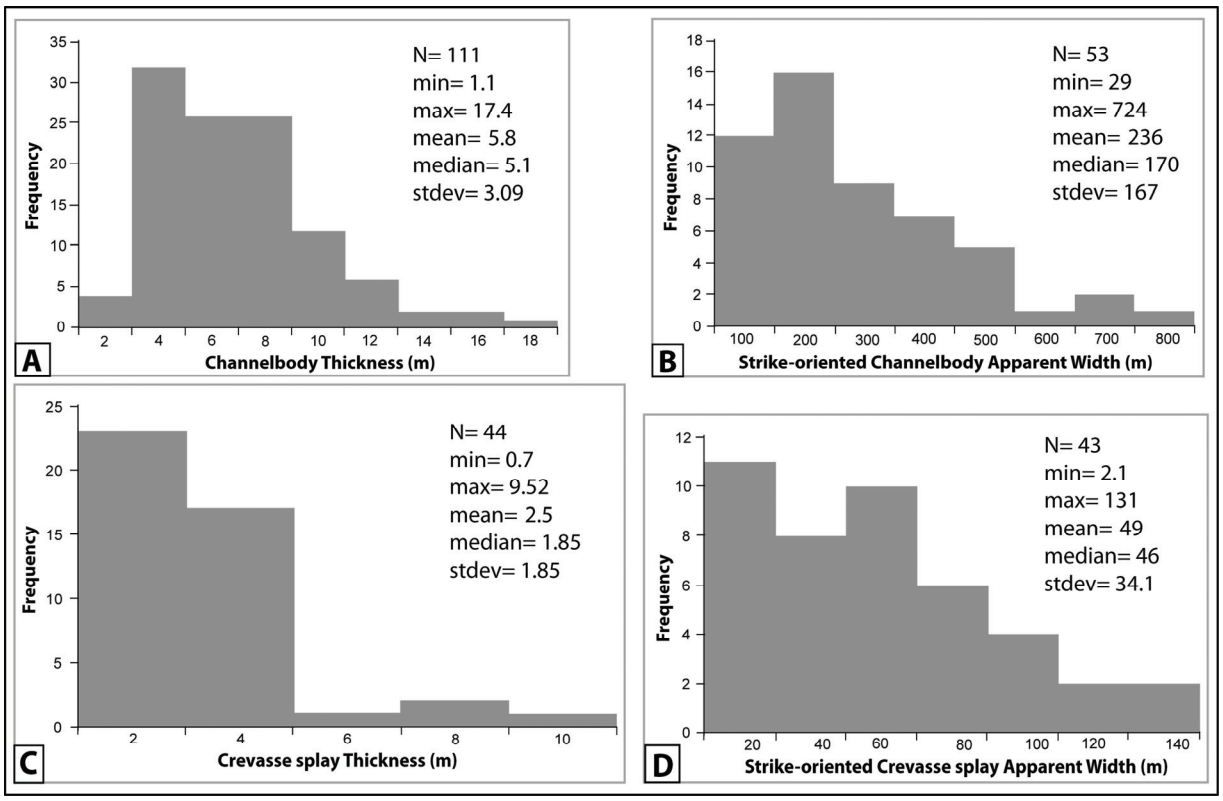

Figure 2.11. Frequency histograms for the dimensions of channelized fluvial sandbodies (composed of architectural elements A and B; Table 2) and crevasse splay sandbodies (architectural element E; Table 2) as measured from studied outcrop data (Figure 3): A) thickness and B) apparent width of preserved channelized fluvial sandbodies; C) thickness and D) apparent width of crevasse splay sandbodies. Many channelized sandbodies are truncated by erosion at their tops, resulting in a decrease in their preserved thickness (Figure 2.10).

amalgamation results in increased sandbody widths (Figures 2.6, 2.7). Lateral trends in channelized sandbody amalgamation in the study area can be related to changes in the thickness of underlying coal seams, as explained below.

Thickness variations in coals and overlying sandstones:

Field documentation on cliff faces 1 and 2 (Figures 2.6, 2.7) demonstrates a general positive correlation between coal thickness and the thickness of overlying sandstones, in the form of

amalgamated channelized sandbodies. Compaction of coal-precursor peat can profoundly affect the subsidence patterns and thus accommodation available for fluvial sedimentation (e.g., Hunt et al., 1996; Hofmann et al., 2011), because peat compacts soon after deposition by a factor of 10 or more (e.g., Ryer and Langer, 1980). Along cliff face 1 (Figure 2.3), the coal seam at the base of the studied startigraphic interval (Axel Anderson coal zone; Sanchez and Brown, 1986) varies in thickness by ~ 1 m (Figure 2.6). The outcrop panel along this cliff face shows that channelized sandbodies are amalgamated above thicker coal sections, but isolated in areas overlying thinner coal sections (Figures 2.12A, D). Thicker coal sections likely experienced greater compactional subsidence, which may have generated topographic depressions that acted as sites of channel reoccupation, resulting in thicker and more amalgamated channelized sandbodies. This observation is consistent with adjacent subsurface coal thickness data (unpublished reports of Energy West Mining Company), and with findings in other coal-bearing basins (Michaelsen et al., 2000; Rajchl and Uličný, 2005; Hofmann et al., 2011).

Intermediate-scale heterogeneity (1's of m vertically, 10's of m laterally)

Different types of architectural elements, each with characteristic depositional and geomorphic attributes (Table 2.2) condition intermediate-scale heterogeneity. For field-validation and calibration, we have pursued its representative characterization in cliff faces 1 and 2 (Figures 2.6, 2.7). In cliff face 1, oriented along depositional-strike, the abundance of architectural elements is as follows (Figure 2.13): (A, B) channel and bar-accretion macroform (36%, in combination); (C) overbank fines (~ 54%); (D) crevasse delta (~ 0.1%); and (E) overbank and crevasse splays (10%). In cliff face 2, oriented along depositional-dip, their abundance differs

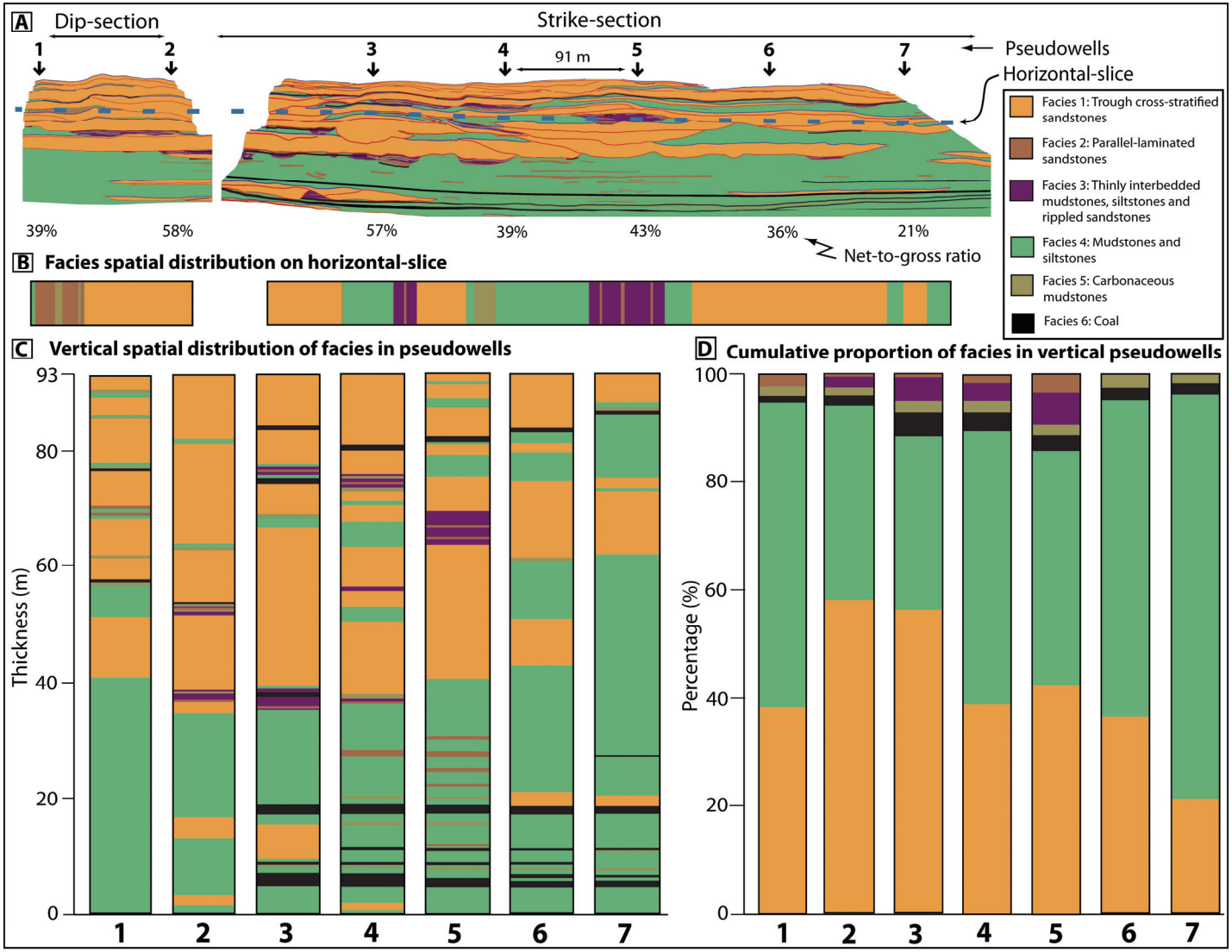

Figure 2.12. A) Position of pseudowells (numbered 1 to 7) in both the strike-oriented (Figure 2.6A) and dip-oriented outcrop panels (Figure 2.7A), and a hypothetical horizontal slice dissecting these two panels. Inter-well spacing was set to 91 m to match that in the tight-gas producing Jonah

field, Wyoming, USA. An approximate net-to-gross ratio has been calculated for each pseudowell. B) Spatial distribution of facies (Table 2.1) on horizontal slice, and C) in vertical pseudowells. D) Cumulative proportion of facies in vertical pseudowells.

(Figure 2.13): (A, B) channel and bar-accretion macroform (51%); (C) overbank fines (41%); (D) crevasse delta (0%); and (E) overbank and crevasse splays (8%). Overbank fines (architectural element C) display the greatest contrast in abundance (54% in strike-oriented section; 41% in dip-oriented section). Even on the same cliff face, its proportion varies laterally, for example from ~ 35% at the left side of cliff face 1 to ~ 80% at the right side of the cliff face (pseudowells 3 and 7 in Figure 2.12D), and from ~ 60% at the left side of cliff face 2 to ~ 40% at the right side of the cliff face (pseudowells 1 and 2 in Figure 2.12D). Only one crevasse delta (architectural element D) is present, on cliff face 1, with a preserved thickness of ~ 7 m and lateral extent of ~ 50 m. The proportion of overbank and crevasse splay deposits (architectural element E) is markedly higher in cliff face 1 (~ 10%; Figures 2.6, 2.13) than in cliff face 2 (~ 8%; Figures 2.7, 2.13). Crevasse splay deposits have been documented (n = 44) in outcrop dataset (Figures 2.11C, D).

Small-scale heterogeneity (10's of cm vertically, 1's of m laterally)

Small-scale heterogeneity is related to the abundance and spatial distribution of sedimentological facies (Table 2.1) nested within architectural elements. For its representative documentation, we have targeted cliff faces 1 and 2 (Figures 2.6, 2.7). Trough cross-stratified sandstones (facies 1) are the dominant facies, occupying 36% of cliff face 1 and 51% of cliff face 2 (Figure 2.13A). This facies, of which channel and bar-accretion macroform elements

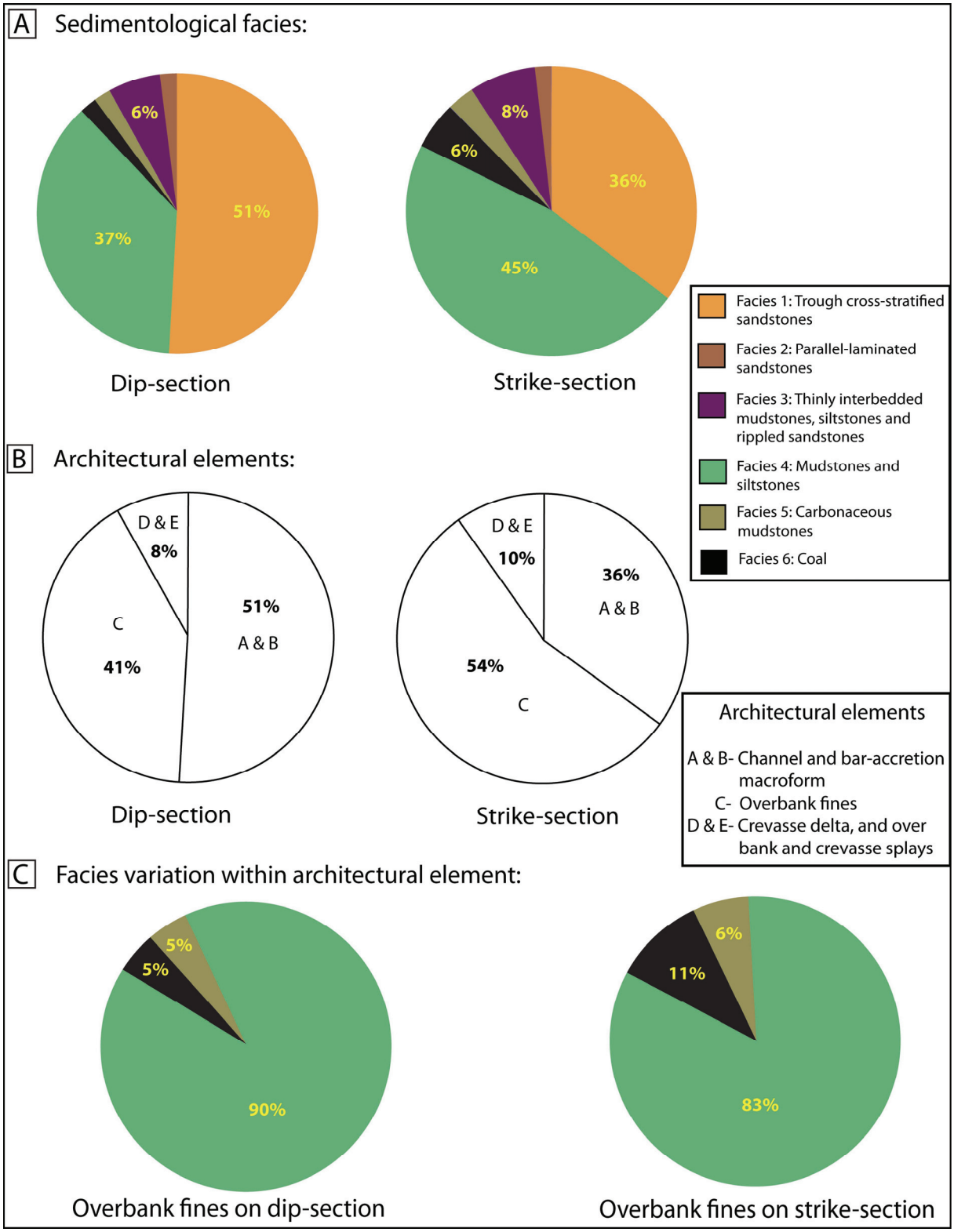

Figure 2.13. Relative proportions of A) facies (Table 2.1), B) architectural elements (Table 2.2), and C) facies proportions within overbank fines (architectural element C), in depositional-dip-oriented cliff face 2 (Figure 2.7) (left), and -strike-oriented cliff face 1 (Figure 2.6) (right).

(architectural elements A and B, respectively) are almost entirely composed, is characterized with predominantly trough cross-stratified, medium- grained sandstones (> 90%) passing upwards into subordinate, ripple cross-laminated, very fine- to fine-grained sandstones (< 10%) (e.g., Lithologs 1-11; Figure 2.14). In this facies, scattered mudstone chips as rip-up clasts additionally contribute to their lithologic heterogeneity. Individual beds in the bar-accretion macroform elements (architectural element B) are inclined and show a gradual up-dip decrease in grain size from lower medium- to upper fine-grained to finer-grained sandstones and intercalated siltstones (Figure 2.5B). Overbank fines (architectural element C) are the most abundant architectural element (Figure 2.13B), and they are composed of a diverse assemblage of constituent facies (Figure 2.13C). Their abundance in cliff face 1 is as follows: mudstones and siltstones (facies 4; 83%), carbonaceous mudstones (facies 5; 6%), and coal (facies 6; 11%). In contrast, their abundance in cliff face 2 is as follows: mudstones and siltstones (facies 4; 90%), carbonaceous mudstones (facies 5; 5%), and coal (facies 6; 5%). Crevasse delta, and overbank and crevasse splays elements (architectural elements D and E) consist predominantly of parallel-laminated, fine-grained sandstones (facies 2) and thinly interbedded mudstones, siltstones and rippled sandstones (facies 3).

2.5 Potential for Stratigraphic Compartmentalization and Implications for Tight-Gas Reservoir Character

Stratigraphic architecture exerts a fundamental control on reservoir compartmentalization that can be evaluated through appropriate connectivity analysis, encompassing net-to-gross ratio,

sandbody geometry and spatial distribution (Ainsworth, 2005), and assessment of facies-dependent rock fabrics. These aspects are constrained below through assessment on potential impact of each fluvial heterogeneity towards stratigraphic compartmentalization of fluvial reservoirs.

2.5.1 Impact of large-scale heterogeneity

Large-scale heterogeneity as shown in Figure 2.11 reveals that >50% (28 out of 53) of sandbodies have width values in the range of 1-200 m. This implies a major production uncertainty because majority of these sandbodies can be penetrated by one well or two wells at maximum with 100 m well spacing. Another manifestation of large-scale heterogeneity that quantifies reservoir net thickness is net-to-gross distribution. We have documented net-to-gross ratio for channelized sandbodies by positioning pseudowells at a uniform spacing (~ 100 m distance) in our study area (Figure 2.15). Documentation of net-to-gross ratio on eight cliff faces shows highest (73%), lowest (17%), mean (41%), and median (39%) values (Figure 2.15). Overally, low net-to-gross values (17-50%) constitute ~ 80% of all estimation, and hence, represent bulk distribution on studied dataset (Figure 2.15). Albeit cliff face 3 which shows higher net-to-gross values (> 50%) consistently, all other cliff faces are permeated with wide ranging values of net-to-gross (Figure 2.15B), implying that these cliff faces require improved risk analysis for exploration and production target. One of the major uncertainties that confront appraisal and exploration strategy of tight gas reservoirs is their dramatic and distinct anomalous net-to-gross distribution. This uncertainty has been constrained on our dataset.

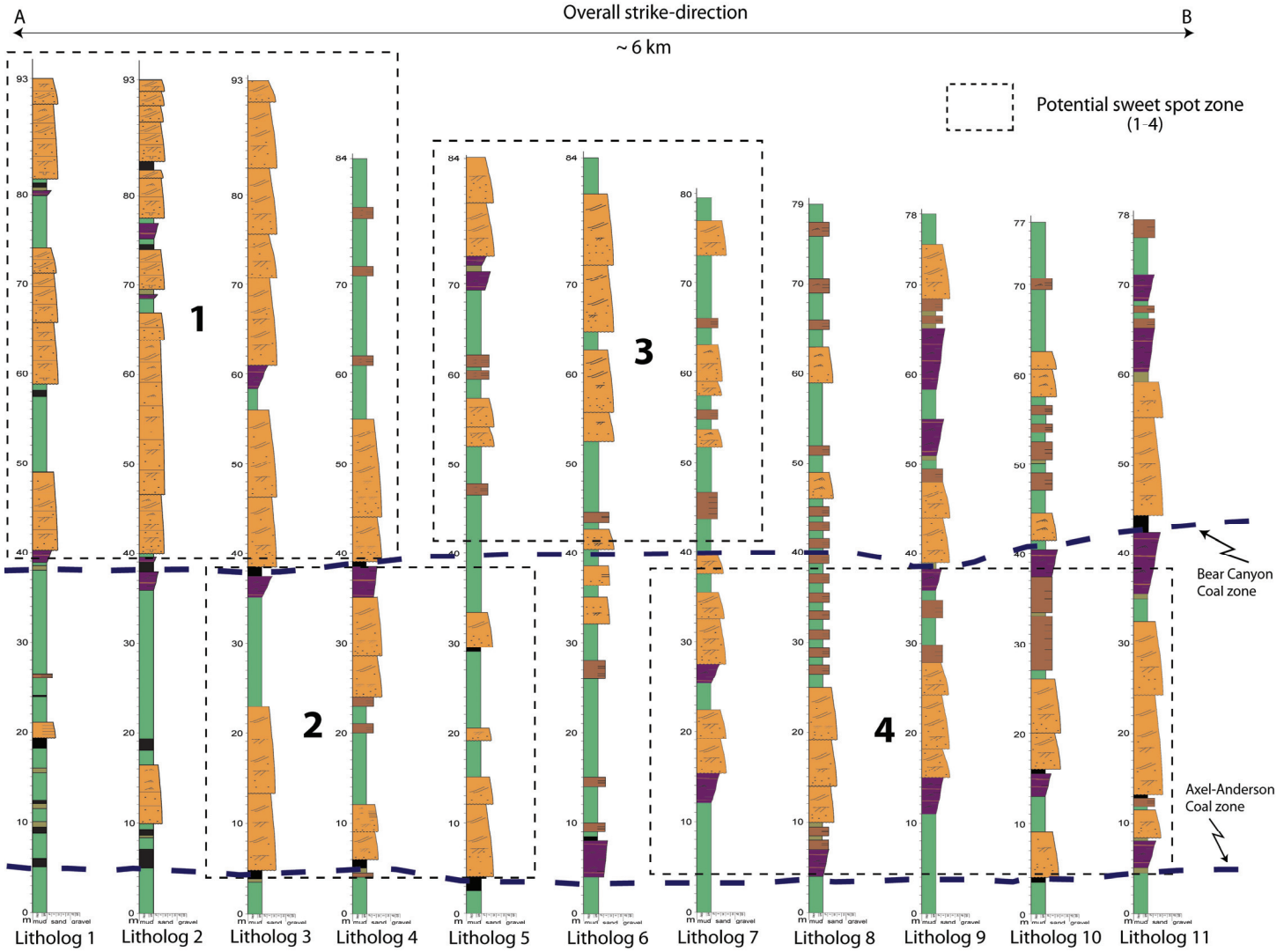

Figure 2.14. Along depositional-strike correlation panel of the study area (for location, see Figure 2.3). Lithologs (1-11) have been correlated using two stratigraphic datums- bottom (Axel Anderson coal zone), and top (Bear Canyon coal zone). Four potential sweet spot zones (1-4) have been identified based on geological parameters (see text for details). For legend see Figure 2.6.

Distinct decrease of net-to-gross values laterally over ~ 100 m distance (inter-pseudowell spacing on our dataset) - 36% to 21 % (pseudowells 6-7, cliff face 1, Figure 2.12; Figure 2.15), 58% to 19%, 48% to 26% (cliff face 5; Figure 2.15), 46% to 25% (cliff face 7; Figure 2.15), 51% to 37%, and 61% to 44% (cliff face 8; Figure 2.15) - emphasizes how these contrasting net-to-gross values can be conditioned within a short distance (here, ~ 100 m) that may contribute to extraction challenges. Through conceptual modeling of channel connectivity, Larue and Hovadik (2006) demonstrated a relationship between channelized sandbody connectivity, net-to-gross ratio, and channelized sandbody sinuosity. Our calculated lateral variability of net-to-gross values, and estimated channel sinuosity (which is likely more than sandbody sinuosity) from paleohydraulic calculation provide a quantitative dataset that can be targeted for further evaluation in this type of fluvial modeling.

Additionally, we have addressed the impact of large-scale heterogeneity through identifying potential sweet spot zones in our dataset. Successful identification of sweet spot zones is crucial to tight-gas producibility and profitability (*sensu* Meckel and Thomasson, 2008). Key geologic parameters that define sweet spot conditioning are 1) greater thickness of reservoir, and 2) a change of reservoir-bearing (*sensu* Meckel and Thomasson, 2008). Utilizing these two parameters, we have identified four potential sweet spot zones (Figure 2.14) where 1) thickness of reservoir has been assigned to combined thickness of channelized sandbodies within the zone, and 2) predominant facies (i.e. trough cross-stratified sandstones; Facies 1) have been considered as analogous reservoir facies. To better constrain boundary conditions for each potential sweet spot zone, we have followed certain geological and operational-comfort guidelines. Both the top and base of each zone have been defined in reference to

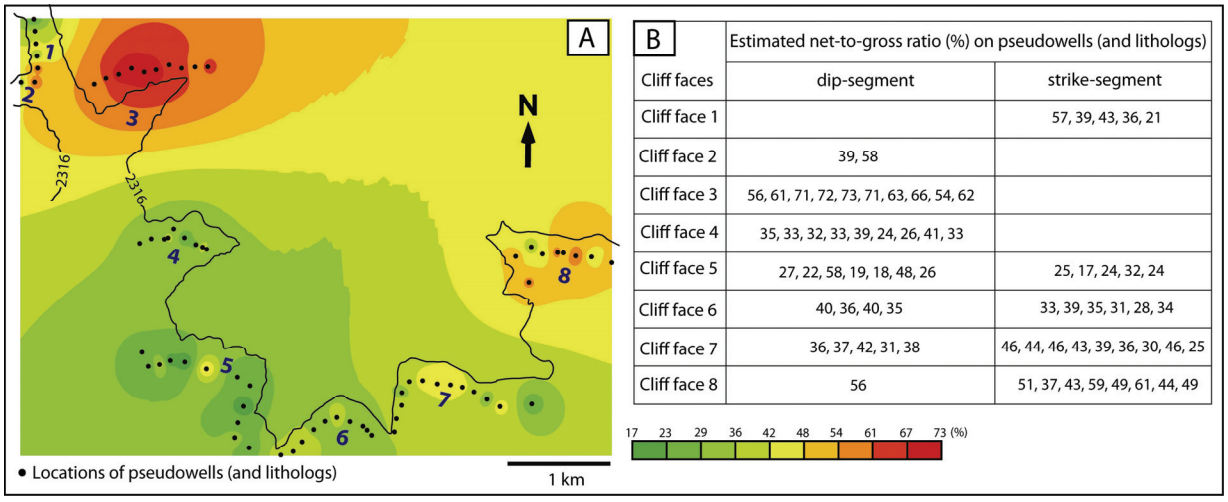

B

Cliff faces	Estimated net-to-gross ratio (%) on pseudowells (and lithologs)	
	dip-segment	strike-segment
Cliff face 1		57, 39, 43, 36, 21
Cliff face 2	39, 58	
Cliff face 3	56, 61, 71, 72, 73, 71, 63, 66, 54, 62	
Cliff face 4	35, 33, 32, 33, 39, 24, 26, 41, 33	
Cliff face 5	27, 22, 58, 19, 18, 48, 26	25, 17, 24, 32, 24
Cliff face 6	40, 36, 40, 35	33, 39, 35, 31, 28, 34
Cliff face 7	36, 37, 42, 31, 38	46, 44, 46, 43, 39, 36, 30, 46, 25
Cliff face 8	56	51, 37, 43, 59, 49, 61, 44, 49

Figure 2.15. A) Net-to-gross map of the study area. Black circles represent locations of pseudowells that were positioned at a ~ 100 m well spacing. B) Quantification of net-to-gross ratio of pseudowells on cliff faces (1-8) along both dip- and strike-orientation.

stratigraphic datum present in the study area. Two laterally extensive coal seams, Axel-Anderson coal seam (~ 2 m thick) and Bear Canyon coal zone (~ 1-2 m thick), constitute bottom and top datum respectively. Additionally, we have demarcated lateral limit of each zone, where 1) we could trace lateral continuity of constituent sandbodies before it ceased to adjacent floodplain fines, and 2) for operational-comfort, we looked for sandbody amalgamation, at least honored by two individual channelized sandbodies. With both the vertical and lateral boundary of each zone adequately constrained, we analyzed the impact of large-scale heterogeneity on each zone by delineating degree of amalgamation of sandbodies and net-to-gross estimation (Figures 2.14, 2.16). For zone 1, net-to-gross increases from 63 to 90% before it steeply decreases to 35%. Within this zone, maximum thickness of amalgamated sandbodies is ~ 32 m. For zone 2, net-to-gross follows a steadily declining trend from 54 to 44%. Within this zone, maximum thickness of amalgamated sandbodies is ~ 18 m. For zone 3, net-to-gross pattern

distinctly increases from 37 to 62% and then decreases to 28%. Within this zone, maximum thickness of amalgamated sandbodies is ~ 15 m. For zone 4, net-to-gross distribution shows modestly decreasing trend from 49 to 37% and then increasing upto 58%. Within this zone, maximum thickness of amalgamated sandbodies is ~ 19 m.

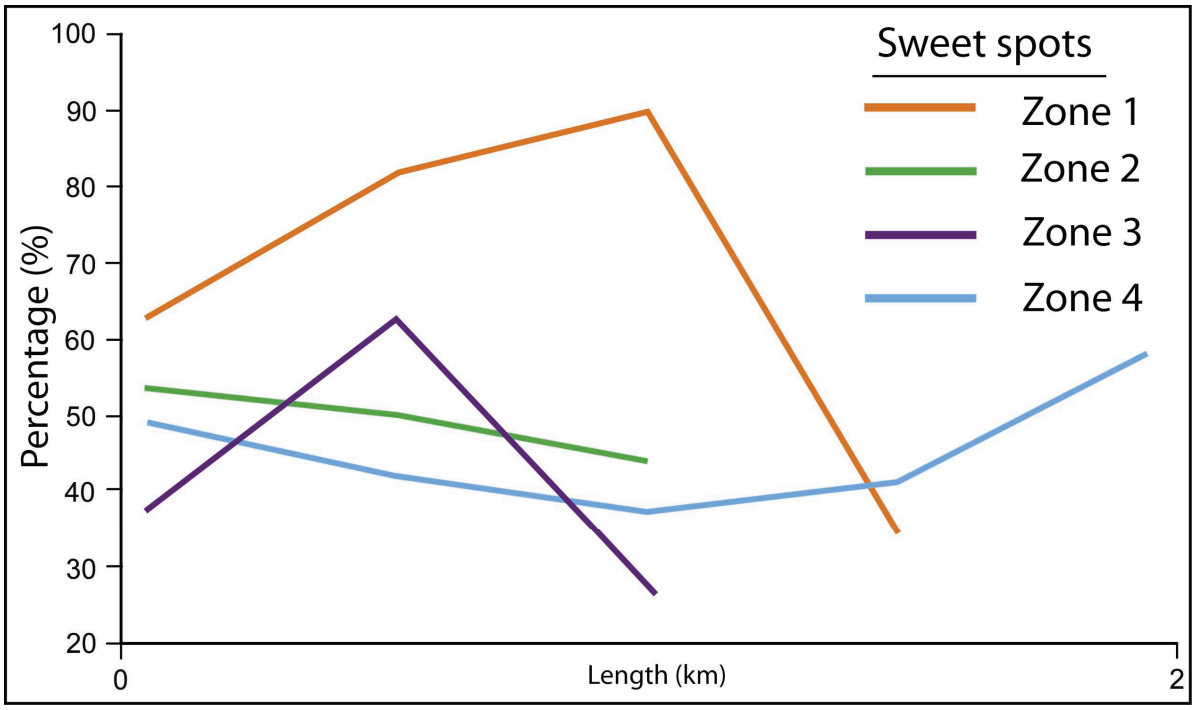

Figure 2.16. Spatial variability of net-to-gross ratio within each potential sweet spot zone (Figure 2.14).

2.5.2 Impact of intermediate-scale heterogeneity

Production behavior of fluvial tight-gas reservoirs is notoriously complex and unpredictable. This can be analogously realized only if an appropriate outcrop data suitably characterize unpredictable and/or uncorrelatable trends of fluvial sedimentologic entities present within a reservoir body. These intriguing relationships have been honored in our studied dataset. Lateral variability trends of five architectural elements within each sweet spot zone (as a percentage of individual sweet spot thickness) show that there are no predictable trends, and occurrences of these elements mostly do not correlate with each other (Figure 2.17). These increasing-decreasing trends developed as either singular or composite path, lend to the insights of reservoir complexities that can be conditioned, particularly in tight gas reservoirs.

For analogous reservoir analysis, documentation of these five architectural elements provides following insights. Channel and bar-accretion deposits (architectural elements A and B, mainly composed of facies 1; Table 2.2) are most likely contribute to net pay. Crevasse delta, and overbank and crevasse splays elements (architectural elements D and E; Table 2.2) form smaller, less abundant and finer-grained sandbodies (mainly composed of facies 2 and 3) that may not contribute to net pay. However, the large lateral extent of these bodies may significantly increase sandbody connectivity if they have sufficiently high permeability to contribute to flow (e.g., Shanley, 2004; Larue and Hovadik, 2006). Overbank fines (architectural element C, composed of facies 3-6; Table 2.2) are too fine-grained to form net pay, and they are likely to form barriers or baffles to flow between stratigraphic reservoir compartments that are composed of connected channelized fluvial sandbodies.

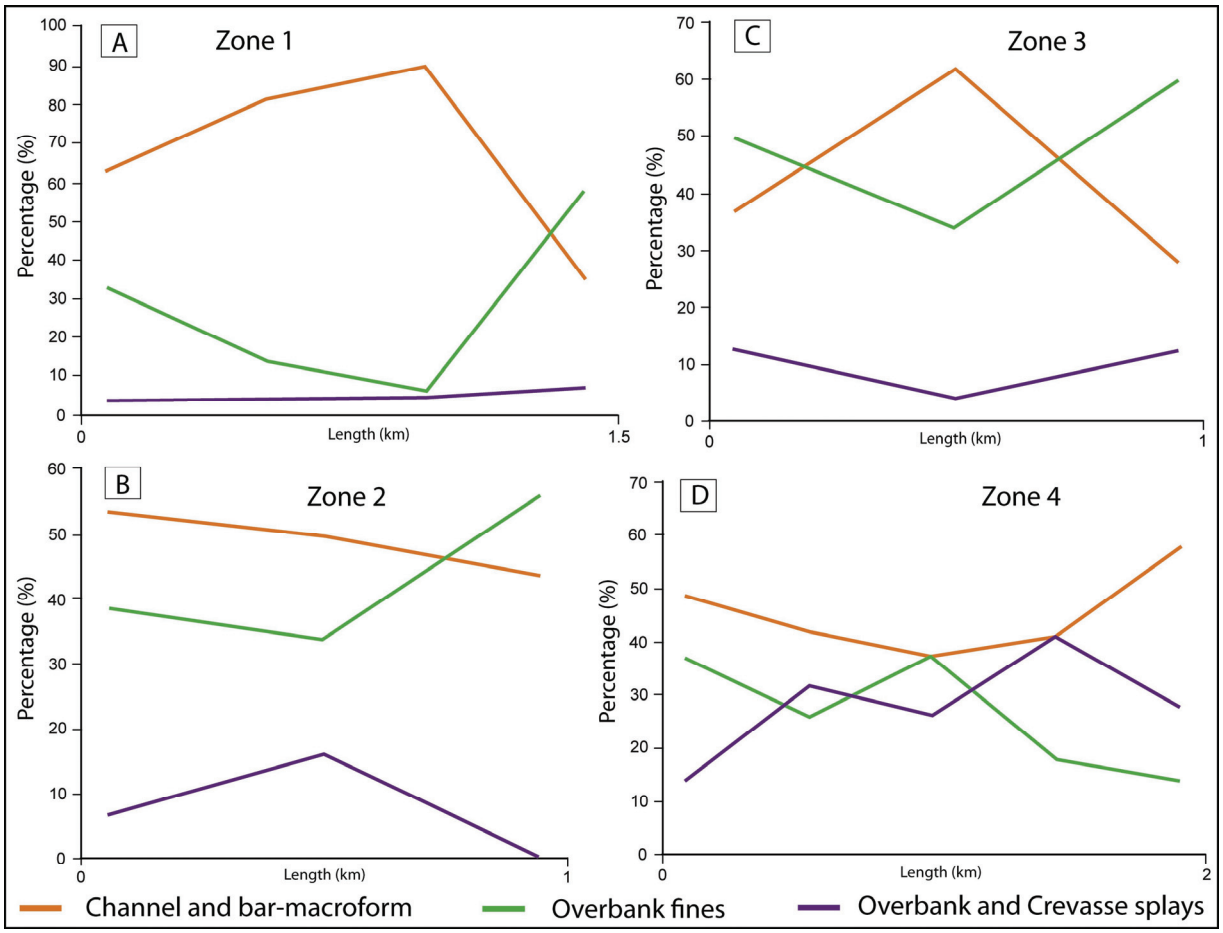

Figure 2.17. Spatial variability of architectural elements (Table 2.2; Figure 2.5) within each potential sweet spot zone (Figure 2.14).

Detailed sedimentological investigation of individual architectural element reveals important attributes of grain size, lithology and sedimentary structure that can potentially control porosity and permeability anisotropy within reservoir compartments, as outlined below. Fining-upward grain-size trends in channel and bar-accretion deposits (architectural elements A and B; Table 2.2) probably result in a subtle upward decrease in permeability. The occurrence of inclined beds in bar-accretion deposits, comprising downdip coarser sandstones to updip finer sandstones and siltstones (Figure 2.5B), introduces an oblique horizontal component to

permeability anisotropy within these elements. Lateral and vertical variation in grain size within sandstone beds of ribbon, sheet and lenticular geometry that occur within overbank and crevasse splays elements (architectural element E; Table 2.2) defines their internal permeability structure, but intercalated mudstones and siltstones result in these elements having much lower vertical than horizontal permeability.

Dimensional attributes of architectural elements as well as ranges of anisotropy nested within each architectural element provide insights to improved exploration and production strategy. For example, directional permeability anisotropy within architectural elements i.e. along the dip of clinoformal sandstone beds in bar-accretion elements (Jones et al., 1987; Hartkamp-Bakker and Donselaar, 1993; Anderson 2005; Pranter et al., 2007) may influence drainage patterns around wells. Width range of crevasse splay elements (Figure 2.11D) demonstrates an important uncertainty that almost all crevasse splay sandbodies (~ 91%; 39 out of 43) are less than 100 m wide, which implies that either these sandbodies will be penetrated by one well at most (for example- pseudowells 2, 3, 4 and 5 penetrate crevasse splay deposits; Figure 2.12) or left un-intersected (for example- crevasse delta and ~ 50% of crevasse splay deposits are not penetrated by pseudowells; Figure 2.12). In this case, high well density is required to drain reservoir compartments formed by unconnected sandbodies of this type.

2.5.3 Impact of small-scale heterogeneity

Attributes of grain size, lithology, and sedimentary structure associated with individual facies have proven impact on reservoir flow anisotropy, and hence, exert control on reservoir quality

(e.g., Weber, 1982; Ringrose et al., 1993, Moreton et al., 2002; Shanley 2004). We have documented these facies charactistics by pursuing grain size analysis, and meticulously populating sedimentary structures on their near-exact spatial position (Figures 2.6-2.8). Additionally, we have quantified lateral and vertical facies-diversity pattern encountered on pseudowells and a horizontal slice on outcrop panels (Figure 2.12) to demonstrate how it can potentially impose uncertainties to lateral and vertical communication of reservoir flow units. Breaks in facies continuity are adequately constrained at a meter to sub-meter scale (Figures 2.12B, 2.12C) which can likely exert boundary conditions to individual flow compartment.

Cross-stratified sandstones (Facies 1) are known lithofacies of superior reservoir quality (e.g., Shanley, 2004), and mudstones (Facies 4) act as barrier to fluid flow (e.g. Weber, 1982). Hence, for analogous reservoir quality assessment of the four sweet spot zones (Figure 2.14), we have documented spatial distribution pattern of these two facies in each sweet spot zone (Figure 2.18). In zones 1 and 3, spatial distribution of these two facies demonstrates the expected inverse relationship, which is conventional (Figure 2.18A). However, in zones 2 and 4, their coupling relationship does not confirm to this norm. In zone 2, on the left side, their spatial distribution trend is positively correlated which gradually becomes inverse towards right side (Figure 2.18B). Likewise, in zone 4, contrary to a single decreasing-increasing trend of trough cross-stratified sandstones, spatial distribution of mudstones and siltsones facies illustrates a composite trend (Figure 2.18D). This could be due to complex interference of other constituent facies nested within this zone.

Quantification of these trends associated to facies types provides spatial data that can be utilized by reservoir engineers and modelers for porosity-permeability class evaluation

commensurate to calibration of facies efficiency towards reservoir flow behavior (e.g., Moreton et al., 2002). Assessment of directional permeability anisotropy, especially for trough cross-stratified sandstones (Facies 1) which constitute principal reservoir facies within sweet spot zones, should also be pursued that can guide well layout strategy in regard to paleoflow direction (e.g. Jones et al., 1987; Anderson 2005).

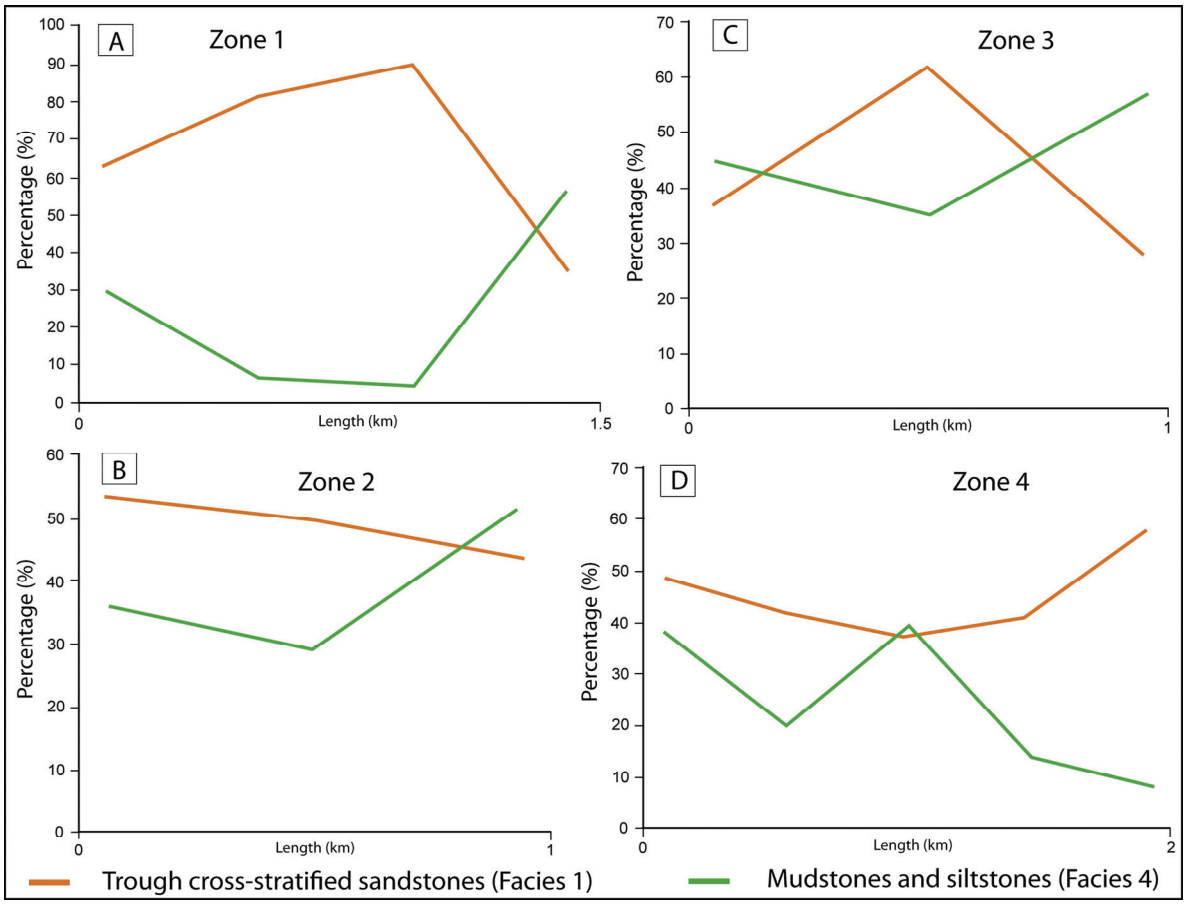

Figure 2.18. Spatial variability of trough cross-stratified sandstones (Facies 1; Table 2.1; Figure 2.4), and mudstones and siltstones (Facies 4; Table 2.1; Figure 2.4) within each potential sweet spot zone (Figure 2.14).

2.5.4 Comparison with subsurface tight-gas reservoirs

The Blackhawk Formation outcrops in Cottonwood Creek are particularly analogous to the Lance Formation reservoir of the Jonah field, Green River Basin, Wyoming, which is the largest fluvial tight-gas reservoir in the onshore US (Robinson and Shanley, 2004). The Jonah field reservoir has a low-to-moderate net-to-gross ratio overally (10-35% to 40%; Cluff and Cluff, 2004; Shanley, 2004). Nearly all net-to-gross ratios (80% of total estimation) of our dataset demonstrate a similar range (17-46%) (Figure 2.19A). Likewise, moderate-to-high net-to-gross values (40-80%) in localized "sweet spots" of the Jonah field (Shanley, 2004) are comparable to the net-to-gross range (35-90%) of four potential sweet spot zones of this study (Figure 2.19B). Channel sandbody single-storey thickness of Jonah field is ~ 3-5 m (Shanley, 2004) which appreciably matches to 3-7 m thickness range attained by two-third majority of single-storeyed channel sandbodies of our dataset (Figure 2.19C). A broadly positive correlation has been achieved between width range of Jonah-Pinedale channel sandbodies having 2.5-5m thickness (Shanley, 2004) to the same thickness-bearing channel sandbodies on our dataset (Figure 2.19D). Particularly, this relationship is more apparent in 30-100% range.

In regard to reservoir quality assessment analysis, net pay in the Jonah field reservoir is dominated by trough cross-stratified sandstones (cf. facies 1; Table 2.1) (Shanley, 2004) that occur in sinuous-channel and point-bar sandbodies (cf. architectural elements A and B; Table 2.2) (Dubois et al., 2004). Crevasse splay sandbodies provide conduits to reservoir connectivity, which enhances reservoir drainage, in the Jonah field (Shanley, 2004); similar sandbodies (architectural elements D and E; Table 2.2) constitute a significant component of our four potential sweet spot zones as well as entire dataset. Based on the analogy, our outcrop data

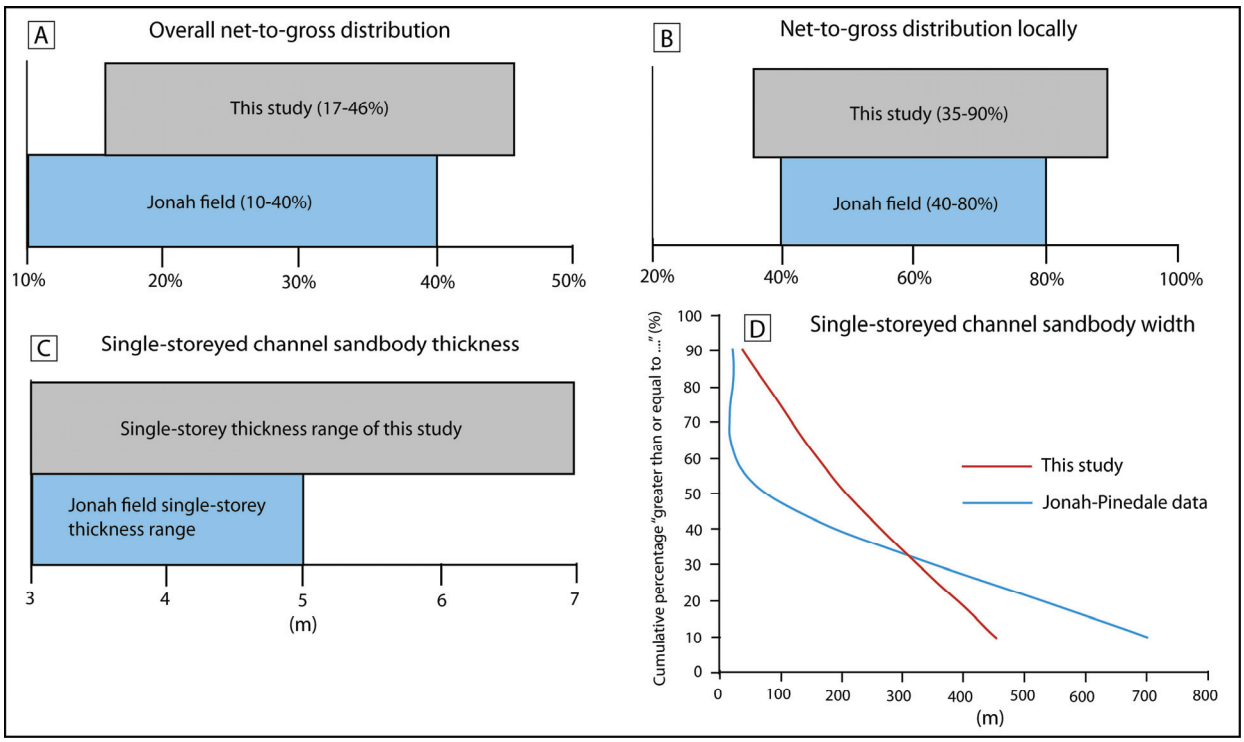

Figure 2.19. Comparative analysis of study results with tight-gas producing Jonah field of Wyoming. Data of Jonah field have been adopted from Cluff and Cluff (2004), and Shanley (2004). A) Overall net-to-gross distribution, B) net-to-gross distribution locally, C) single-storey channel sandbody thickness, and D) single-storeyed channel sandbody width. Overally, these comparisons demonstrate a good correspondence.

(Figures 2.6, 2.7, 2.12) may provide insights to inter-well architecture in the subsurface, which cannot be achieved from interpreting seismic, core, and well-log data. Inter-well connectivity of sandbodies is a major uncertainty in fluvial tight-gas reservoirs. For example, little well-to-well communication between fluvial sandbodies is encountered in interference tests in the Rulison field, Piceance Basin, Colorado, even for well spacing of 280 m (Shanley, 2004), while individual sandbodies are hardly correlatable in the Jonah field, even for well spacing of 91 m (House and Shemeta, 2008). We illustrate this uncertainty on the outcrop panels by positioning

pseudowells at 91 m spacing in Figure 2.12. From the total population of channelized sandbodies (n=39; 100%), a few remain un-intersected (n=2; 5%), several are penetrated by one pseudowell (n=8; 21%) or two adjacent pseudowells (n=6; 15%), and most are intersected by three or more pseudowells (n=23, 59%). However, even if the same sandbody is encountered in multiple wells, stratigraphic compartmentalization may still potentially be induced by the spatial distribution of constituent architectural elements (i.e., intermediate-scale heterogeneity), and facies variation within these elements (i.e., small-scale heterogeneity), if these features are associated with very large permeability contrasts. Similarly, other fine-grained sandbody types like crevasse deposits (one crevasse delta and 24 crevasse splays) show very limited well-penetration or are not intersected.

2.6 Conclusions

Field-validation and calibration of entire range of fluvial heterogeneities have been constrained on a single outcrop dataset that is hard to capture from subsurface reservoir data (i.e., seismic, well-log, and core cuttings). Evaluation of the range of these heterogeneities at various length scales, contributes towards better predictability of reservoir uncertainties in inter-well volumes of fluvial tight-gas reservoirs.

Large-scale heterogeneity (10's of m vertically, 100's of m laterally) is constrained by geometry and spatial distribution of channelized fluvial sandbodies encased within coastal-plain mudstones. Individual sandbodies are medium-grained, 1-17 m thick, 29-724 m wide, and they constitute different sandbody suites: single-storey sandbodies (thickness ranging from 1 to 17

m, width from 29 to 724 m), through multi-lateral channel-belt sandbodies (~ 15 m thick, ~ 230 m wide), to multi-storey channel-belt-complex sandbodies (~ 25 m thick, ~270 m wide). Width of >50% (28 out of 53) individual sandbodies is in the range of 1-200 m, implying that majority of these sandbodies can be penetrated by one well or maximum of two wells with 100 m well spacing. Although estimated net-to-gross ratio shows a very broad range (17-73%), two production challenges have been recognized : 1) 80% of its total estimation confirms to a low value range (17-46%), and 2) several drastic decrease of values (36% to 21 % , 58% to 19%, 48% to 26%, 46% to 25% , 51% to 37%, and 61% to 44%) has been encountered between two adjacent pseudowells at ~ 100 m well spacing. For favorable producibility and profitability, four localized, potential sweet spot zones (where >73% of net-to-gross values show the range of 40-90%) have been characterized, with conspicuous spatial distribution of net-to-gross and sandbody amalgamation development for each zone.

Intermediate-scale heterogeneity (1's of m vertically, 10's of m laterally) is conditioned by the spatial distribution of five architectural elements (channel; bar-accretion macroform; overbank fines; crevasse delta; and overbank and crevasse splays). Fining-upward trend of both channel and bar elements with distinct dowdndip to updip transition from coarser to finer grain-size, respectively, along clinoformal sandstone beds of bar element are type of sedimentologic attributes that can contribute to porosity and permeability anisotropy. These two elements are the predominant constituent of studied sandbodies. Crevasse splay element also illustrates proximal to distal lateral grain-size variation (from coarser to finer, respectively) that can potentially generate horizontal anisotropy. Almost all crevasse splay sandbodies (~ 91%; 39 out of 43) are less than 100 m wide, which indicates that either these sandbodies will

be penetrated by one well at most or left un-intersected if they lie at an inter-well spacing of 100 m.

Small-scale heterogeneity (10's of cm vertically, 1's of m laterally) is related to the diversity and organization of six facies (trough cross-stratified sandstones; parallel-laminated sandstones; thinly interbedded mudstones, siltstones and rippled sandstones; mudstones and siltstones; carbonaceous mudstones; and coal) within architectural elements. Breaks in facies continuity, as documented both laterally and vertically, can potentially induce compartmentalization of reservoir units.

Study results provide closely matching correlation to subsurface characteristics of the giant, tight-gas producing Jonah field, Wyoming. Rendering good correspondence to both overall and localized (i.e. sweet spot) net-to-gross pattern, sandbody thickness and width estimates, and depositional fabric characterization in terms of facies and architectural element abundance, hence, this outcrop dataset can be integrated towards improved subsurface analysis of tight-gas reservoirs like the Jonah field.

Chapter 3

LiDAR-integrated Fluvial Organization Analysis in Rock Record

Abstract

Integration of LiDAR, a cutting-edge photorealistic technology, has been applied to fluvial rock record characterization of this study that enables to improved fluvial analysis at architectural-scale (e.g. avulsion cycle ~1's-10's kyr) to basin-scale (~100's kyr-1's myr). Using an integrated outcrop, LiDAR, and core dataset, this study focuses a high-quality outcrop "window" of fairly large spatial (~25 km^2 area encompassing six contiguous, clean, and vertical cliff faces with their 3D orientation) and temporal (~4 my) scales from the upper Cretaceous Blackhawk Formation in the Cottonwood Canyon area, eastern Wasatch Plateau, Utah.

Channelized sandbodies were mapped and populated on a 3D outcrop model extracted from geo-referenced LiDAR data, ground-truthed with measured sections, and containing mapping of sandbody was guided by paleoflow direction. The model shows that compensational stacking of sandbodies (i.e. lateral shifting of depocenter through time) is better developed in the lower Blackhawk Formation but gradually decreases stratigraphically upward. In contrast, sandbody vertical-clustering (i.e. depocenter fixed through time) is more apparent for the middle and upper Blackhawk Formation. Our study also reveals that single-storey sandbodies (a single bar-macroform combined with a laterally-adjacent channel-fill

deposit) show affinity for vertical clustering, whereas multi-lateral sandbodies (discrete bar deposits that are laterally stacked together at the same stratigraphic level; i.e. channel-belt) are prone to compensational stacking. Floodplain facies diversity, quantified from measured sections and core description, is high for the lower Blackhawk Formation, where sandbodies are prone to compensational stacking, but low for the middle and upper Blackhawk Formation, where sandbodies are more clustered.

Constrained fluvial sandbody organization and associated floodplain diversity coupling relationship help to delineate river characteristics of the Blackhawk Formation. Study suggests that rivers in the lower Blackhawk Formation, as distal distributary threads located closer to paleoshoreline, were sand-prone or of frequent flooding affinity that delivered relatively coarser sediment (i.e. sand) to the floodplain area. As a consequence, heterogeneous bank was developed that, owing to its easy erodibility, facilitated multi-lateral (i.e. channel-belt) sandbody formation. Additionally, laterally-heterogeneous floodplain compensation (i.e. differential compaction) due to higher floodplain lithologic heterogeneity was the guiding factor for compensational-stacking of sandbodies during fluvial avulsion process in the lower Blackhawk Formation. In contrast, rivers in the upper Blackhawk Formation were of a larger trunk river type that were located distal upstream to the paleoshoreline. They were mud-prone or least prone to flooding affinity that delivered relatively finer sediment to the floodplain. As a consequence, homogeneous and muddy banks develops, hindering lateral activity of channels (i.e. resulting in single-storey sandbodies). Moreover, laterally-homogeneous floodplain compensation due to least floodplain diversity could disfavor compensational channel stacking (i.e. resulting in sandbody clustering).

3.1 Introduction

Most recently, analysis from quite a handful studies reveal aspects of fluvial organization at channel-belt scale (e.g. Hajek et al., 2010, Hofmann et al., 2011, Wang et al., 2011). Overally, these attempts have comprehended fluvial organization into two main arrangements: 1) clustering, and 2) compensational-stacking. However, the limitation each of these studies accompanies inadequacy of utilized data in terms of manifesting both clustering and compensational-stacking organization. For example, Hajek et al. (2010) has deliberated the channel-belt clustering based on outcrop and numerical data, but compensational aspect has been missing therein. Wang et al., 2011 has focused more on compensational phenomena through which it revealed that data utilized by Hajek et al. (2010) is under-compensated. Later, Hofmann et al. (2011) could be able to illustrate both these two aspects honored by channel-belt organization, but at the expense of empirically deriving sandbody extent in subsurface well-log data using analogous outcrop integration. These suggest that characterization of both clustering and compensational-stacking phenomena have been poorly evaluated from the same fluvial rock record. Moreover, our current understanding of fluvial organization at a lower scale i.e. channel-storey level is also in speculative realm.

Characterizing fluvial organization in the rock record at a high resolution scale remains challenging owing to 1) limitation of resolution in conventional dataset like seismic, well log, and core data, and 2) limited usefulness of 2D outcrop data where extracting the fully-preserved single-storey sandbody or tracing the channel-belt development as lateral stacking of individual single-storey sandbody at the same stratigraphic level. The latter case is particularly hindered by limited exposure issues apparent to outcrop cliff faces as well as difficulty in joining

individual single-storey sandbody from cliff face to cliff face in absence of georeferenced data (i.e. X, Y, and Z). Additionally, the lateral extent or the fully-preservation of sandbodies can only be best constrained from depositional strike-oriented outcrop data which are not amply abundant in rock record studies thus far. In this study, we have targeted a robust outcrop window which comprises a series of cliff faces containing strike-oriented exposures. To offset the inadequacy of our outcrop data, we have incorporated photorealistic technology like LiDAR into our characterization which, with its 3D documentation ability with proper georeferencing, help us pursuing a high-resolution analysis of fluvial organization at the individual channel-storey level. Furthermore, it is worthy to note that little is known about mutual dependencies of floodplain characteristics and avulsion dynamics (e.g. Hajek and Wolinsky 2012). Our knowledge regarding constraining effects of floodplain heterogeneity towards resultant fluvial organization at both spatial and temporal scale is poorly documented in rock record analysis.

3.2 Geology and Regional Context

The studied outcrop section is from Cottonwood Creek in the Wasatch Plateau, central Utah (Figure 3.1). The Wasatch Plateau is contiguous with, and crops out approximately perpendicular to the extensively studied Book Cliffs of Utah and Colorado, which have served as the natural laboratory underpinning sequence stratigraphic concepts in shallow- and marginal-marine settings (e.g., Van Wagoner, 1995; Howell and Flint, 2003; Hampson 2010). These strata were deposited in the Cretaceous Western Interior Seaway, which formed in response to higher sea-levels during greenhouse late Cretaceous as a vast epicontinental sea stretching

from Alaska to northern Mexico. The Seaway occupied the retro-arc foreland basin formed by subduction-related kinematics of the Farallon Plate (e.g., Liu et al., 2011), and was bordered by the tectonically active highlands of the Sevier orogenic belt in the west and by stable, cratonic lowlands in the east (Kauffman and Caldwell, 1993; DeCelles and Coogan, 2006). The coeval Columbian-Sevier orogeny uplifted areas west of the seaway, and rivers sourced from these highland fold-and thrust-zones dispersed sediments eastward to the Seaway over a source-to-sink distance of ~100 km. This sediment flux resulted in the development of prograding siliciclastic wedges of coastal-plain and shallow-marine deposits that transition eastward into offshore mudstones (e.g., Young, 1955; Hampson, 2010). The combined effect of subduction tectonics, greenhouse eustasy, and varying sediment supply from the Sevier fold-and-thrust zone principally controlled relative sea-level fluctuations in the Seaway, as reflected in the stratal stacking pattern of shallow-marine sandbodies and their intertonguing relationships with offshore shales (Houston et al., 2000; Miall and Arush, 2001; Hampson, 2010).

In comparison to strata exposed in the Book Cliffs, the contemporaneous strata of the Wasatch Plateau are markedly less well documented. The study provides a detailed outcrop characterization of the Cretaceous Blackhawk Formation, Mesaverde Group (Figure 3.2) from cliff faces in the eastern Wasatch Plateau, which forms a continuous 100-km long escarpment oriented roughly parallel to regional depositional strike.

In this Wasatch Plateau, the Blackhawk Formation is mudstone- and coal-prone (proportion of sandstone is c. 10-30% over the entire outcrop belt; Hampson et al., 2012), and consists of marginal-marine, coastal-plain deposits in its lower part that transition to continental, alluvial-plain deposits in its upper part (e.g., Flores et al., 1984; Dubiel et al., 2000;

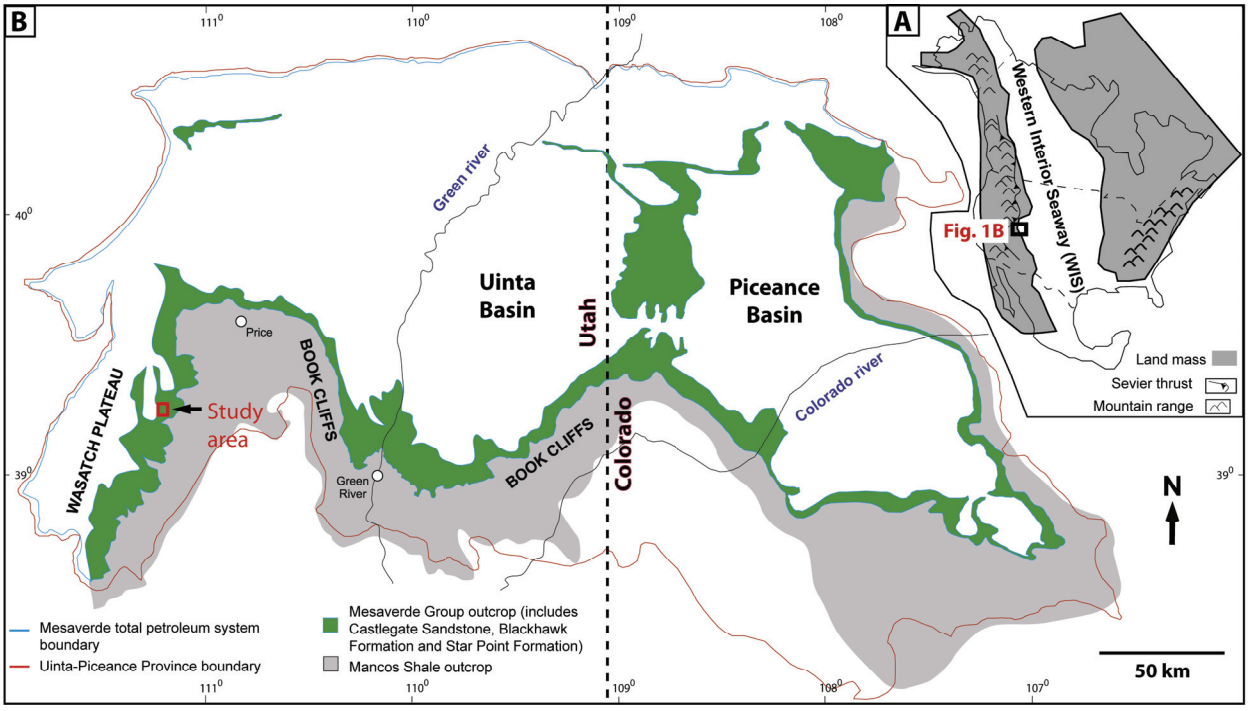

Figure 3.1. A) Late Cretaceous paleogeography of the study area (after Gani and Bhattacharya, 2007). B) Location of the study area in the Wasatch Plateau, central Utah. The Upper Cretaceous Blackhawk Formation, Mesaverde Group, crops out in the study area (modified from Johnson and Roberts, 2003; Hampson, 2010).

Adams and Bhattacharya, 2005; Hampson et al., 2012). Previous works on fluvial characterization of this formation provide following information: rivers in the lower Blackhawk Formation were distributary threads dissecting the coastal-plain paleo-landscape at a proximal distance to shoreline, whereas rivers in the upper Blackhawk Formation were of a trunk, feeder river system in the upstream hinterland region at a distal distance to shoreline (e.g. Hampson et al., 2013; Hampson et al., 2012; Rittersbacher et al., 2012). Rivers flowing in the middle Blackhawk Formation were of transitional nature to the rivers of upper and lower Blackhawk Formation, respectively.

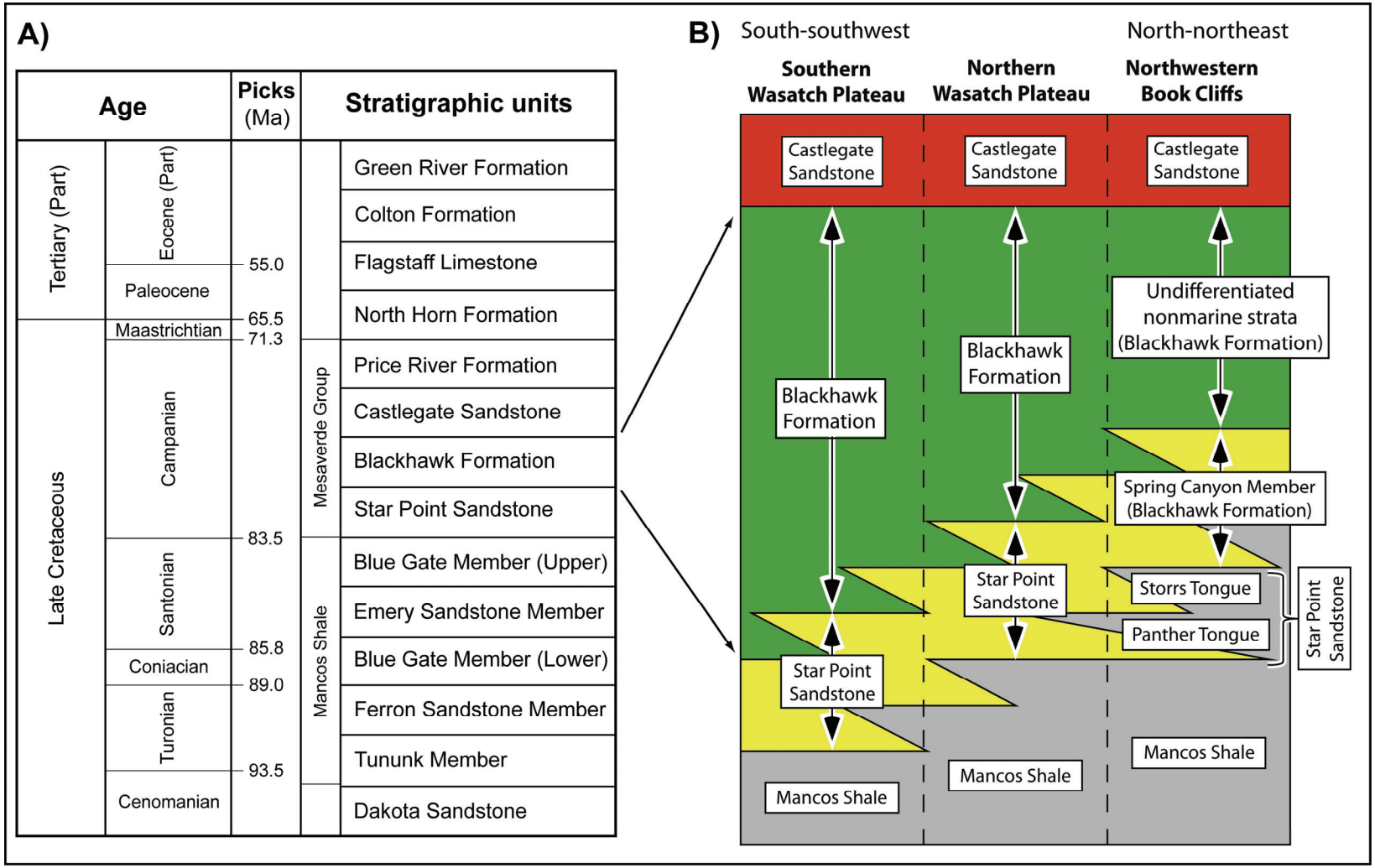

Figure 3.2. A) Stratigraphic succession of the Cretaceous and Tertiary sedimentary rocks in the Wasatch Plateau (modified from Henry and Finn, 2003). B) Lithostratigraphic summary chart of the Blackhawk Formation and surrounding strata in the Wasatch Plateau and northwestern Book Cliffs (from Hampson et al., 2011). The study area lies in the northern Wasatch Plateau (central column). The Blackhawk Formation comprises coastal-plain to alluvial-plain deposits in the study area.

3.3 Dataset and Methodology

Dataset of this study comprise six contiguous, and vertical cliff faces in the Cottonwood Creek, eastern Wasatch Plateau, Utah (Figure 3.3). Overally, individual cliff face contains high-quality exposures oriented in both depositional-dip and -strike direction (Figure 3.3). Depositional dip vs. strike orientations were interpreted from paleocurrent analysis (Figure 3.3C). The investigated outcrop dataset show stratigraphic thickness of ~250 m, and encompass an areal extent of ~5 x 5 km^2.

In the field, serial photos covering cliff faces were collected. All photos in each cliff face were taken serially at the same distance from the cliff face to ensure scale preservation, and with a ~30% overlap with the adjacent photos to maintain the continuity of sedimentologic features during generation of photomosaics. Photomosaics have been constructed by stitching together individual photos in commercially available software ensuring that the correct geometry of sedimentologic features is maintained with minimal parallax error. Bedding diagrams have been constructed from the photomosaics, documenting the preserved geometry of channelized sandbodies (e.g., apparent thickness and width, truncation relationships) and stratigraphic architecture (e.g., sandbody abundance, horizontal and vertical facies distributions, net-to-gross ratio). Lithologs were generated to document vertical facies distributions, and to calibrate the bedding diagrams of cliff faces (Figure 3.4). A detailed subsurface core (EM-137C) analysis has also been included (Figures 3.3 and 3.4).

To augment to the fluvial characterization from conventionally pursued outcrop investigation of these six cliff faces, a low airborne helicopter-based LiDAR scanning method was integrated (Figure 3.5). Compared to the terrestrial LiDAR scanning, this scanning method

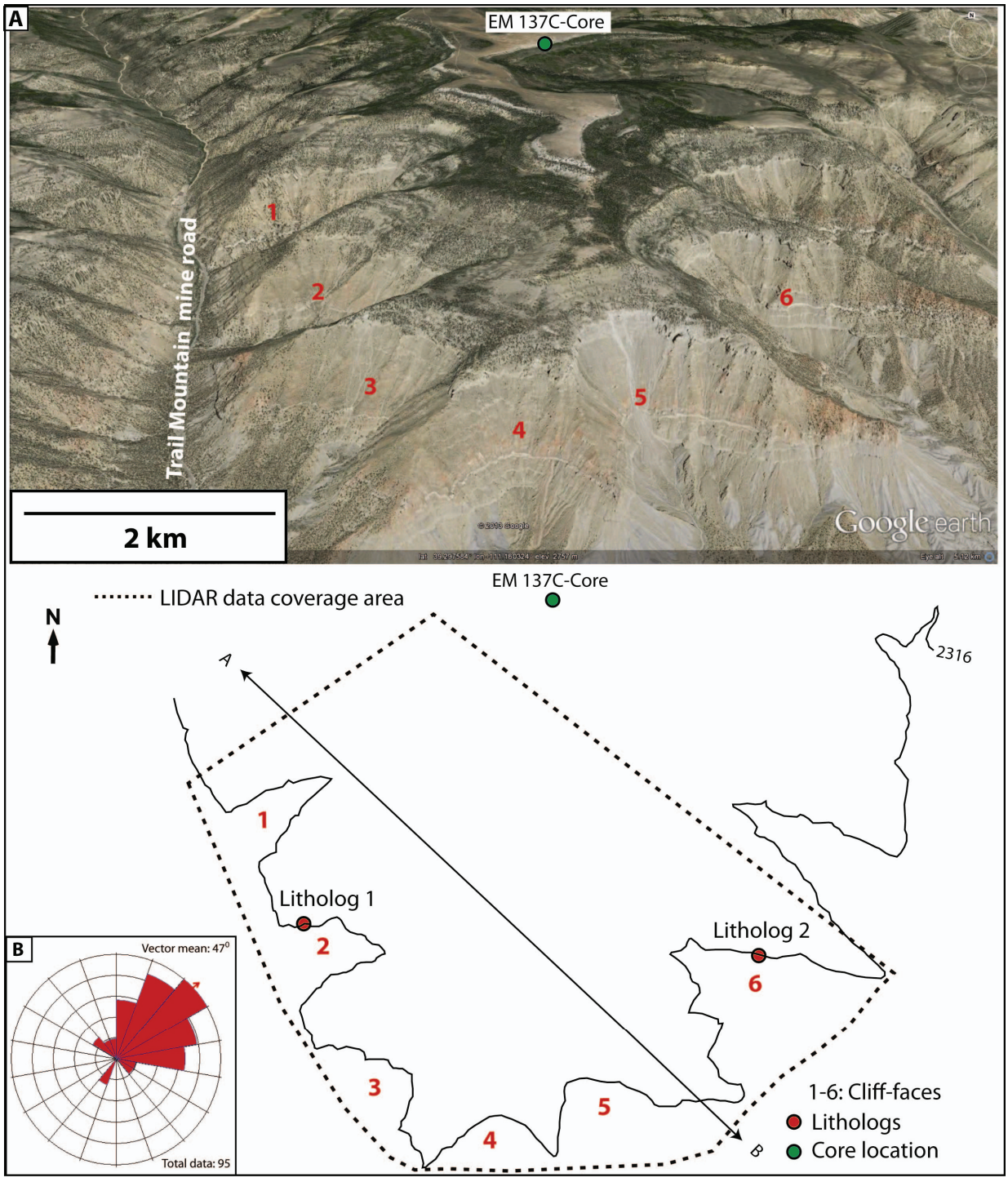

Figure 3.3. A) GoogleEarth view (upper) and map view (lower) of the study location showing dataset comprising six contiguous, and vertical cliff faces (1-6), and one core (2316 m contour line is shown for reference). Along-strike transect line AB perpendicular to paleoflow direction has been drawn for 2D projection of corrected channel sandbodies. B) Paleocurrent rose diagram for dune and ripple cross-strata of the studied outcrop showing an overall northeast paleoflow direction.

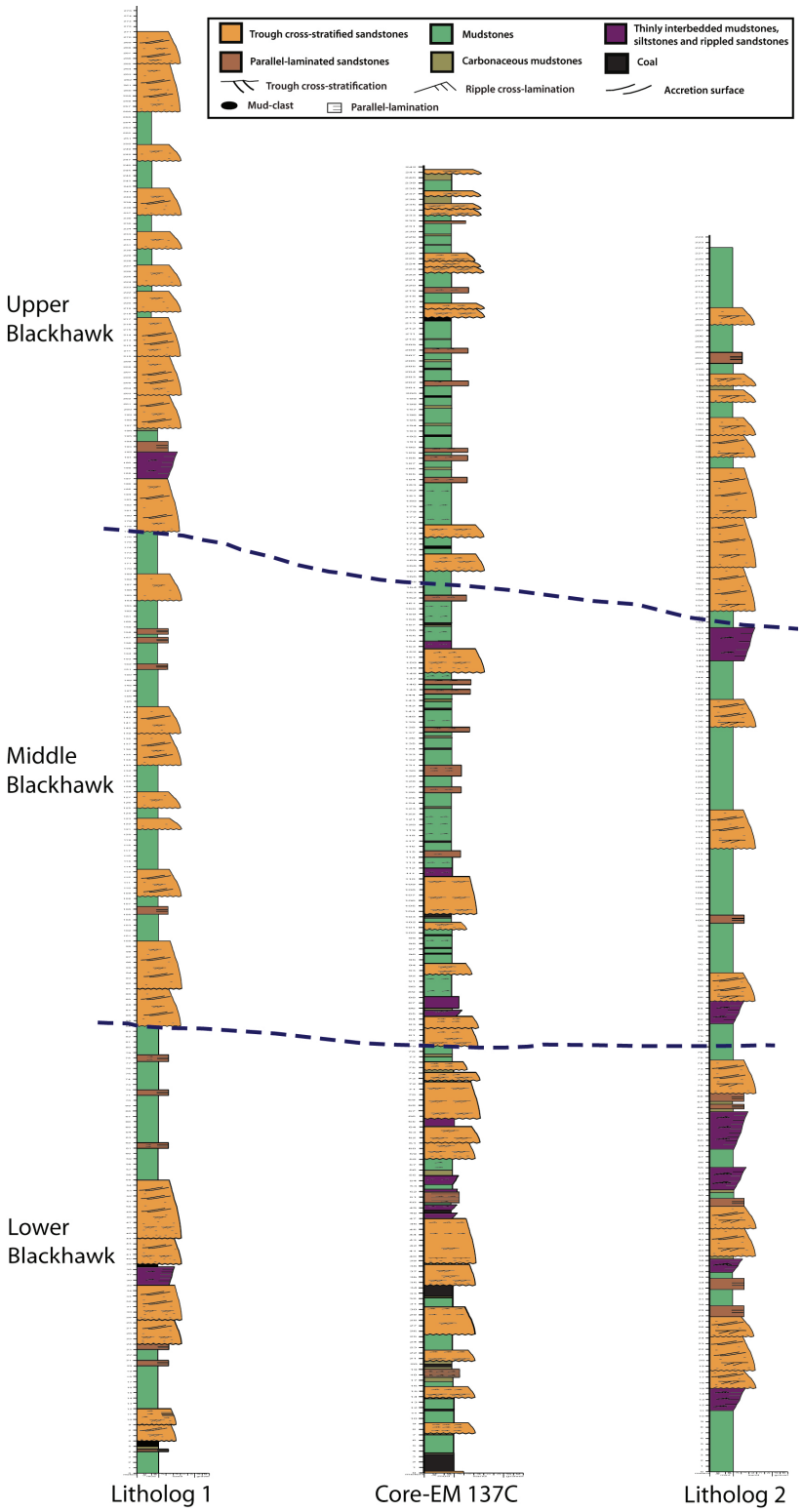

Figure 3.4. Vertical descriptions of lithologs and EM-137C core. Locations of lithologs and core have been shown in Figure 3.3.

is more advantageous for locations where steepness and accessibility of outcrop exposures render difficulty in data acquisition (Buckley et al. 2008a). Unlike to terrestrial LiDAR system that scans from a position usually located at the foot of a cliff, oblique helicopter-based LiDAR scanning uses the scanner system mounted on the side of a flying helicopter, ensuring data capture close to normal to the outcrop. The acquisition process works as a feedback between the instrumentation in the helicopter and a target (i.e. outcrop) like this: flight of laser pulses emitted by the scanner unit hits outcrop face and reflection emanated from that face returns to the detection system of the scanner. Distances to the target are recorded, and as the position and angular orientation of the scanner system is known at all times (using a dual frequency GNSS [global navigation satellite system] and an inertial measurement unit), X, Y, and Z coordinates are calculated for each scan point (Buckley et al. 2008a, Rittersbacher et al. 2012). Recording thousands to hundreds of thousands of points per second, the scanner is able to collect a point cloud containing millions of points for several kilometers of outcrop section in a very short time (usually <1 hour). Together with the point cloud, a series of high-resolution digital photographs covering the scanned area is taken. In this study, the Helimap System, encapsulating a Riegl LMS Q240i-60 airborne laser scanner, Hasselblad H1 22-megapixel digital camera, GNSS and inertial systems were used for data collection. The used Helimap System has proven utility for geological purposes (e.g. Buckley et al. 2008a; Rittersbacher et al. 2012; Vallet & Skaloud 2004).

Upon helicopter-based LiDAR data collection, processing of raw field-data goes through several steps. The first step includes thinning and smoothing of the acquired point cloud which is generally heavily oversampled with respect to outcrop topography (Buckley et al. 2008b).

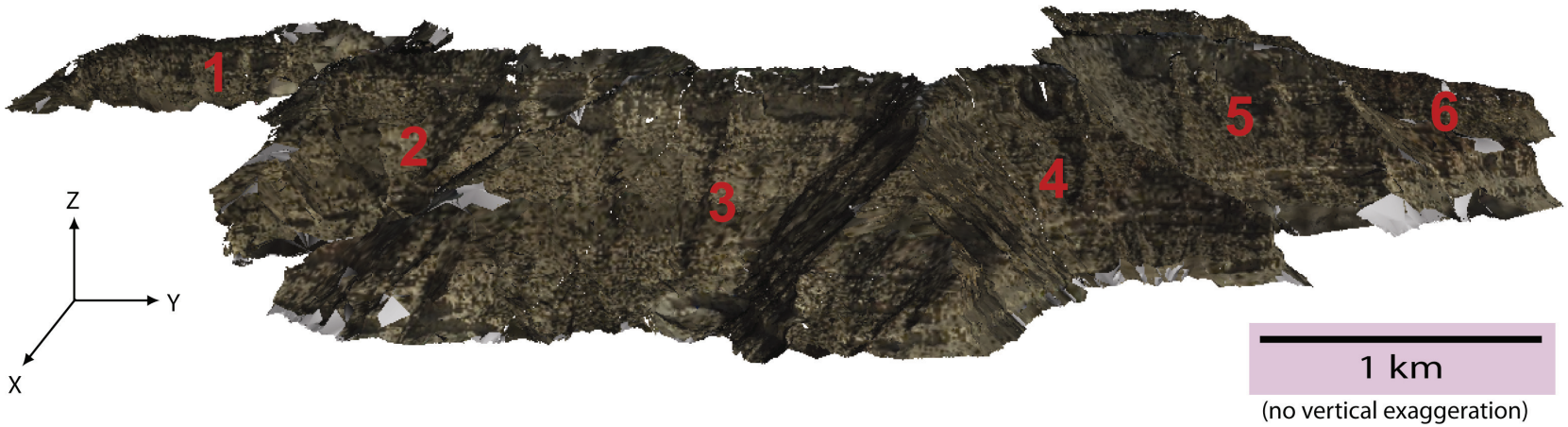

Figure 3.5. LIDAR data of the six cliff-faces in Cottonwood Creek that illustrates 3D virtual outcrop of fluvial strata of the Blackhawk Formation for ~25 km^2 area.

Subsequent to this step, using PolyWorks version 11.0.12, triangulation of the thinned point cloud is pursued that creates a digital terrain model called mesh based on triangles connecting the individual points of the point cloud (Bellian et al. 2005; Buckley et al. 2008b). This mesh is then textured with the digital photos based on optimal angles of the photos and their distances in relation to the mesh. Draped with digital photos, the final model is processed to contain high resolution to low resolution mesh to make the virtual outcrop model responsive to user zoom preference as well as hardware efficiency (Buckley et al. 2008a). In essence, developed virtual outcrop model is a photorealistic three-dimensional depiction of an outcrop, which can readily be interrogated for geological analysis.

On this virtual outcrop model, the base and top of individual channel-storey sandbody were mapped by tracing their continuity from cliff face to cliff face (Figures 3.6, 3.7). These mapping informations were saved as individual ASCII file. Subsequently, each ASCII file was exported onto ArcMap interface to correct the width extent of that sandbody with respect to paleoflow direction. Then, from these corrected data, basal and top topographic surfaces of that sandbody were created on ArcMap and illustrated on ArcGIS (Figure 3.7). Finally, 3D volume of that sandbody was generated by extruding between the top and basal topographic surfaces (Figure 3.7). Generated 3D geobodies of channel-storey sandbodies were populated for fluvial analysis (Figure 3.8).

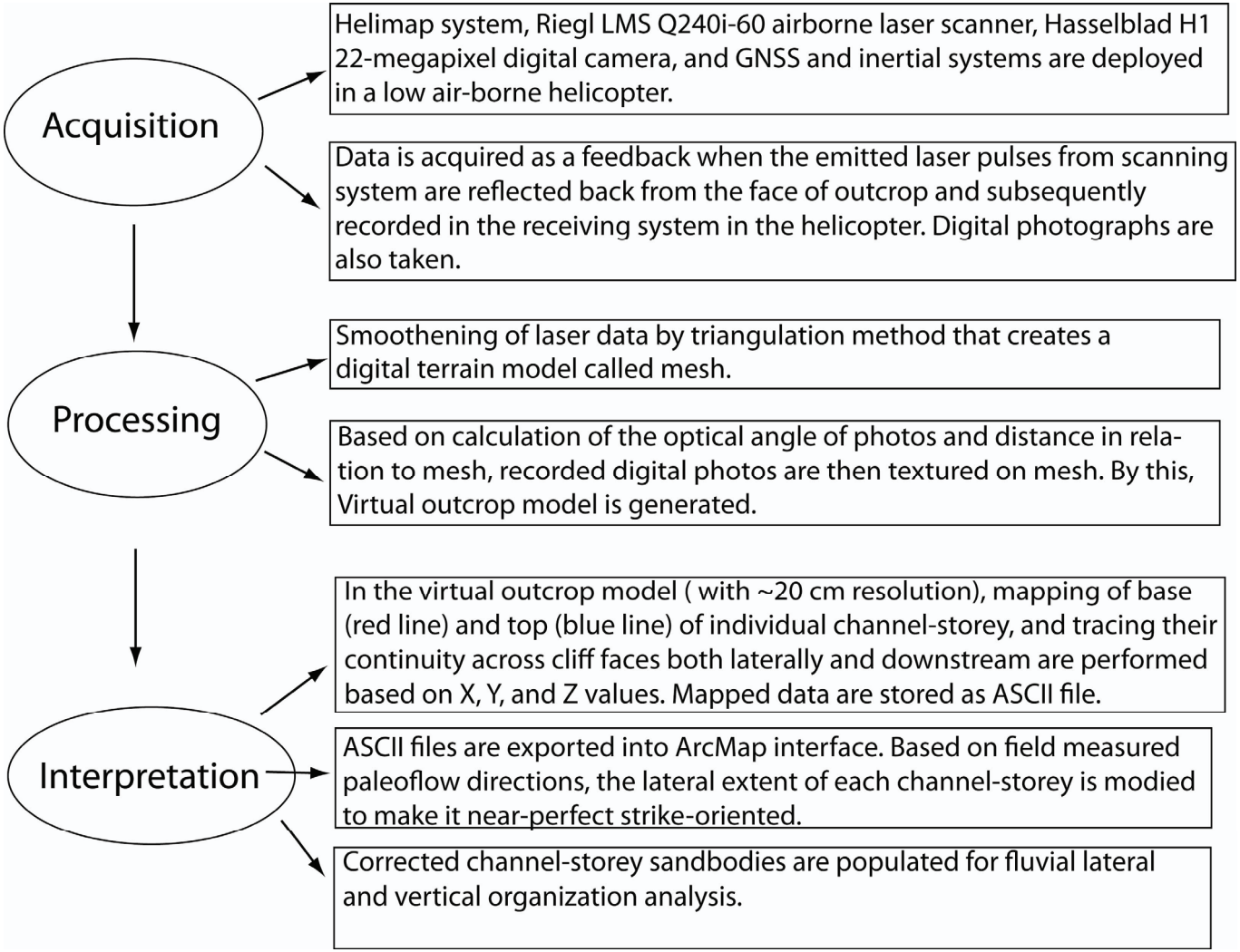

Figure 3.6. Flow chart diagram describing from data acquisition to processing to interpretation of LiDAR data.

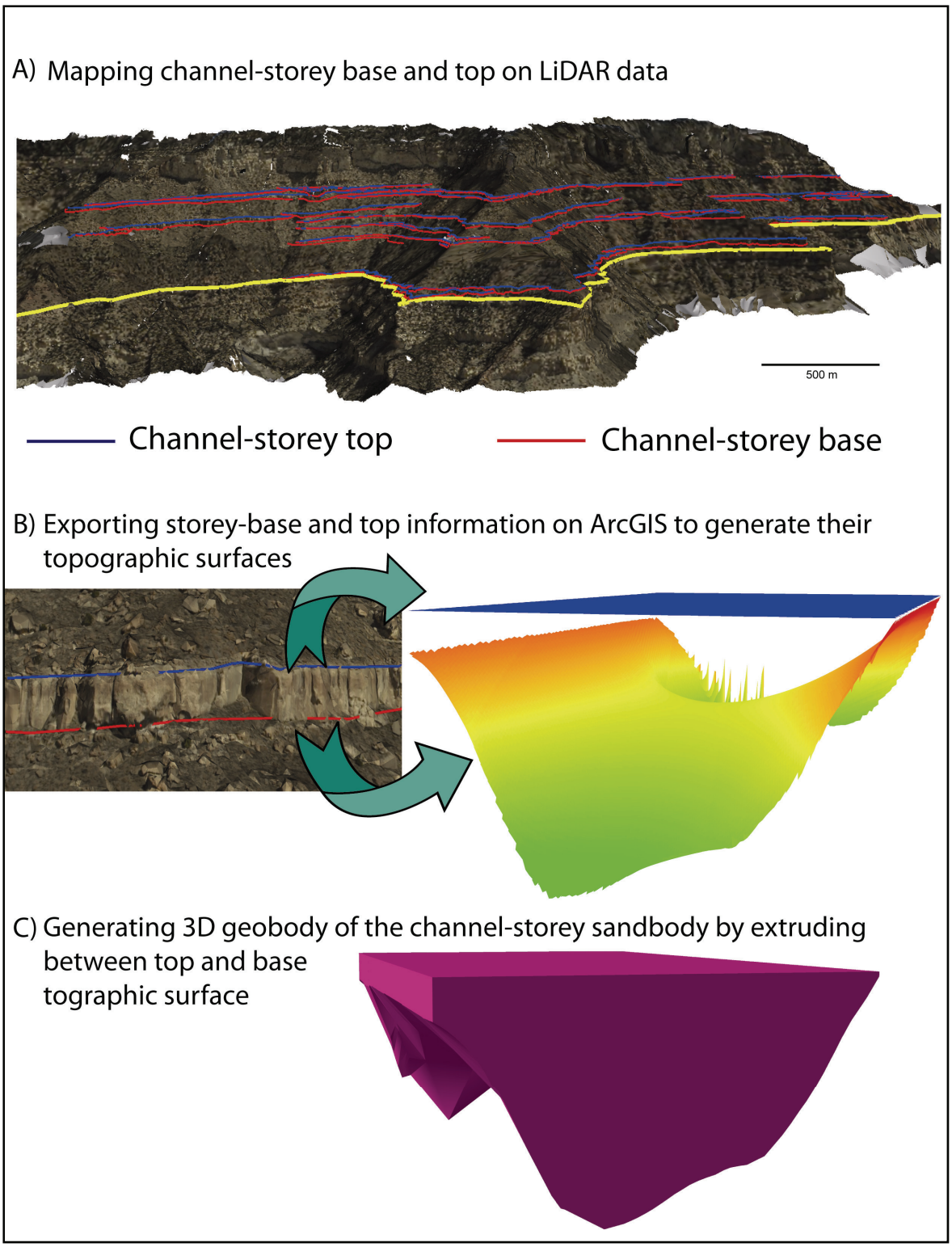

Figure 3.7. Steps followed for the 3D volume body creation of individual channel-storey sandbody on the LiDAR data.

3.4 Results and Discussions

Existing conceptual fluvial models as described in Gibling (2006) provide illustration of tying channel lateral mobility to avulsion-related reoccupation, but do not emphasize lateral characterization of channelized sandbodies. This lateral characterization, as a manifestation of channel mobility, needs to be evaluated for its control on channel avulsion (e.g. Hajek et al., 2010). There exists an ambiguity when studies (i.e. Pranter et al., 2009; Hofmann et al., 2011) have combined multi-storey and multi-lateral channelized sandbodies in the same category, creating confusion about scale relationships. Multi-storey (vertically-stacked) sandbodies happen at different temporal-scale (hence, avulsion-mandated), whereas multi-lateral sandbodies happen at same temporal-scale (i.e. same stratigraphic level; hence, indicative of lateral migration of the same channel). This distinction can have implication towards avulsion dynamics and, in that context, the differentiation of single-storey, multi-lateral and multi-storey is pertinent (Figure 3.9). However in most cases, conventional data render insufficient for a detailed characterization of these fluvial depositional elements. Subsurface core and well data (e.g. Sinha et al., 2005; Hofmann et al., 2011) cannot constrain this lateral storey issue to its fullest extent, given their limited lateral extent. Seismic data cannot resolve truncation of individual channel-storeys juxtaposed laterally. Even, 2D cliff face outcrop data may miss the full extent of lateral juxtaposition of single-storeys forming a channel-belt if it extends to a different cliff face. More importantly, on different and adjoining 2D cliff face outcrop data, joining two or more individual single-storey sandbodies is problematic in absence of precise coordinate values (X, Y, and Z). To remedy this inadequacy of 2D outcrop data, LiDAR integration with its georeferencing precision offers a true 3D rendering of channelized

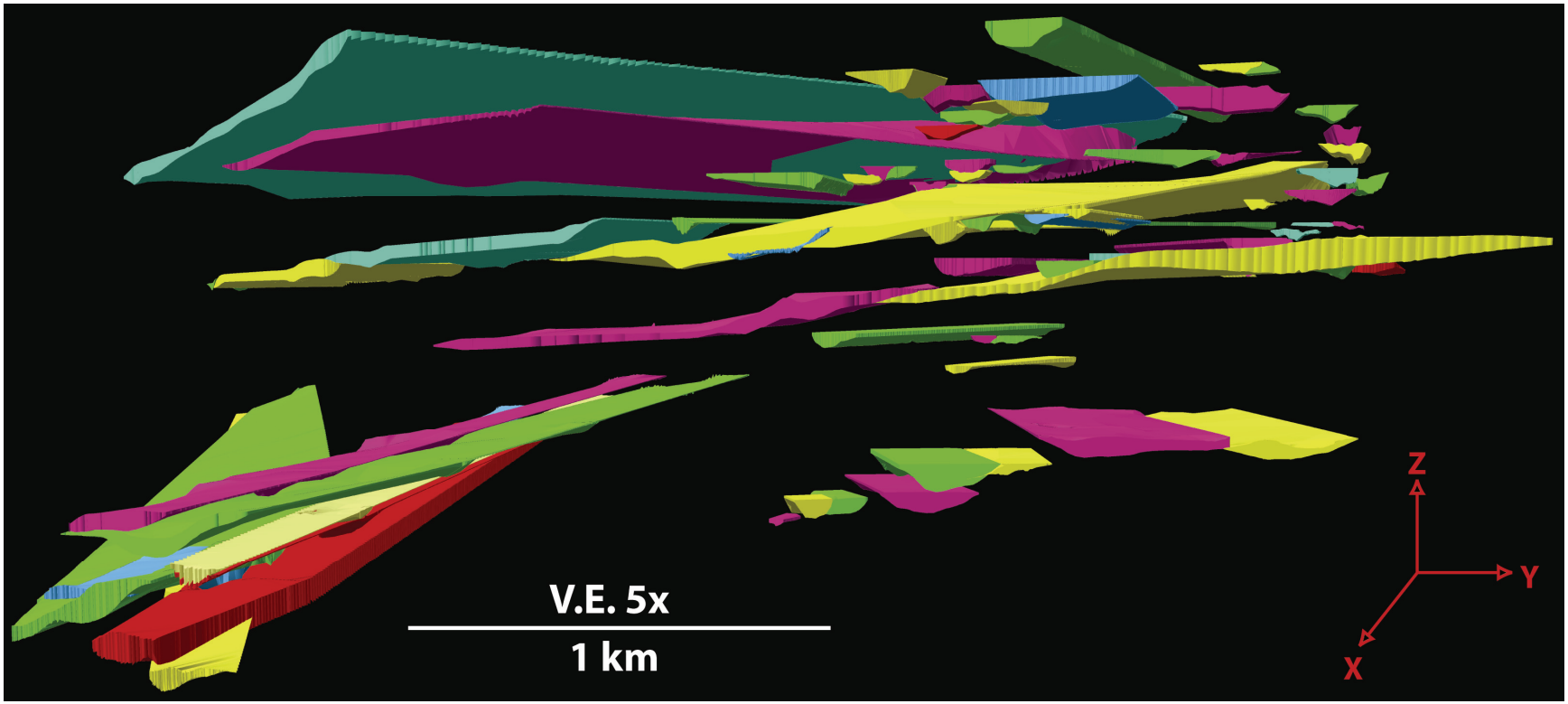

Figure 3.8. 3D perspective view of the individual channel-storey sandbodies of the Blackhawk Formation. This LiDAR-extracted geobody creation achieved down to single channel-storey level illustrates 3D volume distribution of channel-storey sandbodies as analogous fluvial reservoir suite encased with flow-barrier fine-grained coastal-plain deposits (background black color).

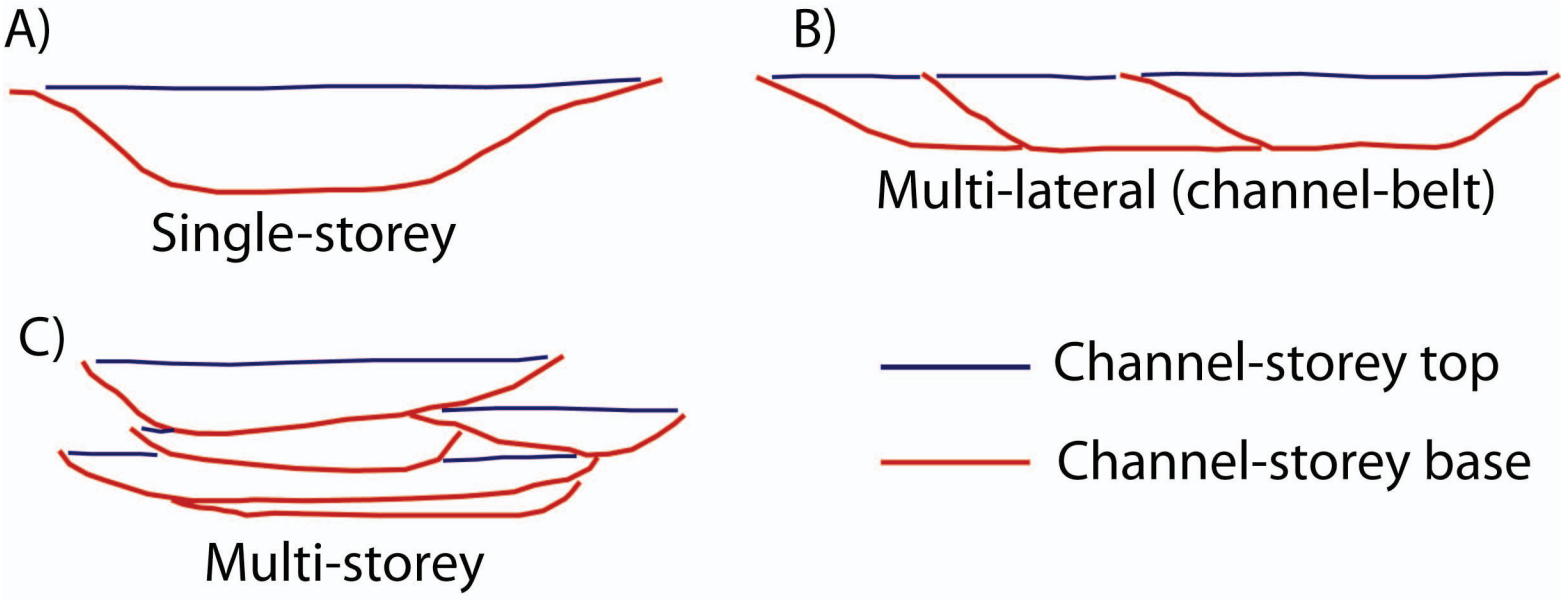

Figure 3.9 Schematic diagram of channelized sandbodies consistent to their genesis relationship. A) Single-storey represents a single bar-macroform combined with its laterally-adjacent channel-fill deposit. B) Multi-lateral sandbody (i.e. channel-belt deposit) is developed when discrete bar deposits are laterally stacked together at the same stratigraphic level. C) Multi-storey sandbody is developed due to vertical juxtaposition of successive single-storey and/or channel-belt sandbodies.

sandbodies in the outcrop (Figures 3.5-3.8). Our acquired LiDAR data were integrated to the outcrop analysis of the entire Blackhawk Formation at a sufficient spatial (5 x 5 km^2) and temporal (~ 4 my) scale in the Western Interior Seaway, Utah. To minimize error margin and maximize near-perfect representation of sandbody dimension, we have focused only on fully preserved sandbodies and their proper orientation were attained through alignment corrections based on ample paleocurrent data (n= ~100; acquired physically through climbing the entire Blackhawk Formation in the LiDAR acquired study area). Study results bring multiple insights of fluvial organization, as comprehended henceforth.

3.4.1. Channel Storey Relationships:

From LiDAR extraction and subsequent correction with respect to paleoflow direction, the dimensional extent of fully-preserved channelized sandbodies has been attained to their near-perfect spatio-temporal position. Populating generated 3D geobodies of near-perfect individual channel-storey sandbodies contributes to a robust illustration of analogous reservoir suite (i.e. sandbody) encased within flow-barrier element (i.e. floodplain fines; background black color; Figure 3.8) for subsurface reservoir characterization. Development of single-storey sandbodies, their lateral stacking leading to channel-belt development (i.e. multi-lateral sandbody), vertical stacking of single-storey and/or channel-belt (i.e. multi-storey sandbody) resulting in channel-belt complex formation have been robustly captured on the projected 2D outcrop template of the Blackhawk Formation (Figure 3.10). This enhanced characterization, which could otherwise be hard to obtain from 2D outcrop data alone, contributes towards robust understanding of fluvial organization in the rock record. In the lower Blackhawk Formation, channel-belt (multi-

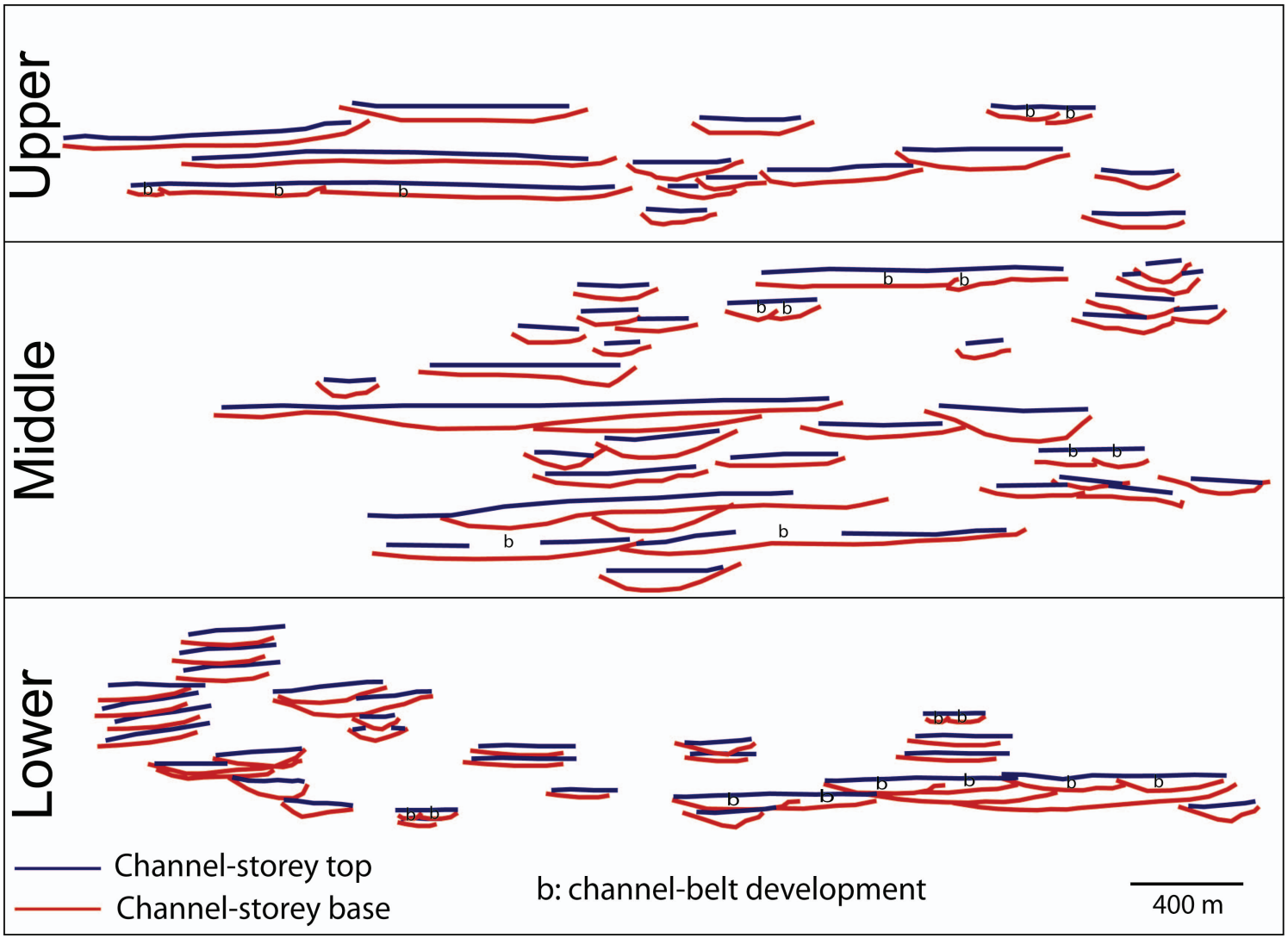

Figure 3.10. 2D projection of fully-preserved 3D channelized sandbodies of the Blackhawk Formation on a strike-transect shown in Figure 3.3A. Broadly, the lower unit is compensational and shows more channel-belt development (multi-lateral sandbodies). However, less compensational-stacking and more clustering are better developed in the middle and upper units. See test for discussion.

lateral) sandbodies are relatively well-developed, whereas the middle and upper Blackhawk Formation show preferential manifestation of single-storey channelized sandbodies. The dimension (both thickness and width) of single-storey as well as channel-belt sandbodies increases from lower to upper Blackhawk Formation. This observation broadly matches with the paleohydraulic estimates of each units of the Blackhawk Formation that were calculated from sedimentological information (cross-stratification thickness, bar-accretion thickness etc.) (Figure 3.11).

Morphological parameters of formative rivers of the Blackhawk Formation

Stratigraphic position	Flow depth (m)	Channel width (m)	Channel-belt width (m)	Sinuosity
Upper Blackhawk	9	160	1,800	1.5
Middle Blackhawk	7	110	1,200	1.6
Lower Blackhawk	6	80	1,000	1.7

Figure 3.11. Paleohydraulic estimation of the formative rivers of the Blackhawk Formation. Note that rivers were increasingly larger in size stratigraphically upward.

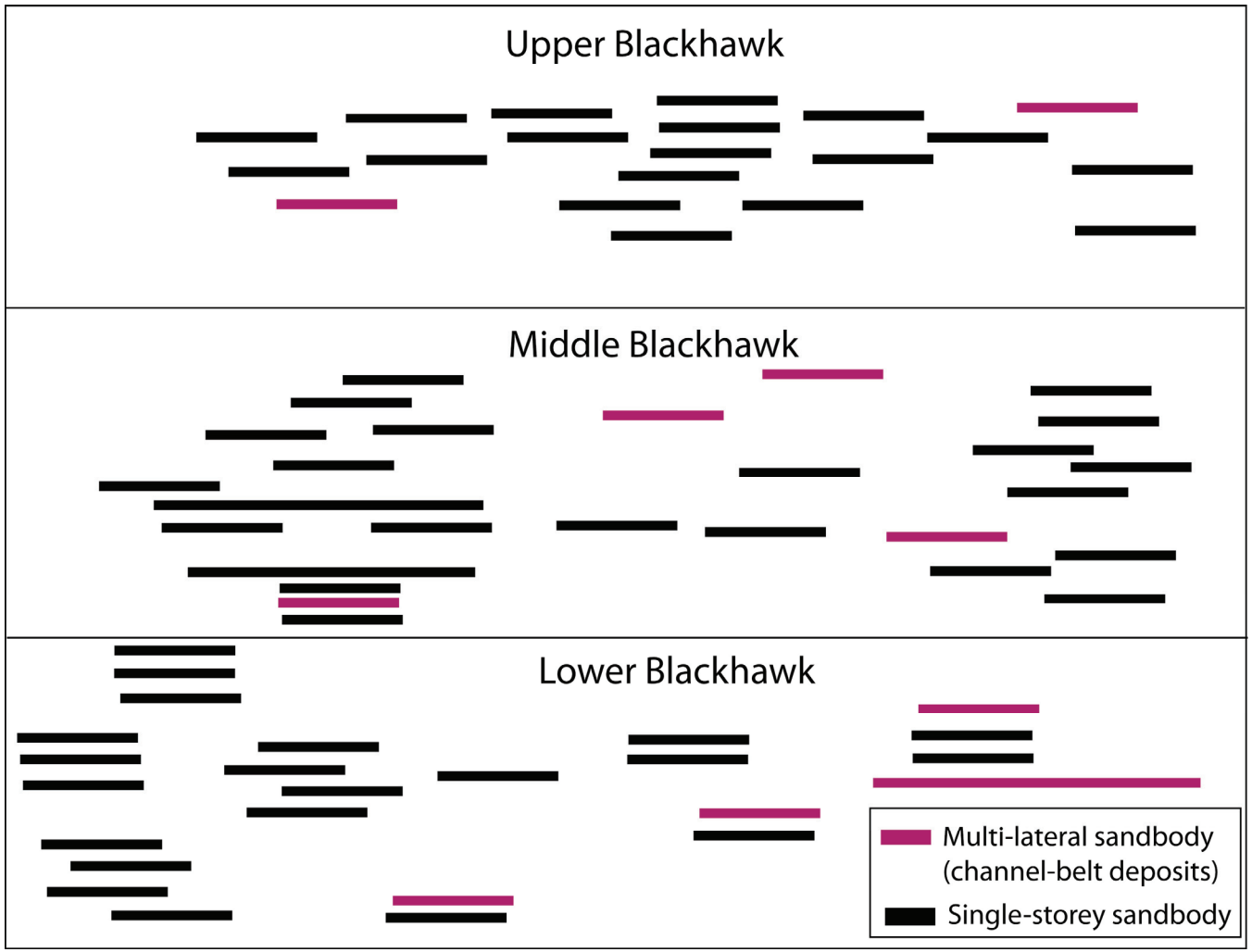

Figure 3.12. Schematic representation of fluvial sandbody distribution of the Blackhawk Formation in the study area. Note: 1) compensational-stacking phenomenon linked to the development of multi-storey lateral sandbodies is apparent in the lower Blackhawk Formation, where floodplain lithologic diversity is high, 2) Middle Blackhawk Formation is moderately compensational to clustered (well developed cluster pockets) with moderate floodplain diversity; 3) Upper Blackhawk Formation is mostly undifferentiated clustered where floodplain diversity is least.

3.4.2. Higher-order Fluvial Organization Analysis

Channelized sandbodies of the Blackhawk Formation projected on a 2D template diagram (Figure 3.10) demonstrate nonrandom vertical fluvial organization structured into two end-member types: clustered and compensationally-stacked. The lower Blackhawk Formation is broadly compensational with localized zones of clustering, middle Blackhawk Formation is moderately compensational to clustered, and the upper Blackhawk Formation is mostly clustered overally (Figures 3.10, 3.12). Empirical observation suggests that single-storey channelized sandbodies show affinity to clustered phenomenon, with or without vertical amalgamation, in all units of the Blackhawk Formation. In contrast, multi-lateral (i.e. channel-belt development) sandbodies are more compensational in nature. Linking the degree of lateral channel activity (i.e. single-storey vs. multi-lateral) to compensational and clustering phenomena has not been documented in previous avulsion studies (e.g. Hajek et al., 2010; Hofmann et al., 2011). Further detailed study is needed for comprehension of this intriguing link. However, this study provides one likely explanation that the observed fluvial organization from clustered to compensationally-stacked in different units of the Blackhawk Formation could have been modulated by a constraining effect of floodplain facies heterogeneity towards channel avulsion dynamics, as discussed henceforth.

3.4.3 Floodplain Diversity Analysis

Relationship between floodplain facies characteristics and avulsion dynamics is virtually unknown to date (e.g. Hajek and Wolinsky 2012). Floodplain deposition is mainly accrued by either flooding, crevassing (incomplete avulsion) or complete avulsion, which in turn provides to development of floodplain internal complexity. However, how this floodplain facies heterogeneity facilitate or hinder channel avulsion dynamics at both spatial and temporal scales is not well realized. By assessing floodplain facies diversity at each unit of the Blackhawk Formation, this study attempts to assess this aspect. In the lower Blackhawk Formation, floodplain diversity is the highest due to a diverse facies assemblage (Figure 3.13). In contrast, floodplain diversity is low to least for the middle and upper Blackhawk Formation (Figure 3.13). Here, two possible explanations are provided to describe this varying degree of floodplain diversity. First, rivers in the lower Blackhawk Formation are relatively sand-prone that delivered relatively more coarser sediments to floodplain during flooding and levee-breaching events, contributing to more overbank and crevasse splay sandbodies as shown in the pie diagram (Figure 3.13). Increased floodplain facies diversity can lead to increased lateral activity of channels (i.e. heterogeneous banks are relatively easy to erode), resulting in multi- lateral sandbodies. Moreover, laterally-heterogeneous floodplain compensation (differential compaction) linked to floodplain facies diversity, can lead to compensational channel stacking, which the lower Blackhawk unit manifests. In contrast, rivers in the middle and upper Blackhawk Formation are relatively mud-prone. Hence, relatively more finer sediments were delivered to floodplain area, as manifested by less proportion of overbank and crevasse splay sandbodies in these two units (Figure 3.13). Decreased floodplain facies diversity can lead to

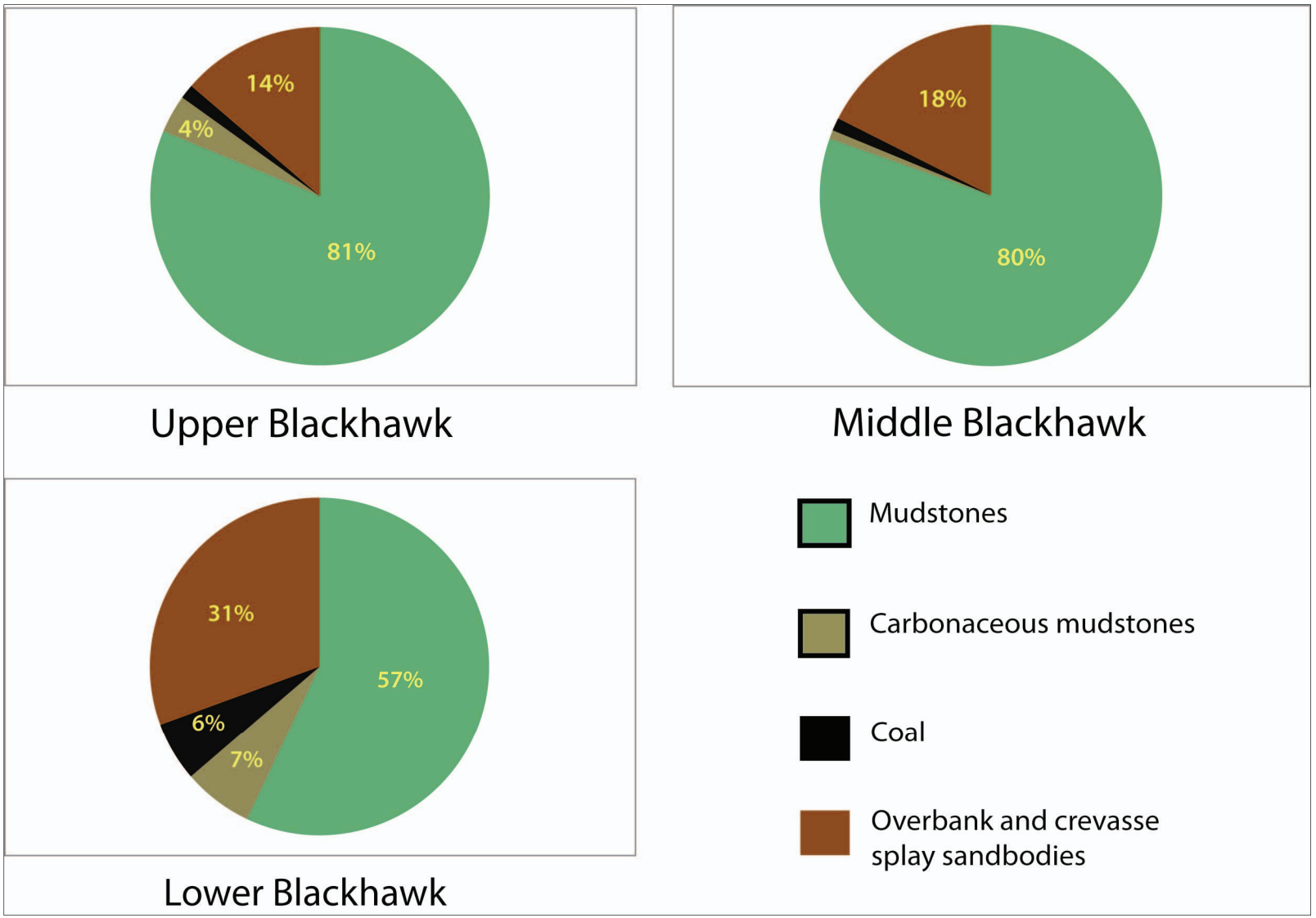

Figure 3.13. Pie diagram of facies assemblage nested within floodplain area of the lower, middle and upper Blackhawk Formation.

decreased lateral activity of channels (i.e. homogenous muddy banks are relatively hard to erode), resulting in single-storey sandbodies. Moreover, laterally-homogenous floodplain compensation can disfavor compensational channel stacking.

Alternatively, assuming the rivers of lower to upper Blackhawk Formation are of similar character instead of varying sand-prone to mud-prone attribution, the second plausible explanation is the varying degree of flooding events for the lower to upper Blackhawk units. As distal distributary threads of the feeder trunk river, rivers in the lower Blackhawk Formation are of smaller size and located in the coastal-plain closer to the paleoshoreline (e.g. Hampson et al., 2012). In this setup, they are more likely to experience frequent flooding. More flooding can route more coarser sediments to floodplain leading to heterogeneous floodplain development, which has been shown for the lower Blackhawk Formation (Figure 3.13). In contrast, rivers in the upper Blackhawk Formation are of larger size demonstrative of a trunk river system located further upstream from the paleoshoreline (e.g. Hampson et al., 2012). In this setup, flooding frequency in those rivers would be less, which, in turn, will hinder routing of coarser sediments to floodplain area, resulting in relatively more homogeneous floodplain (Figure 3.13).

3.5 Conclusions

This study emphasizes the utility of emerging photorealistic technology like the LiDAR in conventional outcrop investigation. The integrated characterization documented here yields far more robust results than can be achieved with conventional outcrop-based investigation alone. Study results provide a high-resolution fluvial organization analysis at the scale of individual

channel-storey level. Our 3D virtual outcrop model provides precise control to analyze sedimentologic-stratigraphic elements in 3D orientation such that both depositional-strike and -dip segments of stratigraphic elements like channelized sandbodies are adequately constrained with proper georeferencing. Mapping of channelized sandbodies using this model (~20 cm resolution) through tracing their continuity across cliff faces with X, Y, and Z control have resulted in capturing of sandbody organization in space and time. Sandbody organization down to the scale of individual channel-storey has been documented: single-storey, multi-lateral (channel-belt), and multi-storey sandbodies. The lateral extent of individual single-storey sandbody has been corrected with respect to paleoflow direction such that near-perfect, strike-oriented width of fully-preserved single-storey sandbody has been attained. Similarly, strike-oriented extent of channel-belt sandbody (lateral-stacking of individual single-storey at the same stratigraphic level) and multi-storey sandbody (vertical-stacking of single-storey and/or channel-belt at different stratigraphic level) have also been constrained from this virtual outcrop model. Study results demonstrate that channel-belt sandbodies show good development in the lower Blackhawk Formation, whereas the middle and upper Blackhawk Formation are more apparent with the development of single-storey sandbodies. Higher-order fluvial organization analysis reveals that single-storey sandbody show affinity towards clustering phenomenon. On the other hand, compensational-stacking was generated preferentially by channel-belt sandbodies. At the stratigraphic-scale, sandbodies of the lower Blackhawk Formation are broadly compensationally-stacked, whereas they show more vertical-clustering phenomenon for the middle and upper Blackhawk Formation. Floodplain facies diversity is high for the lower Blackhawk Formation, within which sandbodies are prone to compensational-

stacking, but low for the middle and upper Blackhawk Formation, where sandbodies are more clustered.

Chapter 4

Autogenic control on allogenic forcing of incised valley formation in rock record

Abstract

Fluvial organization filling incised valleys has traditionally been interpreted to be primarily modulated by allogenic controls like sea-level fluctuations. This allogenic control invokes that 1) a depocenter develops when channel avulsion dynamics is confined to a portion of the basin, and 2) channel sandbody aggradation/amalgamation results when sustained channel occupancy lingers on the same portion of the basin. This attribution of allogenic-controlled mechanism has been overwhelming to the extent that the possibility of autogenic mechanism controlling fluvial organization of incised valley fills was largely overlooked. This has been mainly due to the fact that de-convolving autogenic from allogenic signals remains challenging in the rock record, particularly for incised valley fill deposits. Using an integrated LIDAR, outcrop and core data, we isolate controlling mechanism of autogenic from allogenic process (es) within two successive incised valley fill deposits in the lower Blackhawk Formation (upper Cretaceous) of the Western Interior Seaway, Utah. We illustrate fluvial sandbody organization like depocenter location and sandbody amalgamation trend that can be attributed to a supplanting mechanism of autogenic over allogenic behavior. Studied two incised valley fill deposits, each of which is up to ~15-20 m thick, demonstrate an interplay of both autogenic and allogenic

behavior varying at spatial scales such that they constitute autogenic-controlled and mixed-controlled incised valley fills, unlike conventionally invoked allogenic-controlled type. Differential subsidence linked to underlying coal thickness was the major autogenic control filling incised valleys in our study area. Illustrated supplanting mechanism of the autogenic behavior, when linked at these two successive sequence cycles, appears to be non-compensational in nature. The key implication of this study is that all traditional interpretation of paleovalley fluvial architecture should not be automatically attributed to allogenic modulating processes.

4.1 Introduction

There is a greater degree of unanimity in our current understanding of incised valley fill (henceforth "IVF") that the lower part of coastal-plain IVF comprises amalgamated fluvial sandbodies overlying on an erosional composite surface which is a sequence boundary (e.g. Shanley and McCabe, 1994; Blum et al., 2013). These thicker sandbody suites are deposited in a low accommodation regime mostly during lowstand sea-level rise. Driven by this traditional knowledge, preserved amalgamated fluvial architecture in IVF style deposition, has long been interpreted to be primarily modulated by sea-level fluctuation (an allogenic control). As a consequence, the possibility of autogenic mechanism controlling resultant fluvial organization of IVF has been overlooked. Our study is motivated by the latest observations that: 1) independent of allogenic mechanism, autogenic process can structure amalgamated fluvial organization (e.g. Hampson et al., 2013; Hajek et al., 2012), and 2) autogenic process can

operate at comparable time-scale to that of allogenic mechanism (e.g. Paola et al., 2009; Muto et al., 2007).

Although the convolution of both autogenic and allogenic signals operating in a dynamic natural system like incised valleys is well perceived, differentiating one from the other remains challenging owing to the complexity of this interplay, and equivalent potential of both in sculpting similar fluvial organization (e.g. Blum et al., 2013). One effective way to characterize this differentiation is to find a suitable fluvial organization in a paleovalley architecture that should show discord to modulation of allogenic process like this: how can lateral variation of fluvial organization resulted within a paelovalley be best explained by an allogenic mechanism which is ideally causative of vertical variation of fluvial organization. Conversely, if this variation is correlated with variability of an autogenic mechanism acting during that time, then it merits to be argued that resultant fluvial organization is preferentially controlled by this autogenic rather than allogenic process? This type of distinction has never been attempted in IVF style interpretation of Quaternary, rock record or laboratory experimental studies.

Jerolmack and Paola (2010), based on experimental and numerical study, suggested a threshold value of autogenic signal such that if the amplitude of allogenic signal is below of that threshold value, then it is overprinted by autogenic signal, and consequently never gets reflected in depositional organization. This finding has never been tested in the rock record. Based on this finding and taking IVF as an example, we can build several follow-up questions: 1) Does this filtering process act as a "one to one pass" such that, it is entirely either allogenic-controlled or autogenic-controlled at IVF system scale?, 2) Can both controlling mechanisms co-exist at a spatial scale within the system?, and 3) How these controlling mechanisms traverse in

time in successive IVF style sequences? The objective of our study is to analyze these unknown aspects of IVF style deposition.

4.2 Regional and Geological Context

The studied dataset belong to the lower unit of the Blackhawk Formation, which was deposited along the western margin of the Cretaceous North American Western Interior Seaway (e.g. Krystinik and Dejarnett, 1995). The lower Blackhawk Formation constitutes a mud-prone coastal-plain strata that exhibits numerous well-developed, and regionally extensive coal zones, which were used to develop a high resolution sequence stratigraphic framework of the region (e.g. Dubiel et al., 2000; Hampson et al., 2012). Study area is located in the Cottonwood Creek of the eastern Wasatch Plateau where the Blackhawk Formation crops out in a series of clean, contiguous, and vertical cliff-faces (Figures 4.1).

We target our analysis on two IVFs interpreted (Figure 14 of Hampson et al., 2012) in the study area (Figures 4.2; 4.3). Their attribution to IVF style deposition is based on documented sedimentologic and stratigraphic features: 1) their base is characterized with deep incision, and the basal composite surface is highly erosional and areally extensive, 2) this basal surface is coevally correlated with matured paleosols in the interfluves , and 3) they show multi-storeyed sandbody organization at the bottom, but increasing floodplain preservation towards top, thus recording upward increase in accommodation during valley infilling cycle (e.g. Zaitlin et al., 1994; Reynolds, 1999; Gibling 2006; Hampson et al., 2012). In absence any documented other IVF style deposition between these two so far, we make a note that IVF1

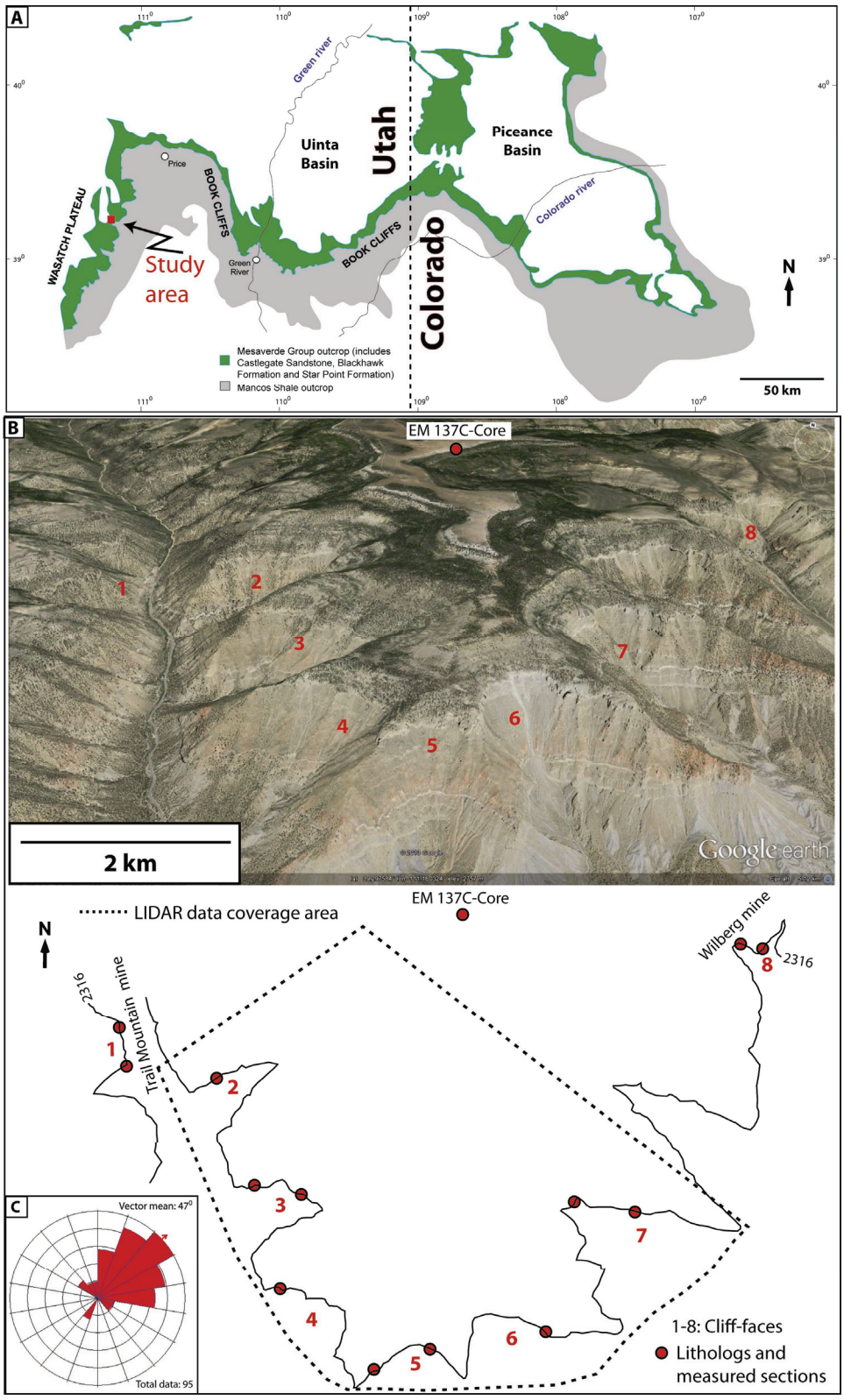

Figure 4.1 A) Location of study area in the Wasatch Plateau, central Utah. The upper Cretaceous Blackhawk Formation (Mesaverde Group) deposited in a coastal-plain setting, crops out in the study

area in a coastal-plain setting. B) Google Earth view (upper) and map view of the studied outcrop dataset comprising eight contiguous, and vertical cliff faces (1-8), and one core (2316 m contour line is shown for reference). C) Paleocurrent rose diagram for dune and ripple cross-strata of the studied outcrop showing an overall northeast direction.

was deposited in a sequence cycle superseded by another sequence cycle where IVF2 was deposited (Figure 4.2).

For a detailed documentation of these two IVFs, we have used an integrated dataset comprising LiDAR, outcrop, and a subsurface core data. Low airborne LiDAR data were acquired on centrally-located, six near-clean, contiguous, and vertical cliff-faces (Figures 4.1B; 4.4). Its acquisition method, and data processing steps have been detailed in Rittersbacher et al., 2012. This LiDAR data is properly geo-referenced, thus, contains three dimensionality of these two IVFs on cliff-faces. For ground-truthing of these two IVFs, outcrop documentation has been pursued on eight adjacent cliff-faces (Figure 4.1B) by performing bedding architecture analysis on photomosaic panels (e.g. Figure 4.2C), and constructing lithologs and measured sections for their lithofacies description (Figure 4.3). A differential GPS of sub-meter accuracy has been used for spatial documentation. Also, we have incorporated a subsurface core data to our analysis that provides additional data control (Figure 4.1B). Two regionally extensive coal zones- Axel-Anderson and Blind Canyon coal zones have been documented on outcrop photomosaics, measured sections, LiDAR, and core data. These two coal zones vary in thickness (0.1-5 m) spatially, and provide the datum for mapping of the two IVFs: Axel-Anderson coal zone for overlying IVF1, and Blind Canyon coal zone for overlying IVF2. This combined dataset provide following descriptions for IVF1 and IVF2: 1) they are larger, amalgamated channel sandbody complexes produced by vertical stacking of ~ 3-4 channel-storeys, showing maximum thickness

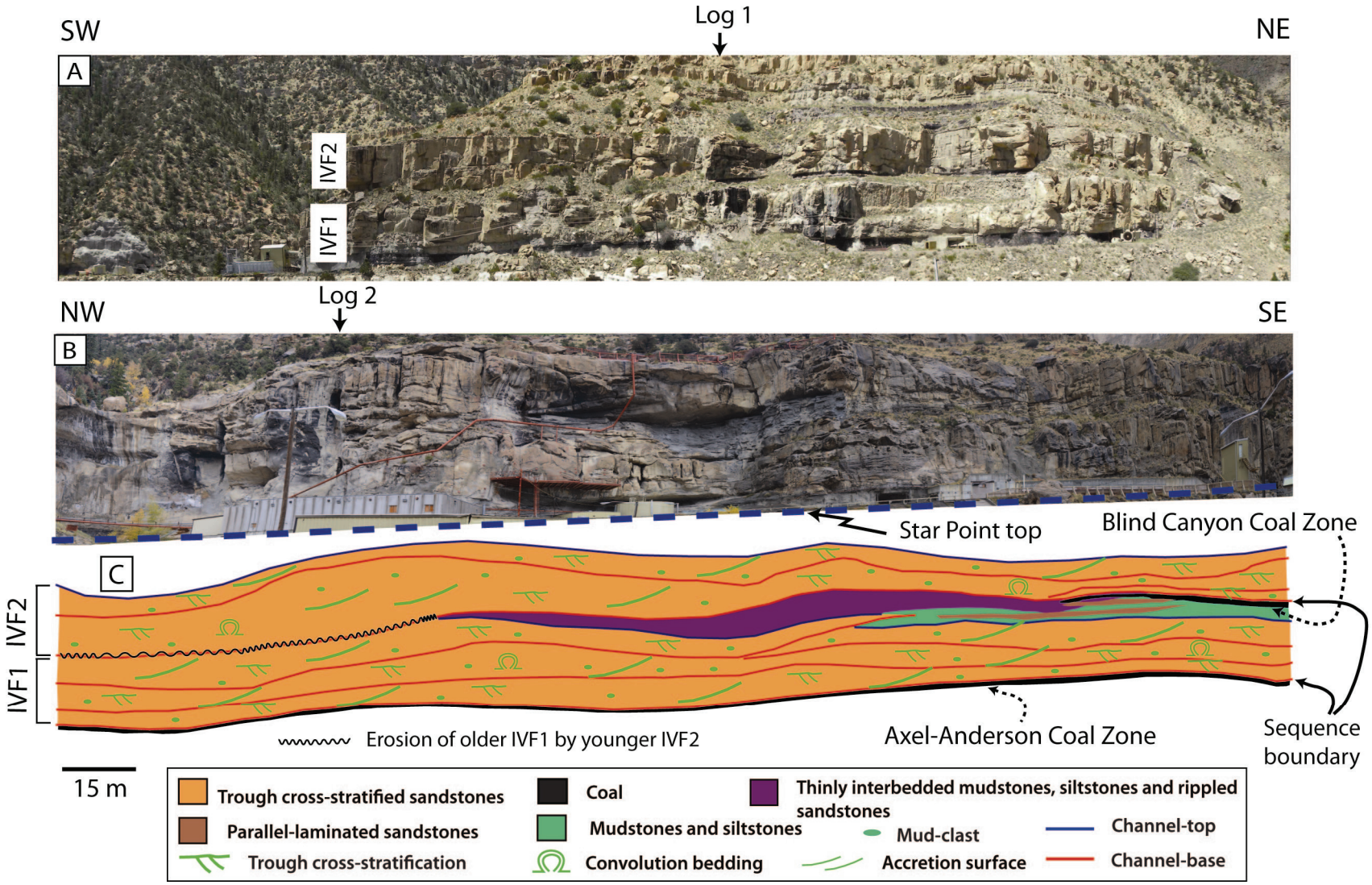

Figure 4.2 Outcrop expression of the two Incised Valley Fill (IVF) deposits at Wilberg Mine (for location, see Figure 4.1B). A) Two IVFs on the depositional-dip oriented section. B) Two IVFs on the depositional-strike oriented section where the overlying IVF2 erodes into underlying IVF1. C) Line drawings of facies distributions with sedimentary structures on the photomosaic panel of this outcrop.

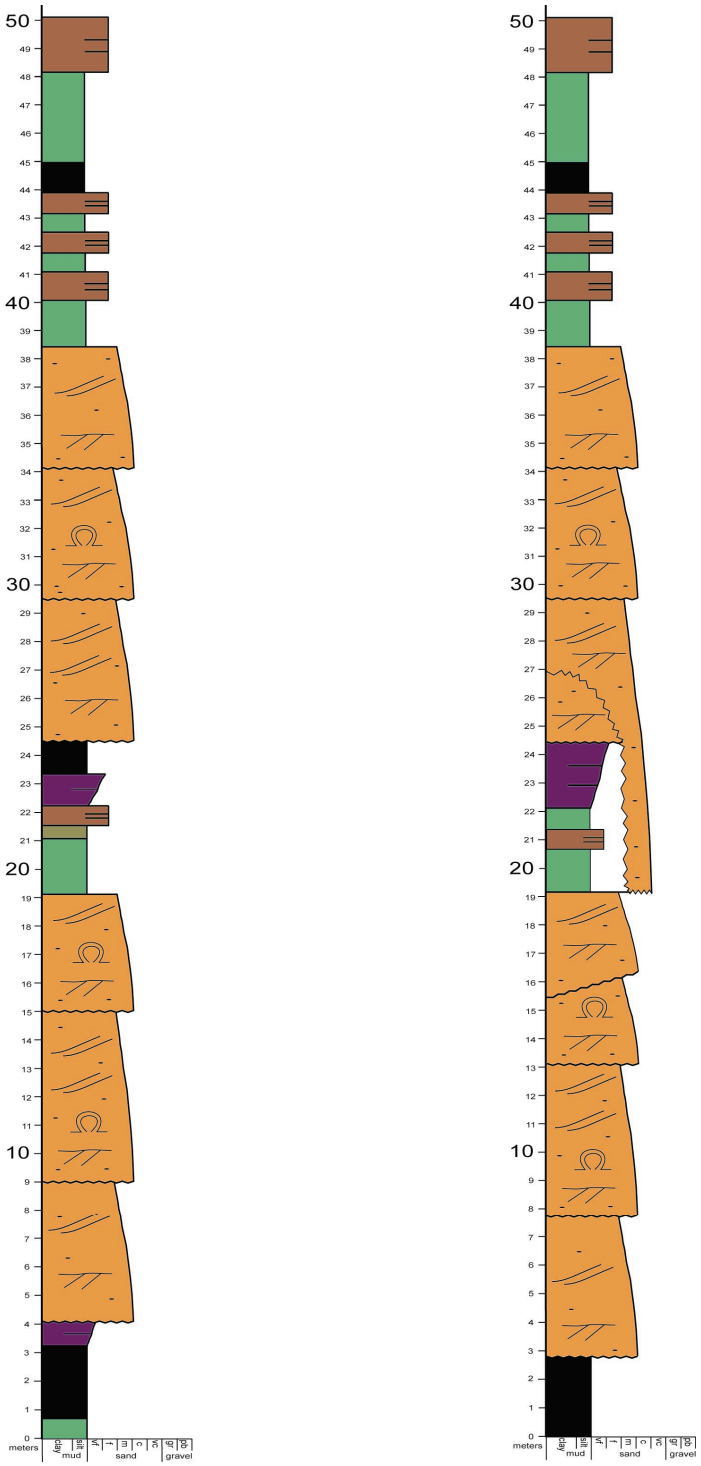

Figure 4.3 Vertical description of two lithologs (for location, see Figure 4.2). Note, IVF2 eroding into IVF1 in Log 2.

of up to ~15-20 m, and 2) internally, they contain predominantly dune cross-stratification, and mud rip-up clasts in addition to localized and patchy convolution bedding (Figures 4.2; 4.3).

Our dataset area (~25 km^2; Figure 4.1B) is broadly aligned in the regional depositional-strike orientation, located c. 50 km landward from coeval shoreline (Hampson et al., 2012). We generated isopach map of sandbody amalgamation thickness for each IVF at the distribution scale of our dataset (Figure 4.5A-B). For thickness analysis of both the Axel-Anderson and Blind Canyon coal zones, we have used the coal map data of Energy West Mining Company and Utah Geological Survey (i.e. Tabet et al., 1999; Gloyn et al., 2003).

4.3 Discussions and Conclusions

Isopach maps of sandbody amalgamation thickness of these two IVFs show preferential depocenter locations where vertically stacked sandbodies shows higher thickness (Figures 4.5A-B). We correlated this observation against available coal datasets of both local coal mining company (i.e. Energy West Mining Company) and Utah Geological Survey (i.e. Gloyn et al., 2003; Tabet et al., 1999), respectively. Interestingly, we found that thickness trend of sandbody amalgamation of both IVFs provided matching correlation to the varying thickness of underlying coal deposition (Figures 4.5A-D). This positive correlation suggests that coal-precursor peat compaction exerted first order control in guiding channel steering and subsequent fluvial organization in these two incised valleys. This channel-steering phenomenon is consistent to documented observation in other coal-bearing basins where coal-precursor peat compaction, through its preferential accommodation creation, acts as an inducing agent steering channels to

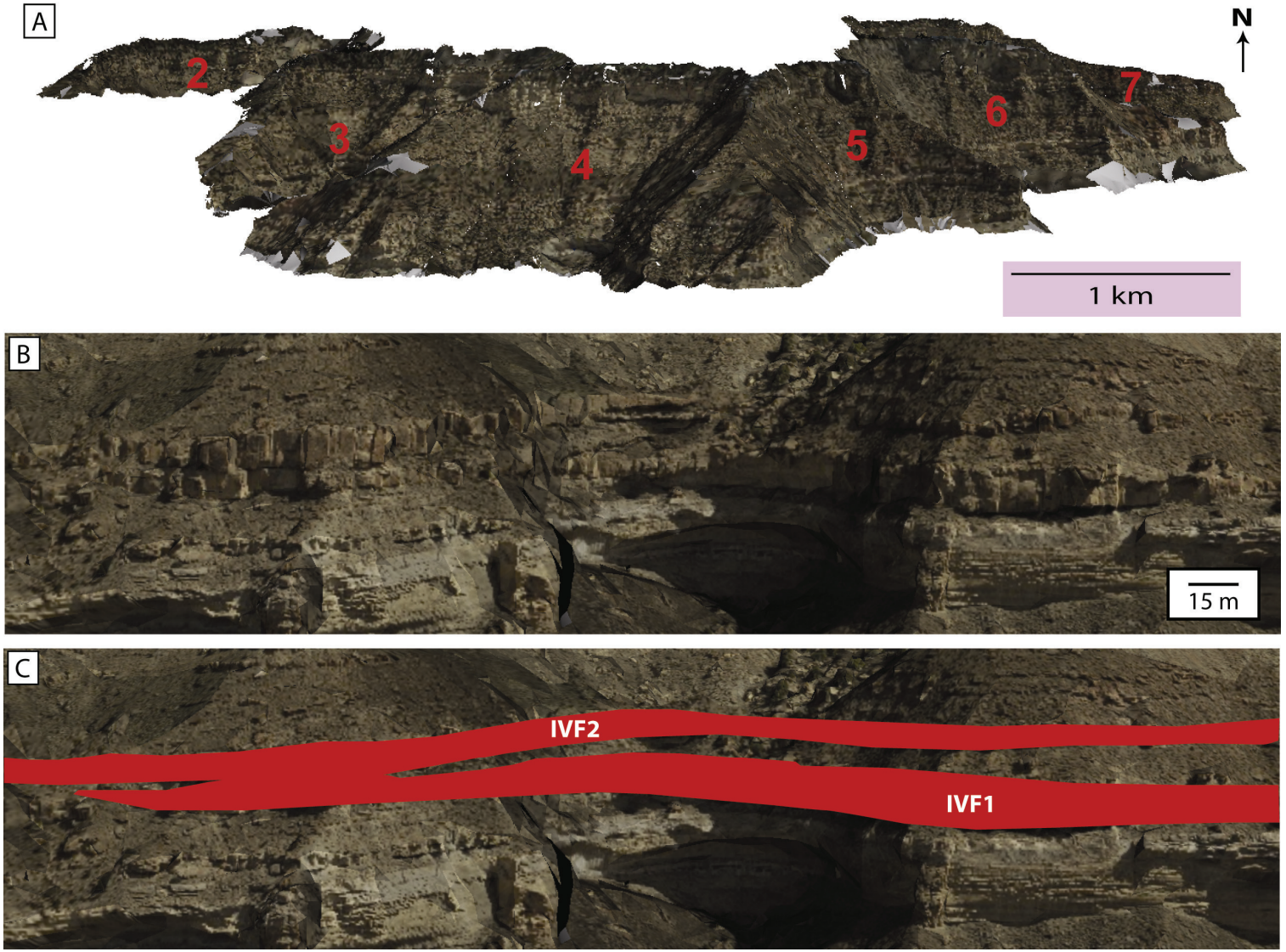

Figure 4.4 A) Processed low-airborne LiDAR data acquired on cliff-faces 2-7 (for location, see Figure 4.1B). B) Zoomed LIDAR data showing IVF1 and IVF2 (un-interpreted). C) Zoomed LIDAR data showing IVF1 and IVF2 (interpreted; red colored).

occupy topographic minima produced by it. Successive channel re-occupations on this topographic minima (i.e. depocenter) result in thicker and amalgamated sandbody development. This process, as an autogenic interplay, has been attributed to be the primary control towards resultant fluvial organization in coal-bearing basin (e.g. Michaelson et al., 2000).

We argue that our data illustrates an IVF style deposition where autogenic process (i.e. coal-precursor peat compaction) has dominated allogenic forcing such that coal thickness and sandbody amalgamation thickness are positively correlated. In this case, autogenic signal has supplanted allogenic one. In contrast, as our data also show, for location where higher sandbody amalgamation is observed above thinner coal ("negative relationship"), it can be argued that allogenic signal has supplanted autogenic one which we conventionally invoke for IVF style deposition. These two types of supplanting mechanisms have been constrained on our dataset for improved characterization of autogenic from allogenic dynamics.

Depositional architecture in IVF1 is demonstrative of a "fully autogenic-supplanting (i.e. autogenic-controlled) model" (Figure 4.5E). Here two depocenters are relatively of bigger sizes, and resultant sandbody amalgamation is in good agreement to thicker coal deposition. We did not find any negative relationship to link resultant fluvial organization with allogenic-supplanting mechanism. The two depocenters are broadly aligned in a less scattered pattern that might have happened due to less heterogeneity in Axel-Anderson coal zone deposition in the study area (Figure 4.5C).

In contrast, we invoke a "mixed-controlled model" for IVF2 (Figure 4.5F) where both autogenic and allogenic signals are preserved in guiding fluvial sandbody organization in incised

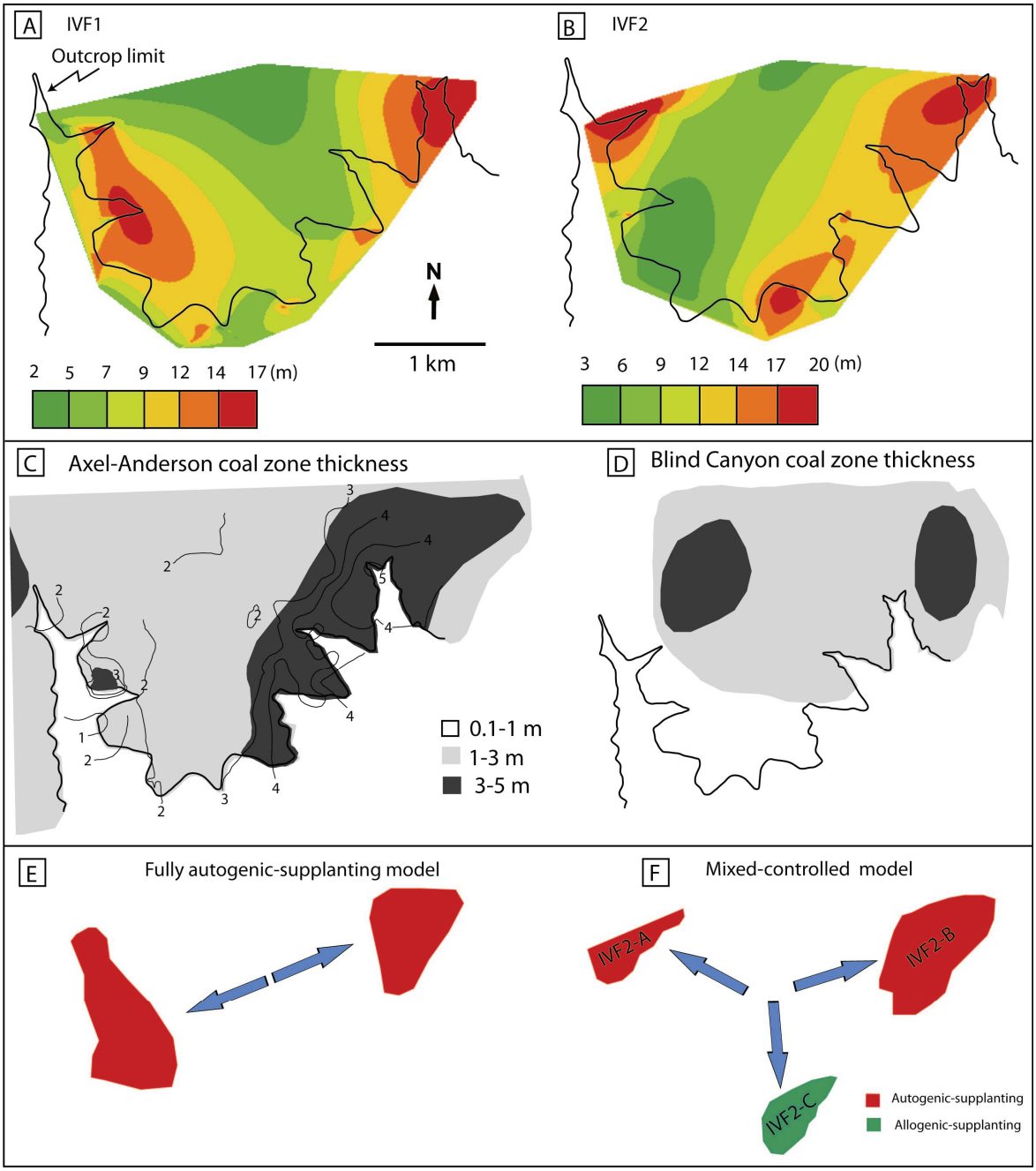

Figure 4.5 A) Isopach map of the amalgamation thickness of IVF1. Black line indicates to the outcrop exposure of cliff-faces shown in Figure 4.1B. B) Isopach map of the amalgamation thickness of IVF2. C) Axel-Anderson coal zone thickness map data provided by Energy West Mining Company. Color shading is redrawn from coal data of Utah Geological Survey (Gloyn et al., 2003; Tabet et al., 1999). D) Blind Canyon coal zone thickness map. Color shading is redrawn from coal data of Utah Geological Survey (Gloyn et al., 2003; Tabet et al., 1999). Note for the bulk part of our study area, no color shading denoting poor deposition (< 1m thick) of Blind Canyon coal zone. E) A fully autogenic-supplanting model for IVF1 showing the depocenters (red colored) are relatively of bigger size, and relatively concentrated. F) A mixed-controlled model for IVF2 showing the depocenters are relatively of smaller size, and spatially-scattered.

valley. For depocenters IVF2-A and IVF2-B, a positive correlation between sandbody amalgamation thickness and coal thickness characterizes autogenic-supplanting behavior. On the contrary, in depocenter IVF2-C, high sandbody amalgamation vs. thinner coal (i.e. negative relationship) demonstrates an allogenic-supplanting behavior. Occurrence of both of these two patterns has resulted in a scattered depocenter distribution that could be attributed to the more heterogeneity in Blind Canyon coal zone deposition in the study area (Figure 4.5D).

From the rock record examination, It is unclear how the threshold value of autogenic signal acts as filter to allogenic signal (i.e. Jerolmack and Paola, 2010). Our data contribute to evaluating this filtering mechanism for IVF style deposition. At a simplest level, we consider the thickness of coal analogous to the strength of autogenic signal. We found that in depocenters of IVF1 , and IVF2-A and IVF2-B where the underlying coal thickness is >1m, the resultant fluvial organization is controlled by autogenic-supplanting mechanism as interpreted above. On the contrary, for depocenter IVF2-C where underlying coal thickness is <1m, the resultant overlying fluvial organization is attributed to allogenic-supplanting mechanism. This analysis brings an analogy that thickness of underlying coal acts as a threshold value such that channels occupying over < 1m thick coal can be preferentially modulated by allogenic control towards resultant fluvial organization. However, if the underlying coal thickness is >1m, then autogenic behavior of coal compaction dominates over allogenic forcing in channel steering and successive fluvial organization.

A depocenter persists at a location within an incised valley for some time before another depocenter is developed at another location (e.g. Blum et al., 2013), which occurs within a sequence cycle. Relationships between autogenic-controlled and allogenic-controlled

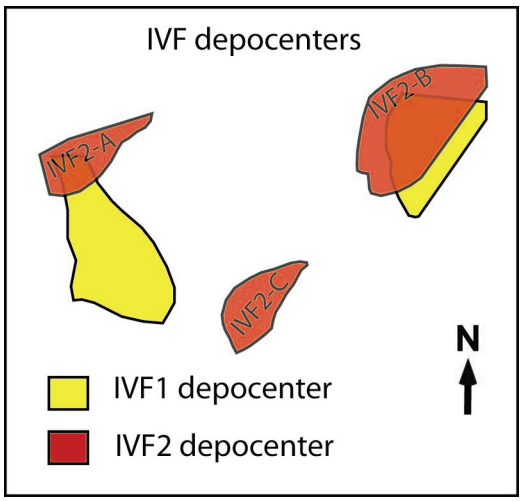

Figure 4.6 Vertical superposition of depocenters of two IVFs of studied dataset.

depocenters in successive sequences is presently unknown. Our results bring perspectives to this. When we superpose the isopach map of sandbody amalgamation thickness of these two IVFs (Figure 4.6), it reveals that depocenters IVF2-A and IVF2-B are located immediately above two depocenters of IVF1, but depocenter IVF2-C locates above the interfluve of two depocenters of IVF1. This is significant at the length scale of our data because depocenters controlled by autogenic-supplanting mechanism are vertically juxtaposed, whereas depocenter controlled by allogenic-supplanting mechanism implies to a compensational style occurrence. Based on this observation, we can make an inference that autogenic supplanting behavior, when linked to successive sequence cycles, could operate randomly or non-compensationally contrary to allogenic-supplanting behavior which could act compensationally, as our data shows, at underlying sequence to overlying sequence. Whether this is unique to our study area

or a new insight, this provoking observation needs to be evaluated by future laboratory experimental and rock record studies.

Finally, study results can aid in more interpretation value to ongoing depositional architecture analysis of the Western Interior Seaway. Obtained knowledge like supplanting mechanism of autogenic and allogenic process in IVF style deposition linked to coal deposition can be applied to important coal-bearing stratigraphic units like Blackhawk Formation and Williams Fork Formation. For example, Blackhawk Formation has been interpreted to be a low-frequency (c. 2.0-3.0 Myr duration) highstand systems tract comprising multiple high-frequency sequences of c. 0.2-1.0 Myr duration (e.g. Hampson et al., 2012, 2013; Howell and Flint, 2003). Given that its fluvial architecture broadly conforms to a modulating process governed by autogenic rather than allogenic forcing at certain locations (i.e. Hampson et al., 2013), our characterization of supplanting mechanism of autogenic vs. allogenic forcing from these two high frequency sequences encourages to similar high resolution sequence by sequence analysis of this Formation. Both Blackhawk Formation and Williams Fork Formation show coal-prone to coal-poor transitional behavior from their lower to upper stratigraphic interval. Evaluation of the degree of magnitude by which the presented autogenic supplanting behavior linked to coal deposition changes as a function of stratigraphic position (lower, middle or upper) in guiding fluvial organization might help refining previous results of these two formation (e.g. Hampson et al., 2013; Hofmann et al., 2011). Finally, study results bring a caution to the IVF style interpretation for both Quaternary and rock record that not all IVF deposits are modulated by allogenic forcing.

Chapter 5

Conclusions and Future Works

5.1 Conclusions

This research underscores the importance of outcrop characterization of fluvial strata as an effective tool in achieving significant sedimentologic and stratigraphic insights. This study embraces to the motivation, which both academic community and petroleum industry have followed: characterization of fluvial depositional elements bears immense intellectual and economic values. This characterization has been attained here from rock record exposures of the upper Cretaceous Blackhawk Formation in Cottonwood Creek of the Wasatch Plateau, Utah. Using a robust and integrated dataset comprising outcrop, core, GPR and LIDAR data on exposed coastal-plain strata, which are of exceptional quality and scales, this study has extracted several knowledge suites that are paramount to both ongoing analysis in fluvial discipline and continuing strive for improved reservoir characterization in petroleum industry.

This research has illustrated field-validation and -calibration of entire range of fluvial heterogeneities constrained on a single outcrop dataset. Large-scale heterogeneity (10's of m vertically, 100's of m laterally), which is associated with stacking of channelized fluvial sandbodies encased within coastal-plain fines, provides a range of geometry and spatial

distribution of channelized sandbodies. Their discrete organization ranging from single-storey sandbodies (thickness ranging from 1 to 17 m, width from 29 to 724 m), through multi-lateral channel-belt sandbodies (~15 m thick, ~230 m wide), to multi-storey channel-belt-complex sandbodies (~25 m thick, ~270 m wide) is captured on outcrop panels at spatial scales. Major sandbody uncertainty like well interference problem has been assessed. Width of >50% (28 out of 53) sandbodies is in the range of 1-200 m indicating that major sandbodies can be intersected by one well or maximum of two wells at 100 m well spacing, which is typical for tight-gas problem of onshore US. Estimated net-to-gross ratios demonstrate production challenges: 1) bulk estimation confirms to a low value range (17-46%), which is usually accompanied by fluvial reservoirs of low net-to-gross system like those in the hydrocarbon-prolific Uinta and Piceance Basins of Utah and Colorado, and 2) dramatic decrease/increase of estimated values at short distances that adds to analogous reservoir complexity. Broadly, four sweet spot zones have been identified for favorable exploration and production prospect. Spatial distribution of five architectural elements (channel, bar-accretion macroform, overbank fines, crevasse delta, and overbank and crevasse splays) have conditioned intermediate-scale heterogeneity (1's of m vertically, 10's of m laterally). Their efficacy as reservoir body (e.g. channel, bar-accretion macroform), reservoir conduit (e.g. crevasse splay) or flow-barriers (e.g. overbank fines) has been comprehended. Small-scale heterogeneity (10's of cm vertically, 1's of m laterally) has been attributed to spatial variability of six facies (trough cross-stratified sandstones, parallel-laminated sandstones, thinly interbedded mudstones, siltstones and rippled sandstones, mudstones and siltstones, carbonaceous mudstones, and coal) within architectural elements. Illustrated lateral and vertical breaks of these facies contribute to local-

scale heterogeneities nested within the studied coastal-plain strata. Overally, these fluvial heterogeneities generate a range of stratigraphic compartmentalization potential at field-scale that can be integrated towards improved reservoir analysis of low net-to-gross system like tight-gas fluvial reservoirs including the giant Jonah Field of Wyoming.

Integrating cutting-edge photorealistic technology like LiDAR, this study has achieved far robust sedimentological and stratigraphic results. LiDAR data (~20 cm resolution) have been acquired on six vertical and contiguous cliff faces spanning ~5 x 5 km^2 area. As the LiDAR data is properly georeferenced and contains three dimensionality of outcrop elements (X, Y, and Z), it have generated a 3D virtual outcrop model. Using this model, this study has been able to trace and map the continuity of individual sandbody from one cliff face to the next. This LiDAR-extracted information has been exported to ArcMap interface to generate 3D volume of sandbody exposed on 2D outcrop template. Upon correction with respect to paleoflow direction, the near-perfect, three-dimensional extent of individual channel-storey sandbody has been attained. Using this novel approach of generating 3D fluvial geobody, all geobodies have been populated to illustrate analogous distribution of reservoir suite (i.e. sandbody) encased within flow-barrier element (i.e. floodplain fines) of subsurface reservoir development. For fluvial organization analysis, these geobodies have been projected onto a 2D plane perpendicular to paleoflow direction. Projected sandbody population has brought multiple insights of fluvial organization: 1) single-storey deposits show affinity towards clustering phenomenon in contrast to compensational behavior demonstrated by multi-lateral deposits (i.e. channel-belt), 2) sandbody organization is broadly compensationally-stacked for the lower Blackhawk Formation where floodplain diversity is the highest, unlike in both the middle and

upper Blackhawk Formation where vertical-clustering phenomenon of sandbodies is more apparent along with the least floodplain diversity. This shows that floodplain diversity can control fluvial sandbody stacking pattern.

The study has contributed to the growing call of de-convolving autogenic from allogenic signal, particularly where their interplay is complex like in the case of paleovalley system. Using two interpreted incised valley fill deposits, each of which is up to ~15-20 m thick, this study has targeted the spatial variability of fluvial architecture nested within these two valley fills. Trend of sandbody amalgamation thickness within these two valley fills brings a significant observation that it is positively correlated to the thickness variation of underlying coal deposit. This sandbody amalgamation vs. coal thickness relationship can be attributed to the following reasoning: differential subsidence linked to underlying coal thickness (i.e. an autogenic mechanism) was the major autogenic control filling incised valleys in the study area. In that process, this autogenic mechanism was dominating over allogenic control (i.e. sea-level fluctuation) such that its supplanting behavior preferentially guided resultant fluvial organization of these two valley fill deposits. Thus, this finding brings a caution that resultant fluvial architecture of paleovalley system should not be automatically attributed to the allogenic modulating process.

5.2 Future Works

Outcropped coastal-plain strata of the Wasatch Plateau, Utah offers significant future research potential. Some future works can be pursued towards improved fluvial rock record understanding as specified below

- As invoked by the latest fluvial review studies, instead of simplistically attributing formative channel as end-member types (i.e. straight, meandering or braided) in rock record studies, 3D description of bar sandbody should be pursued to document all sedimentologic variability, which can potentially furnish information appreciable to wide-ranging variability manifested by modern rivers. Suitable, 3D-oriented outcrops of bar sandbodies in the Wasatch Plateau can be targeted as part of this ancient vs. modern fluvial integrative analysis.

- As the Wasatch Plateau itself is classified as an exploratory tight-gas basin, in addition to its location proximity to the tight-gas producing Uinta and Piceance Basins of Utah and Colorado, it can offer to improved analysis of unconventional tight-gas reservoir development. 3D outcrop and petrophysical models of analogous tight-gas reservoir development and spatial distribution of source, reservoir and seal elements can be constructed from LiDAR-integrated outcrop data of the Wasatch Plateau.

- Upstream vs. downstream changes in fluvial avulsion characteristics have largely been investigated in numerical or experimental (flume tank) work. Superbly exposed fluvial

strata in the Wasatch Plateau and their downstream reach at the Book Cliffs can be analyzed to evaluate and/or validate these modeled fluvial avulsion behavior.

- For a better understanding of the evolutionary depositional characteristics in the broader Western Interior Seaway of Utah and Colorado, depositional aspects of the coal-bearing Blackhawk Formation can be evaluated in comparison to the highly-producing younger Williams Fork Formation, which bears similar coastal-plain depositional character and depositional duration. This comparative analysis will shed light on similarity/dissimilarity of the same coastal-plain depositional character as it evolved through time.

References

Adams, M.M., and Bhattacharya, J.P., 2005, No change in fluvial style across a sequence boundary, Cretaceous Blackhawk and Castlegate Formations of central Utah, USA: Journal of Sedimentary Research, v. 75, p. 1038-1051.

Ainsworth, R. B., 2005, Sequence stratigraphic-based analysis of reservoir connectivity: influence of depositional architecture – a case study from a marginal marine depositional setting: Petroleum Geoscience, v. 11, p. 257-276.

Allen, J. R. L., 1963, Henry Clifton Sorby and the sedimentary structures of sands and sandstones in relation to flow conditions: Geologie en Mijnbouw, v. 42, p. 223–228.

Allen, J. R. L., 1970, Physical processes of sedimentation: London, Allen and Unwin, 248 p.

Allen, J. R. L., 1984, Sedimentary Structures; Their character and Physical Basis: Amsterdam, Elsevier, 1256 p.

Allen, J.R.L., 1965, The sedimentation and palaeogeography of the Old Red Sandstones of Anglesey, North Wales: Proceedings of the Yorkshire Geological Society, v. 35, no. 8, p. 139–185.

Anderson, D. S., 2005, Architecture of crevasse splay and point-bar bodies of the nonmarine Iles Formation north of Rangely, Colorado: Implications for reservoir description: The Mountain Geologist, v. 42, p. 109–122.

Barnaby, R. j, and Ward, W. B., 2007, Outcrop analog for mixed siliciclastic-carbonate ramp reservoirs-stratigraphic hierarchy, facies architecture, and geologic heterohenity: Grayburg Formation, Permian Basin, U.S.A.: Journal of Sedimentary Research, v. 77, p. 34-58.

Bellian, J. A., Kerans, C. and Jennette, D. C., 2005, Digital Outcrop Models: Applications of Terrestrial Scanning Lidar Technology in Stratigraphic Modeling. Journal of Sedimentary Research, v. 75, p. 166-176.

Bhattacharya, J. P., and Tye, R. S., 2004, Searching for modern Ferron analogs and applications to subsurface interpretation, in T. C. Chidsey, Jr., R. D. Adams, and T. H. Morris, eds., Regional to Wellbore Analog for Fluvial-Deltaic Reservoir Modeling, The Ferron Sandstone of Utah: AAPG Studies in Geology 50, p. 39-57.

Blum, M., Martin , J., Milliken, K., and Garvin, M., 2013, Paleovalley systems: Insights from Quaternary analogs and experiments: Earth-Science Reviews, v. 116, p. 128-169.

Bohacs, K., and Suter, J., 1997, Sequence stratigraphic distribution of coaly rocks: fundamental controls and paralic examples: AAPG Bulletin, v. 81, p. 1612–1639.

Bridge, J. S., and Tye, R. S., 2000, Interpreting the dimensions of ancient fluvial channel bars, channels, and channel belts from wireline-logs and cores: AAPG Bulletin, v. 84, p. 1205-1228.

Bryant, I., D. Carr, P. Cirilli, N. Drinkwater, D. McCormick, P. Tilke, and J. Thurmond, 2000, Use of 3D digital analogs as templates in reservoir modeling: Petroleum Geoscience, v. 6, p. 195–201.

Buckley, S. J., Vallet, J., Braathen, A., and Wheeler, W., 2008a, Oblique helicopter-based laser scanning for digital terrain modelling and visualisation of geological outcrops. International Archives of the Photogrammetry, Remote Sensing and Spatial Information Sciences, 37. Part B4, 493-498.

Buckley, S. J., Howell, J. A., Enge, H. D., and Kurz, T. H., 2008b, Terrestrial laser scanning in geology: data acquisition, processing and accuracy considerations. Journal of the Geological Society, v. 165, p. 625-638.

Cluff, S. G., and Cluff, R. M., 2004, Petrophysics of the Lance Sandstone Reservoirs in Jonah Field, Sublette County, Wyoming, in J.W. Robinson and K.W. Shanley, eds., Jonah Field: Case study of a giant tight-gas fluvial reservoir: AAPG Studies in Geology 52, p. 215-241.

Cole, R. D., and Cumella, S. P., 2005, Sand-Body architecture in the lower Williams Fork Formation (Upper Cretaceous), Coal Canyon, Colorado, with comparison to the Piceance Basin subsurface: The Mountain Geologist, v. 42, p. 85–107.

Cumella, S. P., Shanley, K. W., and Camp, W. K., 2008, Introduction, in S. P. Cumella, K. W. Shanley and W. K. Camp, eds., Understanding, exploring and developing tight-gas sands: AAPG Hedberg Series 3, p. 1-4.

DeCelles, P. G., and Coogan, J. C., 2006, Regional structure and kinematic history of the Sevier fold-and-thrust belt, central Utah: Geological Society of America Bulletin, v. 118, p. 841–864.

Dubiel, R.F., Kirschbaum, M.A., Roberts, L.N.R., Mercier, T.J., and Heinrich, A., 2000, Geology and coal resources of the Blackhawk Formation in the Southern Wasatch Plateau, Central Utah, in Kirschbaum, M.A., Roberts, L.N.R., and Biewick, L.R.H., eds., Geologic Assessment of Coal in the Colorado Plateau: Arizona, Colorado, New Mexico, and Utah: U.S. Geological Survey, Professional Paper 1625-B, Chapter S (CD-ROM only).

Dubois, D. P. , Wynne, P. J. , T. M. Smagala, T. M. , Johnson, J. L. , and Engler, K. D., 2004, Geology of Jonah Field, Sublette County, Wyoming *in* J.W. Robinson and K.W. Shanley, eds., Jonah field: Case study of a giant tight-gas fluvial reservoir: AAPG Studies in Geology 52, p. 37-59.

Flores, R. M., Blanchard, L. F., Sanchez, J. D., Marley, W. E. and Muldoon, W. J., 1984, Paleogeographic controls of coal accumulation, Cretaceous Blackhawk Formation and Star Point Sandstone, Wasatch Plateau, Utah: Geological Society of America Bulletin, v. 95, p. 540-550.

Friend, P. F., M. J. Slater, and R. C. Williams, 1979, Vertical and lateral building of river channels, Ebro Basin, Spain: Geological Society (London), v. 136, p. 39–46.

Gani, M. R., and Bhattacharya, J. P., 2007, Basic building blocks and process variability of a Cretaceous delta: Internal facies architecture reveals a more dynamic interaction of river, wave, and tidal process than is indicated by external shape: Journal of Sedimentary Research, v. 77, p. 284-302.

Gibling, M.R., 2006, Width and thickness of fluvial channel bodies and valley fills in the geological record: a literature compilation and classification. Journal of Sedimentary Research 76, p. 731–770.

Gloyn, R. W., Tabet , D. E., Tripp, B. T., Bishop, C. E., Morgan, C. D., Gwynn, J. W., and Blackett, R. E., 2003, Energy, mineral, and ground-water resources of Carbon and Emery Counties, Utah: Utah Geological Survey Bulletin 132, 161 p.

Hajek and Wolinsky, 2012, Simplified process modeling of river avulsion and alluvial architecture: Connecting models and field data. Sedimentary geology, 257-260, p. 1–30.

Hajek, E. A., Heller., P. L., and Schur, E. L., 2012, Field test of autogenic control on alluvial stratigraphy (Ferris Formation, Upper Cretaceous–Paleogene, Wyoming): GSA Bulletin, v. 124, p. 1898-1912.

Hajek, E.A., Heller, P.L., Sheets, B.A., 2010, Significance of channel-belt clustering in alluvial basins. Geology 38 (6), p. 535–538.

Hampson, G. J., 2010, Sediment dispersal and quantitative stratigraphic architecture across an ancient shelf: Sedimentology, v. 57, p. 96-141.

Hampson, G. J., and Howell, J. A., 2005, Sedimentologic and geomorphic characterization of ancient wave-dominated deltaic shorelines: Upper Cretaceous Blackhawk Formation, Book Cliffs, Utah, U.S.A., *in* L. Giosan and J.P. Bhattacharya, eds., River deltas – concepts, models and examples, SEPM, 2005, p. 133 - 154.

Hampson, G. J., Gani, M. R., Sharman, K. E., Irfan, N., and Bracken, B., 2011, Along-strike and down-dip variations in shallow-marine sequence stratigraphic architecture: Upper Cretaceous Star Point Sandstone, Wasatch Plateau, central Utah, U.S.A: Journal of Sedimentary Research, v. 81, p. 159-184.

Hampson, G. J., Gani, M. R., Sahoo, H., Rittersbacher, A., Irfan, N., Ranson, A., Jewell, T. O., Gani, N. D. S., Howell, J. A., Buckley, S. J., and Bracken, B., 2012, Controls on large-scale patterns of fluvial sandbody distribution in alluvial to coastal plain strata: Upper Cretaceous Blackhawk Formation, Wasatch Plateau, Central Utah, USA: Sedimentology, v. 59, p. 2226-2258.

Hampson, G. J., Jewell, T. O., Irfan, N., Gani, M. R., and Bracken, B., 2013, Modest change in fluvial style with varying accommodation in regressive alluvial-to-coastal-plain wedge: upper cretaceous Blackhawk Formation, Wasatch Plateau, central Utah, U.S.A.: Journal of Sedimentary Research, v. 83, p. 145-169.

Hartkamp-Bakker, C. A., and M. E. Donselaar, 1993, Permeability patterns in point bar deposits: Tertiary Loranca Basin, central Spain, in S. S. Flint and I. D. Bryant, eds., The geological modelling of hydrocarbon reservoirs and outcrop analogs: International Association of Sedimentologists Special Publication 15, p. 157– 168.

Henry, M. E., and Finn, T. M., 2003, Petroleum Assessment of the Ferron/ Wasatch Plateau Total Petroleum System, Upper Cretaceous Strata, Wasatch Plateau and Castle Valley, Utah: U.S. Geological Survey Digital Data Series DDS–69–B, Chapter 8 (CD only).

Higgs, K. E., Zwingmann, H., Reyes, A. G., and Funnel, R. H., 2007, Diagenesis, porosity evolution, and petroleum emplacement in tight gas reservoirs, Taranaki Basin, New Zealand: Journal of Sedimentary Research, v. 77, p. 1003-1025.

Hofmann, M. H., Wroblewski, A., and Boyd, R., 2011, Mechanisms controlling the clustering of fluvial channels and the compensational stacking of channel belts: Journal of Sedimentary Research, v. 81, p. 670-685.

House, N., and Shemeta, J., 2008, Understanding hydraulic fractures in tight-gas sands through the integration of borehole microseismic data, three-dimensional vertical seismic profile data: A Jonah field case study, in S.P. Cumella, K.W. Shanley, and W.K. Camp, eds., Understanding, Exploring and Developing tight-gas sands: AAPG Hedberg Series, no. 3, p. 5-12.

Houston, W. S., Huntoon, J. E. and Kamola, D. L., 2000, Modeling of Cretaceous foreland-basin parasequences, Utah, with implications for timing of Sevier thrusting: Geology, v. 28, p. 267-270.

Howell, J.A., and Flint, S.S., 2003, Siliciclastics case study: the Book Cliffs, *in* A. Coe, ed., The sedimentary record of sea level change: Cambridge University Press, p. 135-208.

Hunt, D., Allsop, T., and Swarbrick, R.E., 1996, Compaction as a primary control on the architecture and development of depositional sequences: conceptual framework, applications and implications, in J.A. Howell and J.F. Aitken, eds., High Resolution Sequence Stratigraphy: Innovations and Applications: Geol. Soc. Spec. Publ., v. 104, p. 21–345.

Jackson, R. G., 1977, Preliminary evaluation of lithofacies models for meandering alluvial streams, in A. D. Miall, ed., Fluvial sedimentology: Canadian Society of Petroleum Geologists Memoir 5, p. 543–576.

Jerolmack, D., and Paola, C., 2010, Shredding of environmental signals by sediment transport: Geophysical Research Letters, v. 37, L 19401.

Johnson, R. C., and Roberts, S. B., 2003, The Mesaverde Total Petroleum System, Uinta-Piceance Province, Utah and Colorado. In: Petroleum systems and geologic assessment of oil and gas in the Uinta-Piceance Province, Utah and Colorado: U.S. Geol. Survey, Digital Data Series, DDS-69-B, Chapter 7 (CD only).

Jones, J. R., A. J. Scott, and L. W. Lake, 1987, The geologic aspects of reservoir characterization for numerical simulation: Mesaverde meander-belt sandstone, northwestern Colorado: Society of Petroleum Engineers Formation Evaluation, v. 2, p. 97–107.

Kamola, D. L., and Van Wagoner, J. C., 1995, Stratigraphy and facies architecture of parasequences with examples from the Spring Canyon Member, Blackhawk Formation, Utah, *in* J.C. Van Wagoner and G.T. Bertram, eds., Sequence stratigraphy of foreland basin deposits: AAPG Memoir 64, p. 27-54.

Kauffman, E. G., and Caldwell, W. G. E., 1993, The Western Interior Basin in space and time, in W.G.E. Caldwell and E.G. Kauffman, eds., Evolution of the Western Interior Basin: Geological Association of Canada Special Paper, v. 39, p. 1–30.

Kraus, M. J., 1987, Integration of channel and floodplain suites: II. Vertical relations of alluvial paleosols: Journal of Sedimentary Petrology, v. 57, p. 602–612.

Krystinik, L. F., and Dejarnett, B. B., 1995, Lateral variability of sequence stratigraphic framework in the Campanian and Lower Maastrichtian of the Western Interior Seaway, in Van Wagoner, J.C., and Bertram, G.T., eds., Sequence Stratigraphy of Foreland Basin Deposits: Outcrop and Subsurface Examples from the Cretaceous of North America: American Association of Petroleum Geologists, Memoir 64, p. 11–26.

Larue, D. K., and Hovadik, J., 2006, Connectivity of channelized reservoirs: a modeling approach: Petroleum Geoscience, v. 12, p. 291-308.

Lasseter, T. J., J. R. Waggoner, and L. W. Lake, 1986, Reservoir heterogeneities and their influence on ultimate recovery, in L. W. Lake and H. B. Carroll, Jr., eds., Reservoir characterization: Orlando, Academic Press, p. 545–559.

Laubach, S. E., and Gale, J. F. W., 2006, Obtaining fracture information for low-permeability (tight) gas sandstones from sidewall cores: Journal of Petroleum Geology, v. 29, no. 2, p. 147–158.

Law, B. E., 2002, Basin-centered gas systems: AAPG Bulletin, v. 86, no. 11, p. 1891– 1919.

Law, B. E., and Spencer, C. W., 2004, Basin-centered gas systems and the Jonah field, in J.W. Robinson and K.W. Shanley, eds., Jonah field: Case study of a giant tight-gas fluvial reservoir: AAPG Studies in Geology 52, p. 147-158.

Leclair, S. F., and Bridge, J. S., 2001, Quantitative interpretation of sedimentary structures formed by river dunes: Journal of Sedimentary Research, v. 71, p. 714-717.

Liu, S., D. Nummedal, and L. Liu, 2011, Migration of dynamic subsidence across the Late Cretaceous United States Western Interior Basin in response to Farallon plate subduction: Geology, v. 39, p. 555-558.

Meckel, L. D., and Thomasson, M. R., 2008, Pervasive tight-gas sandstone reservoirs: An overview, in S.P. Cumella, K.W. Shanley, and W.K. Camp, eds., Understanding, Exploring and Developing tight-gas sands: AAPG Hedberg Series, no. 3, p. 13-27.

Miall, A. D. and Arush, M., 2001, The Castlegate Sandstone of the Book Cliffs, Utah: sequence stratigraphy, paleogeography, and tectonic controls: Journal of Sedimentary Research, v. 71, p. 537–548.

Miall, A. D., 1988, Reservoir heterogeneities in fluvial sandstones: Lessons from outcrop studies: AAPG Bulletin, v. 72, no. 6, p. 682– 697.

Miall, A. D., 2006, The geology of fluvial deposits: Springer, 582 p.

Michaelsen, P., Henderson, R.A., Crosdale, P.J., and Mikkelsen, S.O., 2000, Facies architecture and depositional dynamics of the Upper Permian Rangal Coal Measures, Bowen Basin, Australia: Journal of Sedimentary Research, v. 70, p. 879-895.

Moreton, D. J., Ashworth, P. J., and Best, J. L., 2002, The physical scale modeling of braided alluvial architecture and estimation of subsurface permeability: Basin Research, v. 14, p. 265-285.

Muto, T., Steel, R.J., Swenson, J.B., 2007, Autostratigraphy: a framework norm for genetic Stratigraphy. Journal of Sedimentary Research, v. 77, p. 2–12.

Nehring, R., 2008, Growing and indispensable: The contribution of production from tight-gas sands to U.S. gas production, in S.P. Cumella, K.W. Shanley, and W.K. Camp, eds., Understanding, Exploring and Developing tight-gas sands: AAPG Hedberg Series, no. 3, p. 5-12.

Nuccio, V. F., and Roberts, L. N. R., 2003, Thermal maturity and oil and gas generation history of petroleum systems in the Uinta-Piceance Province, Utah and Colorado: U.S. Geol. Survey, Digital Data Series, DDS-69-B, Chapter 4 (CD only).

Olson, J. E., Laubach, S. E., and Lander, R. H., 2009, Natural fracture characterization in tight gas sandstones: Integrating mechanics and diagenesis: AAPG Bulletin, v. 93, no. 11p. 1535–1549.

Owen, G., 1986, Experimental soft-sediment deformation: structures formed by the liquefaction of unconsolidated sands and some ancient examples: Sedimentology, v. 43, p. 279-293.

Paola, C., Straub, K., Mohrig, D., and Reinhardt, L., 2009, The “unreasonable effectiveness” of stratigraphic and geomorphic experiments. Earth-Science Reviews, v. 97, p. 1–43.

Pattison, J. A., 1995, Sequence stratigraphic significance of sharp-based lowstand shoreface deposits, Kenilworth Member, Book Cliffs, Utah: AAPG Bulletin, v. 79, no. 3, p. 444–462.

Pettijohn, F. J., Potter, P. E., and Siever, R., 1972, Sand and Sandstone: New York, Springer-Verlag, 618 p.

Pranter, M. J., and Sommer, N. K., 2011, Static connectivity of fluvial sandstones in a lower coastal-plain setting: An example from the Upper Cretaceous lower Williams Fork Formation, Piceance Basin, Colorado: AAPG Bulletin, v. 95, no. 6, p. 899–923.

Pranter, M. J., Cole, R. D., Panjaitan, and Sommer, N. K., 2009, Sandstone-body dimensions in a lower coastal-plain depositional setting: Lower Williams Fork Formation, Coal Canyon, Piceance Basin, Colorado: AAPG Bulletin, v. 93, no. 10, p. 1379–1401.

Pranter, M. J., Ellison, A. I., Cole, R. D., and Patterson, P. E., 2007, Analysis and modeling of intermediate-scale reservoir heterogeneity based on a fluvial point-bar outcrop analog, Williams Fork Formation, Piceance Basin, Colorado: AAPG Bulletin, v. 91, no. 7, p. 1025–1051.

Rajchal, M., and Uličný, D., 2005, Depositional record of an avulsive fluvial system controlled by peat compaction (Nogene, Most Basin, Czech Republic): Sedimentology, v. 52, p. 601-625.

Reynolds, A.D., 1999, Dimensions of paralic sandstone bodies, AAPG Bulletin, v. 83, p. 211–229.

Richardson, J. G., D. G. Harris, R. H. Rossen, and G. Van Hee, 1978, The effect of small, discontinuous shales on oil recovery: Journal of Petroleum Technology, v. 20, p. 1531– 1537.

Ringrose, P. S., Sorbie, K. S., Corbett, P. W. M., and Jensen, J. L., 1993, Immiscible flow behavior in laminated and cross-bedded sandstones: Journal of Petroleum Science and Engineering, v. 9, p. 103-124.

Rittersbacher, A., Buckley, S.J., Howell, J.A., Hampson, G.J. and Vallet, J., 2012, Helicopter-based laser scanning: a method for quantitative analysis of large-scale sedimentary architecture, , in A.W. Martinius, Howell J. A., and Good. T., eds., Sediment-body Geometry and heterogeneity: Analogue studies for modelling the subsurface: Geological Society of London Special Publication 387.

Robinson, J. W, and Shanley, K. W., 2004, Introduction: Jonah Field- Case study of a tight-gas fluvial reservoir, in J.W. Robinson and K.W. Shanley, eds., Jonah Field: Case study of a giant tight-gas fluvial reservoir: AAPG Studies in Geology 52, p. 1-3.

Ryer, T.A., and Langer, A.W., 1980, Thickness change involved in the peat-to-coal transformation for a bituminous coal of Cretaceous age in central Utah: Journal of Sedimentary Research, v. 50, p. 987-992.

Sanchez, J.D., and T.L. Brown, 1986, Stratigraphic framework and coal resources of the Upper Cretaceous Blackhawk Formation in the Trail Mountain and East Mountain areas of the Wasatch Plateau coal field, Manti 30˚ x 60˚ quadrangle, Emery and Sanpete counties, Utah: U.S. Geological Survey, Coal Investigations Map C-94C, scale 1:24,000.

Schumm, S. A., 1972, Fluvial paleochannels, *in* J.K. Rigby and W.K. Hamblin, eds., Recognition of Ancient Sedimentary Environments: SEPM Special Publication, no. 16, p. 98–107.

Shanley, K. W., 2004, Fluvial reservoir description for a giant, low-permeability gas field: Jonah field, Green river basin, Wyoming, USA, in J.W. Robinson and K.W. Shanley, eds., Jonah Field: Case study of a giant tight-gas fluvial reservoir: AAPG Studies in Geology 52, p. 159-182.

Shanley, K. W., and McCabe, P. J., 1994, Perspectives on the sequence stratigraphy of continental strata: American Association of Petroleum Geologists Bulletin, v. 78, p. 544–568.

Shanley, K. W., Cluff, R. M., and Robinson, J. W., 2004, Factors controlling prolific gas production from low-permeability sandstone reservoirs: Implications for resource assessment, prospect development, and risk analysis: AAPG Bulletin, v. 88, p. 1083–1121.

Sharp, J. M., S. Mingjuan, and W. E. Galloway, 2003, Heterogeneity of fluvial systems; control on density-driven flow and transport: Environmental and Engineering Geosciences, v. 9, no. 1, p. 5– 17.

Sinha, R., Gibling, M.R., Jain, V., and Tandon, S.K., 2005, Sedimentology and avulsion patterns of the anabranching Baghmati River in the Himalayan foreland basin, India, in Blum, M., and Marriott, S., eds., Fluvial Sedimentology VII: International Association of Sedimentologists, Special Publication 35, p. 181–196.

Smith, N.D., Cross, T.A., Dufficy, J.P., and Clough, S.R., 1989, Anatomy of an avulsion: Sedimentology, v. 36, p. 1–24.

Smith, T., Sayers, C. M., and Liner, C., 2010, Introduction to this special section: tight gas sands: The Leading Edge, v. 29, no. 12, p. 1463.

Surdam, R. C., 1997, A new paradigm for gas exploration in anomalously pressured ''tight-gas sands'' in the Rocky Mountain Laramide basins, *in* R. C. Surdam, ed., Seals, traps, and the petroleum system: AAPG Memoir 67, p. 283–298.

Tabet, D.E., Quick, J.C., Hucka, B.P. and Hanson, J.A. (1999) The available coal resource for nine 7.5-minute quadrangles in the northern Wasatch Plateau Coalfield, Carbon and Emery Counties, Utah. Utah Geol. Survey Circular, 100, 46 p.

Tobin, R. C., McClain, T., Lieber, R. B., Ozkan, A., Banfield, L. A., Marchand, M. E., and McRae, L. E., 2010, Reservoir quality modeling of tight-gas sands in Wamsutter field: Integration of diagenesis, petroleum systems, and production data: AAPG Bulletin, v. 94, no. 8, p. 1229–1266.

Tyler, N., and R. J. Finley, 1991, Architectural controls on the recovery of hydrocarbons from sandstone reservoirs, in A. D. Miall and N. Tyler, eds., The three-dimensional facies architecture of terrigenous clastic sediments and its implications for hydrocarbon discovery and recovery: SEPM Concepts in Sedimentology and Paleontology, v. 3, p. 1–5.

Vallet, J. & Skaloud, J. 2004. Development and experiences with a fully-digital handheld mapping system operated from a helicopter. International Archives of the Photogrammetry, Remote Sensing and Spatial Information Sciences, 35, Part B5, 6.

Van Wagoner, J.C., 1995, Sequence stratigraphy and marine to nonmarine facies architecture of foreland basin strata, Book Cliffs, Utah, in J.C. Van Wagoner and G.T. Bertram, eds., Sequence stratigraphy of foreland basin deposits: AAPG Memoir 64, p. 137-224.

Wang, Y., Straub, K.M., Hajek, E.A., 2011. Scale dependent compensational stacking: an estimate of autogenic timescales in sedimentary deposits. Geology 39, p. 811–814.

Weber, K. J., 1982, Influence of common sedimentary structures on fluid flow in reservoir models: Journal of Petroleum Technology, v. 34, p. 665–672.

Willis, B.J., 1997, Architecture of fluvial-dominated valley-fill deposits in the Cretaceous Fall River Formation: Sedimentology, v. 44, p. 735–757.

Willis, B.J., 1998, Permeability structure of fluvial-dominated valley-fill deposits in the Cretaceous Fall River Formation: AAPG Bulletin, v. 82, p. 206–227.

Willis, B. J., 1989, Palaeochannel reconstructions from point bar deposits: A three-dimensional perspective: Sedimentology, v. 36, p. 757–766.

Willis, B. J., and C. D. White, 2000, Quantitative outcrop data for flow simulation: Journal of Sedimentary Research, v. 70, p. 788–802.

Young, R. G., 1955, Sedimentary facies and intertonguing in the Upper Cretaceous of the Book Cliffs, Utah–Colorado: Geological Society of America Bulletin, v. 66, p. 177–201.

Yurewicz, D. A., Bohacs, K. M., Kendall, J., Klimentidis, R., E., Kronmueller, K., Meurer M. E., Ryan, T. C., and Yeakel, J. D., 2008, Controls on gas and water distribution , Mesaverde basin-centered gas play, Piceance Basin, Colorado, in S.P. Cumella, K.W. Shanley, and W.K. Camp, eds., Understanding, Exploring and Developing tight-gas sands: AAPG Hedberg Series, no. 3, p. 105-136.

Zaitlin, B.A., Dalrymple, R.W. and Boyd, R., 1994, The stratigraphic organization of incised-valley systems associated with relative sea-level change. In: Incised-Valley Systems; Origin and Sedimentary Sequences (Eds R.W. Dalrymple, R. Boyd and B.A. Zaitlin), SEPM Sp. Publ., v. 51, p. 45–60.

VITA

Hiranya Sahoo was born in Orissa, India. He completed his school and graduate level education with several scholarships awarded by state and central government. He entered The Post-Graduate Department of Geology at Utkal University, and graduated with a MS degree in geology in 2003. He attended IIT Bombay and completed his Master of Technology (MTech) degree in Geo-Exploration there. During his stay at IIT Bombay, he was a Schlumberger Fellow focusing a Schlumberger-British Gas sponsored research. He joined University of New Orleans in 2008 to pursue his PhD degree in sedimentology and stratigraphy under the supervision of Dr. Royhan Gani. At UNO, he has been awarded student grants from ExxonMobil, AAPG, IAS and Ed Picou Fellowship Grant from GCSSEPM. Additionally, he has been a recipient of Richard Boebel Graduate scholarship from New Orleans Geological Society. He has presented his research works in AAPG and GSA meetings.